PB-202 571

EVALUATION OF A NEW ACID MINE DRAINAGE TREATMENT PROCESS

Black, Sivalls and Bryson, Incorporated
Pittsburgh, Pennsylvania

February 1971

DISTRIBUTED BY:

NTIS
National Technical Information Service
U. S. DEPARTMENT OF COMMERCE
5285 Port Royal Road, Springfield Va. 22151

14010 DYI 02/71

WATER POLLUTION CONTROL RESEARCH SERIES • 14010 DYI 02/71

PB-202571-U

RC/SOD
MF/NTIS
$1.50

Evaluation of a New Acid Mine Drainage Treatment Process

LIBRARY
U. S. E. P. A.
4676 Columbia Pkwy. Cinti, OH 45228

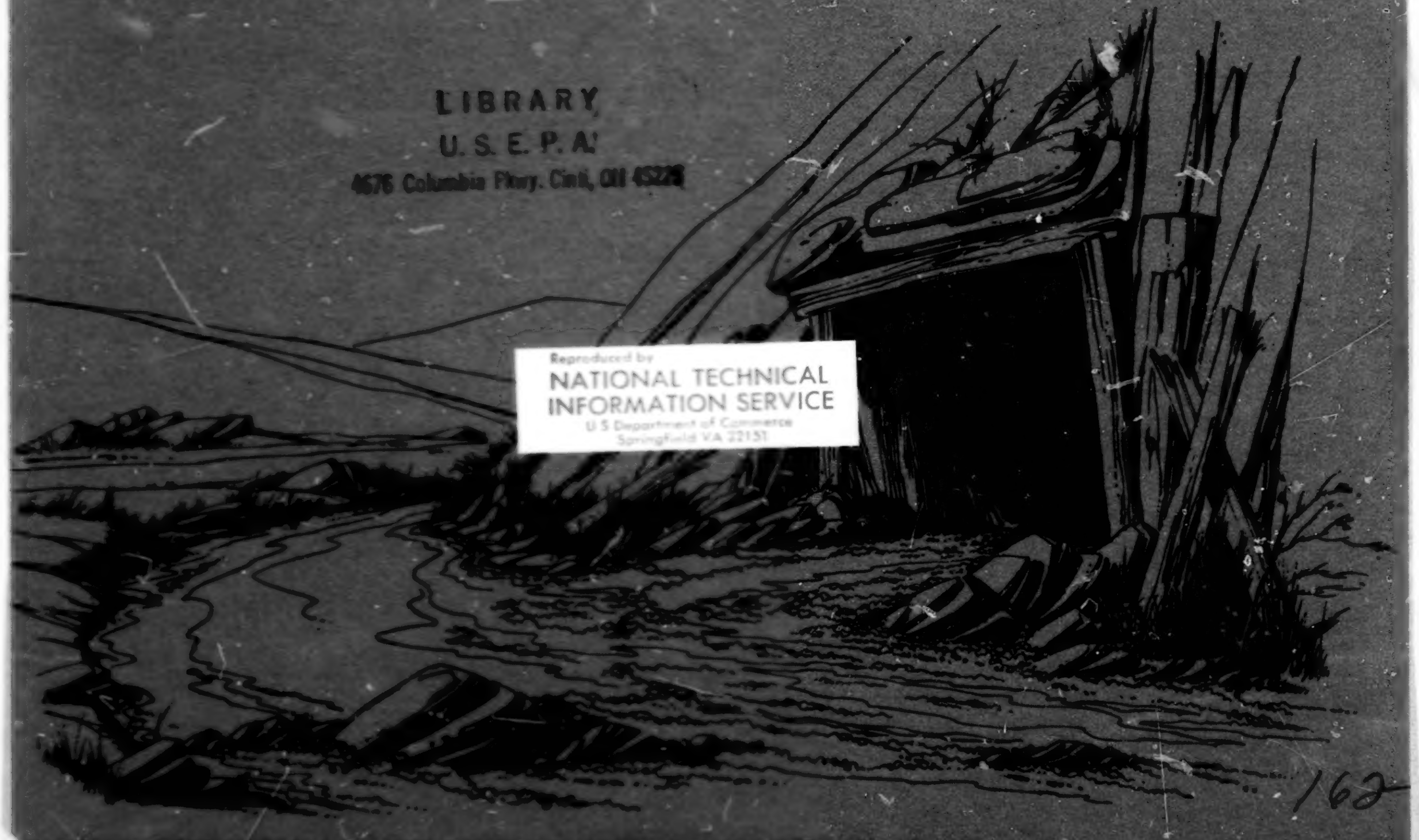

Reproduced by
NATIONAL TECHNICAL
INFORMATION SERVICE
U S Department of Commerce
Springfield VA 22151

162

ENVIRONMENTAL PROTECTION AGENCY • WATER QUALITY OFFICE

WATER POLLUTION CONTROL RESEARCH SERIES

The Water Pollution Control Research Reports describe the results and progress in the control and abatement of pollution in our Nation's waters. They provide a central source of information on the research, development, and demonstration activities in the Environmental Protection Agency, Water Quality Office, through inhouse research and grants and contracts with Federal, State, and local agencies, research institutions, and industrial organizations.

A tripilicate abstract card sheet is included in the report to facilitate information retrieval. Space is provided on the card for the user's accession number and for additional uniterms.

Inquiries pertaining to Water Pollution Control Research Reports should be directed to the Head, Project Reports System, Office of Research and Development, Environmental Protection Agency, Water Quality Office, Washington, D. C. 20242.

Evaluation of a New Acid Mine Drainage Treatment Process

by

Black, Sivalls & Bryson, Inc.
Applied Technology Division
135 Delta Drive
Pittsburgh, Pennsylvania 15238

for the

ENVIRONMENTAL PROTECTION AGENCY
WATER QUALITY OFFICE

Program No. 14010 DYI

Contract No. 14-12-529

February, 1971

For sale by the Superintendent of Documents, U.S. Government Printing Office, Washington, D.C. 20402 - Price $1.50
Stock Number 5501-0075

EPA Review Notice

This report has been reviewed by the Environmental Protection Agency and approved for publication. Approval does not signify that the contents necessarily reflect the views and policies of the Environmental Protection Agency, nor does mention of trade names or commercial products constitute endorsement or recommendation for use.

ABSTRACT

An economic and engineering evaluation of a submerged coal refuse combustion process to convert acid mine water (AMW) to potable water has been made. In this process coal refuse is burned in molten iron to supply energy for distillation or reverse osmosis, and the coal refuse sulfur is trapped in a slag for eventual recovery of sulfur. Laboratory experimentation was conducted on those areas which could profoundly affect the process. These areas were: A laboratory demonstration of slag desulfurization to produce sulfur, the evaluation of slag sulfur retention characteristics, slag capability for neutralizing AMW and determination of slag compositions having acceptable fluidities. Laboratory results indicated that sulfur is obtained, high slag sulfur partition ratios are achieved, fluid slags are produced, and that desulfurized slags are not suitable for neutralization.

Engineering studies show that the process has potential for supplying inexpensive energy for distillation and permits the recovery of sulfur so that distilled water is economically produced. Depending upon the AMW composition and sulfur selling price ($20 to $30/ton) the break-even price of water for a 5 MM GPD plant varies between $.42 and $.16/1,000 gals when a 14 percent capital interest charge is used.

This report was submitted in fulfillment of Program No. 14010 DYI, contract No. 14-12-529 under the sponsorship of the Environmental Protection Agency.

key words: Acid mine water, distillation, slag desulfurization, slag characterization, submerged coal combustion, two-stage coal combustion, coal refuse

CONTENTS

Page

Abstract. i
Conclusions xi
Recommendations xii
Introduction. 1

Process Description 3

Process Engineering 7
  Computer Simulation. 7
  Important Process Parameters 9
  Process Design 12

Economic Evaluation 19
  Determination of Equipment Costs 19
  Determination of Capital Investment Requirement. 26
  Determination of Break-even Price of Water 28
  Determination of Operating Revenue 29
  Break-even Price of Water and Process and Economic Factors . . . 29

Acknowledgements. 44

References. 45

Glossary. 47

Appendix A - Laboratory Studies 49
  Slag Fluidity. 49
    Introduction. 49
    Experimental Procedure - General. 49
    Standardization of Experimental Techniques. 50
    Calibration of the Herty Fluidity Equipment 55
    Discussion of Results - The Effect of Basicity on Fluidity. . 55
    Effect of Calcium Sulfide Content on Fluidity 55
    Significance of Fluidity and Apparent Viscosity Measurements. 60
    Effect of MgO Additions on Slag Fluidity. 61
    Effect of Fluorspar on Slag Fluidity. 63
    Effect of SiO_2/Al_2O_3 Ratio on Fluidity. 64
    Engineering Design Recommendations. 64

  Sulfur Retention by Slag 67
    Introduction. 67
    Experimental Procedure. 68
    Results and Discussion 69
    Engineering Design Specifications. 72

  Detailed Slag Characterization. 73

  Apparent Density of High Sulfur Bearing Slags 75
    Experimental Equipment and Procedure 75
    Discussion of Results. 75

CONTENTS CONT'D

Page

Viscosity Measurements. 77
  Introduction 77
  Experimental Procedure 77
  Discussion of Results. 79
  Engineering Design Recommendations 81

External Surface Area 83
  Introduction 83
  Theory 83
  Equipment and Experimental Procedure 83
  Discussion of Results. 84

Total Specific Surface Area 87
  Introduction 87
  Discussion of Results. 87

Crushing Energy Requirements. 89
  Introduction 89
  Experimental Equipment and Procedure 89
  Calibration of Crushing Energy Equipment 91
  Discussion of Results. 91
  Engineering Design Recommendations 94

Heat Capacity 95
  Introduction 95
  Experimental Equipment and Procedure 95
  Heat Capacity. 95
  Discussion of Results. 96
  Engineering Design Recommendations 96

Acid Mine Water Neutralization With Slag. 99
  Introduction 99
  Experimental 99
  Effectiveness of Slag Alkali for Neutralization. 101
  Continuous Neutralization Tests. 103
  AMW Neutralization 105
  Batch Neutralization Studies 107
  Engineering Design Recommendations 110

Kinetics of Sulfur Recovery from Slag 111
  Introduction 111
  Theory 111
  Experimental Procedure .116
  Discussion of Results. .119
  Engineering Reactor Design Recommendations 127

CONTENTS CONT'D

Page

Refractory Lining Life. 131
  Introduction 131
  Experimental Procedure 131
  Results. 135
  Design Recommendations 137

Appendix B - The Process Working Area Diagram 139

Appendix C - Equipment Cost 145

Appendix D - The Theory of Carbon Solubility Rates. 151
  Introduction 151
  Theory 151
  Discussion of Theoretical Calculations 153

FIGURES

Figure		Page
1	Flow Chart Acid Mine Water Treatment Process	5
2	Effect of Heat Rate on Process Operability	14
3	Effect of AMW Concentration on Process Operability	16
4	Coal Handling Complex	20
5	Neutralization Complex	21
6	Distillation and Waste Heat Boiler Complexes	23
7	Direct Fired Furnace, Steam Turbine-Air Compressor and Combustor Complexes	24
8	Desulfurization Complex	25
9	Rotary Kiln Dryer	27
10	Effect of Sulfur on Break-even Price of Water	34
11	Effect of Plant Capacity on Capital Investment	35
12	Effect of Plant Capacity on Break-even Price of Water	38
13	Process Flow Chart of AMW Treatment Plant	39
14	Effect of Water Selling Price on Payback	40
15	Fluidity Test Apparatus	51
16	Relation Between Fluidity and Residence Time of Sample in Furnace	53
17	Effect of Temperature on Viscosity of a Synthetic Slag	56
18	Effect of Temperature on Slag Fluidity	57
19	Relationship of Slag Fluidity and Slag Viscosity	58
20	Effect of Basicity on Apparent Viscosity of Sulfur-Free Slags	59
21	The Effect of CaS Addition on Apparent Viscosity	59

FIGURES CONT'D

Figure Page

22 The Effect of Magnesia Content on Apparent Slag Viscosity. 62

23 The Effect of Fluorspar on Apparent Slag Viscosity . . . 62

24 The Effect of Silica to Alumina Weight Ratio on Apparent Slag Viscosity. 65

25 The Effect of Time on the Approach to Partition Ration Equilibrium. 70

26 The Effect of Contact Time on the Sulfur Content of Iron. 70

27 The Effect of Slag Basicity on Equilibrium Partition Ratio. 71

28 The Effect of Particle Diameter on Apparent Density. . . 76

29 Viscosimeter 78

30 Effect of Carbon Bob Residence Time in Furnace on Measured Viscosity 80

31 The Effect of Slag Basicity and Particle Size on External Specific Surface. 85

32 The Effect of Basicity on Total Specific Surface Area. . 88

33 Crushing Energy Apparatus. 90

34 Calibration Curve for Aluminum Wire Used in Crushing Energy Test. 92

35 The Effect of Slag Basicity on Grinding Energy Requirements 93

36 The Effect of Basicity and Temperature on Specific Heat Capacity 97

37 Continuous Neutralization Apparatus. 100

38 Effect of Slag Particle Size and Basicity Ratio on Slag Alkali Utilization in Neutralization 102

39 Effect of Slag Particle Size and SiO_2/Al_2O_3 Ratio on the Slag Alkali Utilization Factor 102

FIGURES CONT'D

Figure Page

40 Effect of Operating Parameters on the Neutralization of Acid Mine Water with Sulfur Free Slag. 104

41 The Effect of Throughput on pH of Effluent Leaving Flow Neutralizing Reactor 106

42 Effect of Slag Particle Size on pH as a Function of Neutralization Time. 108

43 Variation of pH with Time as a Function of Slag Basicity. 109

44 Variation of Equilibrium Constant with Temperature. . .113

45 Equilibrium Data for the System, $CaS + xH_2O + yO_2 = CaO + aSO_2 + bH_2S + cS_2 + dS_8$ 114

46 Stainless-Steel Reactor Desulfurization Equipment . . .117

47 Ceramic-Tube Reactor Desulfurization Equipment. 118

48 Temperature Effect on Steam-Slag Reaction 120

49 Effect of Time on Desulfurization, Slag Basicity of 0.82. 122

50 Effect of Time on Desulfurization, Slag Basicity of 0.90. 123

51 Effect of Time on Desulfurization, Slag Basicity of 1.01. 124

52 Effect of Temperature on Specific Reaction Rate 126

53 Correlation Between Actual and Predicated Desulfurization Results. 128

54 The Effect of Slag Contact on Refractory Erosion. . . .136

55 Slag Basicity vs. Spent Slag Recycle Fraction of Various Flux Rates. 140

56 Required Preheated Air Temperature vs. Slag Recycle Fraction of Various Flux Rates. 141

57 Percent Sulfur in Combustor Slag vs. Slag Recycle Fraction at Various Flux Rates. 143

FIGURES CONT'D

Figure Page

58 Process Working Area Diagram for a 2 MM GPD Plant using Partially Neutralized Dilute AMW and a Heat Rate of 2 MM BTUs/1,000 Gals AMW. 144

59 Effect of Particle Radius on Residence Time Needed in Iron Melt to Dissolve Carbon 154

60 Effect of Particle Radius on Hot Metal Depth Required to Dissolve Carbon 155

TABLES

Table		Page
I	AMW Compositions Used in this Study.	12
II	Ultimate Analysis of Coal Refuse (% by Weight)	12
III	Equipment Complex Cost	28
IV	Determination of Break-even Price of Water	30
V	BEPW for Process Operation Under Various Conditions. .	31
VI	Capital Investment for Various Plant Sizes	36
VII	Stream Capacities and Temperatures for 5 MM GPD Plant.	41
VIII	Synthetic Slag Chemical Composition.	52
IX	The Effect of Remelting on Slag Fluidity	54
X	The Effect of Remelting on Slag Fluidity	54
XI	The Variation of Slag Apparent Viscosity with Basicity and CaS Content	60
XII	Slag Compositions Used in Partition Ratio Studies. . .	68
XIII	Slag Compositions Used in Characterization Studies . .	75
XIV	Comparison of Surface Areas for Glass Beads Determined by Air Permeability and Micrometer Methods	83
XV	A Comparison of Crushing Energy Requirements for Silica and Slags	94
XVI	Standard Acid Mine Water Composition	101
XVII	Refractories Used in Laboratory Tests.	133
XVIII	Slag Composition Used in Refractory Study.	134
XIX	Summary of Test Results.	134
XX	Computer Results Used to Generate Process Working Area Diagram	139
XXI	Coal Handling Complex Cost	146

TABLES CONT'D

Table Page

XXII Neutralization Complex Cost. 146

XXIII Direct Fired Heater Complex Cost 147

XXIV Combustor Complex Cost 148

XXV Distillation Complex Cost. 148

XXVI Desulfurization Complex Cost 149

XXVII Rotary Kiln Dryer Cost 149

CONCLUSIONS

This study has advanced the state of the art for using a two-stage coal refuse combustion process for the treatment of acid mine water. An engineering and laboratory study has shown that the process has the technical capability for converting acid mine water into a potable water product. An engineering and economic study of the process indicates that the process can produce distilled water profitably. Some additional work will be required before the process can be demonstrated on a large scale.

Specific conclusions derived from this study are:

1. By combusting coal refuse in a molten bath of iron, low cost energy is available to produce distilled water on a profitable basis. For a plant processing five million gallons per day of acid mine water, the break-even price of water will vary between 16 and 42 cents per thousand gallons depending upon the price of by-product elemental sulfur and the cost of coal refuse.

2. The distilled water will find utility as an industrial or municipal water supply.

3. Using coal refuse as a source of fuel for distillation will eliminate this source of acid mine water production.

4. Slag formed in the combustor is not suitable for neutralization of acid mine water. The process flow chart has been modified to accept limestone neutralization or to distill as-received acid mine water directly.

5. To maintain the slag and iron contained within the combustor in a molten condition, a combustion air preheater will be required. Preheat energy is derived from secondary combustion of the carbon monoxide rich offgas produced in the combustor.

6. Fluid slags exhibiting better than anticipated sulfur retention capacities (partition ratios) have been developed.

7. Slag desulfurization to produce elemental sulfur from combustor slag has been demonstrated. However, data are lacking with regard to optimum sulfur yield and quality.

8. Suitable commercial refractories have been found that can be used in the combustor for operation with high sulfur slags.

9. The process has a high degree of flexibility and can readily accommodate wide variations in acid mine water composition and flow rate.

RECOMMENDATIONS

Based on the results of this study, it is recommended that:

1. The kinetics of slag desulfurization be evaluated on a larger scale in the laboratory using both molten and solid slags to quantitatively determine sulfur yield and quality.
2. The reduction kinetics of calcium sulfate to calcium sulfide in molten slags which come in contact with molten iron containing carbon be evaluated in the laboratory using an induction furnace and synthetic slag.
3. Kinetic data be obtained in the laboratory for carbon solubility rate while pneumatically injecting coal refuse beneath the surface of a molten iron bath.
4. Lances be designed and tested in the laboratory for total immersion in molten iron using water and other liquid media as cooling agents.
5. An evaluation of the refractories selected in this work be made in the induction furnace employing calcium sulfate-bearing slags.
6. A new cost estimate be made for this process based on results of above recommendations.

INTRODUCTION

This report describes the study of a novel process for the elimination of acid mine water (AMW) drainage as a source of water pollution. This process utilizes coal refuse, a source of AMW, as fuel to generate steam for the conversion of AMW to potable water. Energy for steam generation to operate evaporators for distillation or to drive pumps for reverse osmosis, is derived from a two-stage coal refuse combustion process. In the first stage of combustion, high-sulfur coal refuse or similar low-cost fuel is dissolved in a molten iron bath. In the second stage of combustion the fuel carbon is burned with air at the surface of the iron bath, generating hot carbon monoxide which can be further burned to release additional heat in a boiler.

Two-stage combustion makes it possible to use high sulfur bearing fuels without polluting the air. Fuel sulfur is trapped in the iron from which it is removed via a lime-bearing slag in the form of calcium sulfide, without generating sulfur oxides. Sulfur is also recovered from the reduction of the sulfate content of the acid mine water. Sulfates contained in the sludge generated by distillation or reverse osmosis units are dried and added to the combustor as part of the slag. Sulfur is extracted from the calcium sulfide in the slag by treating the hot slag with steam and air to recover elemental sulfur.

The recovery of sulfur from the acid mine water and the fuel, coupled with the utilization of coal refuse as a fuel, provides the economic incentive for treatment of acid mine water using this process.

Earlier preliminary technical and economic evaluations of the concept described above showed that it warranted further study. As a first step towards such a study, the Federal Water Quality Administration funded a program for a limited bench scale study of process parameters that can be readily evaluated in the laboratory. The results of the experimental work were used to arrive at a more reliable technical and economic evaluation of the process.

This report presents the up-dated evaluation of the process, along with a discussion of the process engineering and cost estimating methods used in the evaluation. Laboratory work, on which the engineering was based, is presented as Appendix A of this report. To enable the reader to refer to any part of the laboratory work, each experimental study is presented as an autonomous section of Appendix A. In each section, objective of the work, experimental methods, results, and engineering design recommendations are presented.

PROCESS DESCRIPTION

Figure 1 presents a flow chart of the process. The dotted lines on the flow chart indicate that the acid mine water (AMW) may or may not be partially neutralized. Partial neutralization will be required for concentrated AMW to prevent excessive corrosion of the flash distillation equipment, but for moderately concentrated AMW the process economics are more attractive without neutralization. If neutralization is required, AMW is introduced into a neutralizer (1) where it is contacted with finely divided limestone to partially neutralize the AMW to a pH of three or more. The limestone used for partial neutralization reduces the amount of flux introduced into the dryer (4) for use in combustor (5). The neutralized water which contains suspended solids is pumped to a flash distillation unit (7) to produce potable water and a concentrated brine slurry which is subsequently fed to a rotary kiln dryer (4). If acid mine water is not neutralized, it is fed directly into the distillation unit.

The rotary kiln dryer serves three functions: 1) to dry the concentrated brine slurry from the distillation unit, 2) to calcine dolomitic limestone to produce lime and magnesia for use as flux in the combustor, and 3) to preheat the portion of the desulfurized spent slag from the desulfurization unit. The contents of the dryer are fed to the combustor (5) to minimize the quantity of dolomitic limestone required in the process.

The combustor is a refractory-lined steel vessel that contains molten iron. Coal or coal refuse is pneumatically injected beneath the surface of the iron bath where the carbon is dissolved to free its sulfur for ultimate reaction with the flux floating on the molten iron surface. Air is then injected slightly below the surface of the bath and reacts with carbon to produce a carbon monoxide rich offgas. Heat generated during the combustion of the coal provides the necessary heat of reaction to reduce calcium sulfate contained in the dryer solids to calcium sulfide. In addition, the combustor provides the energy required to produce iron from iron compounds contained in the dryer solids and pyrites contained in the coal. Molten elemental iron is continuously removed from the combustor. Slag containing calcium oxide. magnesium oxide, ash and calcium sulfide is continuously removed from the combustor and sent to the slag desulfurization unit (8) where it is contacted with steam and air to produce a sulfur-rich gas. Elemental sulfur is condensed out of this gas and sent to storage.

Desulfurized spent slag exiting the desulfurization unit is divided into two streams which proceed to the dryer, and to a spent slag storage pile. Spent slag consists of a dry mixture of silica, alumina, magnesium hydroxide and calcium hydroxide.

Carbon monoxide rich offgas generated in the combustor is used to supply energy for operation of auxiliary equipment. A large fraction of the combustor offgas is sent to the waste heat boiler (10) which provides high pressure steam for the steam turbine-air compressors (15) and the exiting low pressure steam for the flash distillation unit. Steam generated in the waste heat boiler undergoes a pressure reduction through the steam-turbine air compressors before entering the distillation unit. In the discussion which follows, steam from the waste heat boiler is assumed to enter the distillation unit directly. Steam turbine air compressors are used to generate pressurized air for combustion and coal pneumatic conveying. Combustor offgas is also used to provide the energy requirements for air preheating (13), for drying and calcining the dryer contents, and drying the incoming coal (14).

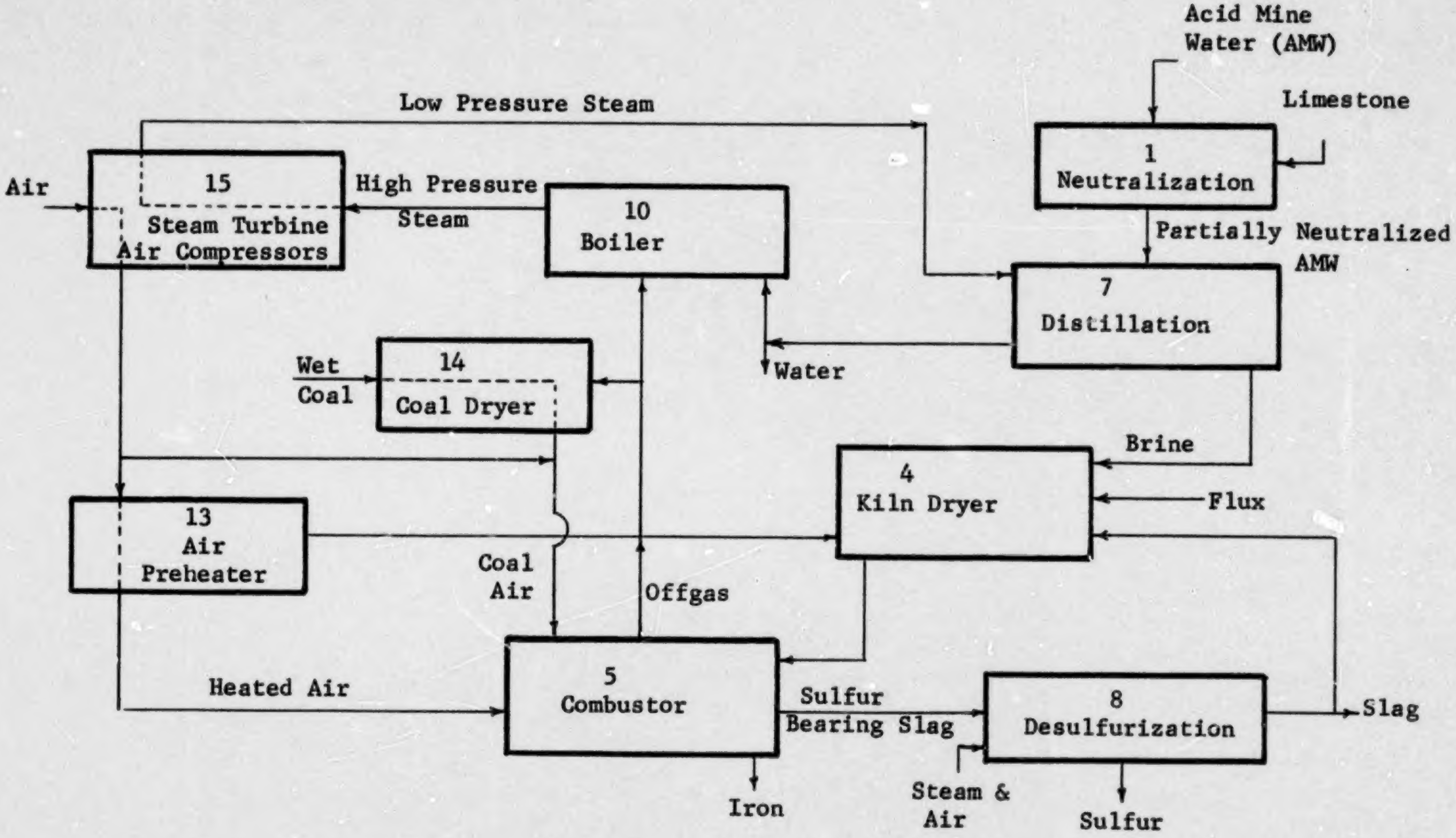

FIGURE 1 - FLOW CHART ACID MINE WATER TREATMENT PROCESS

PROCESS ENGINEERING

Computer Simulation

To simulate the AMW Treatment Process, a computer program of the energy and material balance equations for the process was prepared. The digital computer simulation permits all process parameters to be varied and yields quantities and temperatures of all process streams as output. A brief description of the unit operations involved in the process and the assumptions in their operation is now presented.

An important consideration in operation of the process is the composition and concentration of the AMW. In this study it is assumed that the AMW composition and concentration does not change with time. In reality the acid mine water composition will vary with time. Therefore, values used in the process simulation should be considered as yearly averages.

Partial neutralization of AMW is accomplished by using finely divided limestone. Quantity of limestone required for neutralization depends upon concentration of AMW and effectiveness of limestone in neutralization. In the process it was assumed that the limestone is 80 percent efficient in utilizing its lime content to produce a pH of about three in the partially neutralized water. The partially neutralized water containing suspended solids proceeds to the distillation unit.

As previously stated, if the AMW is moderately acidic it can be used directly in the flash distillation unit. By doing this, the partial neutralization unit operation is eliminated and the AMW proceeds to the distillation unit. Distillation is accomplished by using conventional flash distillation equipment in which the steam requirement for the evaporation of acid mine water is supplied by a waste heat boiler. Combustor offgas serves as the energy source to generate steam in the waste heat boiler. The waste heat boiler is a standard item of equipment in which the carbon monoxide rich offgas from the combustor is reacted with air to produce carbon dioxide. The heat of combustion of carbon monoxide to carbon dioxide and the sensible heat of the incoming combustor offgas supply the energy to convert water to steam for use in the flash distillation evaporators. The combustor offgas entering the boiler is assumed to undergo a ten percent loss in temperature in transit from the combustor. The waste heat boiler is assumed to operate at an efficiency of 90 percent with a flue gas leaving at 280°F. The temperature of the combustor offgas entering the waste heat boiler (and all other auxiliary equipment) will depend upon the combustor operating temperature. In this simulation, the combustor is assumed to operate at 2700°F.

The combustor offgas is used to supply energy for the rotary kiln dryer, combustion air preheater and coal dryer in addition to the waste heat boiler. In the simulated process, the combustor offgas requirements for all auxiliary equipment except the waste heat boiler are determined first. The remaining combustor offgas is then used in the waste heat boiler. The reason for this is that the energy requirements for the auxiliary functions are fixed by the quantities of the process streams, however, some latitude is possible in the design of a flash distillation unit to use more or less steam. In a flash distillation plant, the heat transfer surface area required to evaporate water is related to the economy factor (defined as the pounds of water distilled per pound of steam used). Consequently, within specified design limits, the heat transfer area of the distillation plant can be made to accommodate available steam. To minimize capital cost by minimizing required evaporator heat transfer area, all of the remaining combustor offgas (after all auxiliary functions have been satisfied) is used in the boiler to generate steam.

Potable water and a concentrated brine slurry at 180°F are produced in the distillation unit. Concentrated (60 percent water by weight) brine slurry, containing all of the acid mine water constituents entering the distillation unit, proceeds to a rotary kiln dryer where it is dewatered. The rotary kiln dryer is also used to calcine the dolomitic limestone. Calcination converts the dolomite to lime and magnesia which are required as fluxing agents in the combustor. In this study, dolomitic limestone was used as the flux. However, a calcitic limestone or a combination of calcitic and dolomitic limestones could have been employed to obtain any desired ratio of lime to magnesia in the combustor slag. The dolomitic limestone was assumed to contain 60 percent calcium carbonate and 40 percent magnesium carbonate by weight. Also added to the dryer is a recycle stream of desulfurized spent slag. The stream enters the dryer to be heated to 2200°F for use in the combustor, because reuse of the lime content of the spent (desulfurized) slag decreases the combustor flux costs. In essence, then, combustor offgas is fired directly in the rotary kiln to supply hot gases for heat of vaporization to dry the concentrated brine slurry, the heat of reaction for calcination, and the sensible heat necessary to raise the solids to a temperature of 2200°F.

The dry solids from the rotary kiln dryer are fed to the combustor, which is assumed to operate at 2700°F and the air preheat temperature is adjusted to maintain this temperature. In the combustor, coal refuse is pneumatically injected beneath the molten iron bath where its sulfur and carbon are dissolved in the molten iron. The volatile matter of the coal is cracked to carbon monoxide and hydrogen. Air is also added to the combustor slightly below the molten iron surface to combust the carbon. Combustion of coal serves to supply the necessary heat required to reduce the calcium sulfate contained in the kiln dryer solids to calcium sulfide in the slag layer floating on the molten iron. The ash content of the coal is also transferred to the slag layer. Sulfur present in the coal dissolves in the molten iron and reacts with the lime contained in the slag to produce calcium sulfide. Iron contained in the coal as pyrities is reduced to elemental iron. In combustor operation iron (containing one percent sulfur) and slag rich in calcium sulfide are continuously removed from the unit. Even though laboratory data show that the iron will contain less than 0.3 percent S, iron sulfur content was conservatively established at one percent. A complete energy balance encompassing all reactions occurring in the combustor at a temperature of 2700°F, with kiln solids added at 2200°F and coal pneumatically injected at ambient temperature is used to determine the air preheat temperature necessary to maintain the required temperature in the combustor. Carbon monoxide rich combustor offgas is continually removed from the combustor and, as previously stated, serves as the energy source for the auxiliary equipment.

An important variable in the operation of the combustor is the basicity of the slag. Basicity (defined as the weight percent ratio, $CaO + MgO/Al_2O_3 + SiO_2$) is related to the operational characteristics of the slag. It has been found experimentally that basicity should be in the range of 0.8 to 1.2 to produce a sufficiently fluid slag which can be easily handled. Of equal importance in producing suitable slags for the combustor operation is the sulfur content of the slag. There is a maximum sulfur content in slag above which the sulfur causes the fluidity of the slag to decrease to inoperable levels. Laboratory experimentation has indicated that a maximum of ten weight percent sulfur in the slag is usable.

Combustor offgas, which is rich in carbon monoxide, is combusted to carbon dioxide in a direct-fired heat exchanger to preheat the air entering the combustor. Air heater heat transfer surface and materials of construction are adjusted according to the air preheat temperature requirements. The resulting flue gas, which is assumed to exit at a temperature of 500°F, is used together with additional combustor offgas in a coal dryer. In the coal dryer, coal surface moisture is removed to facilitate pneumatic injection into the combustor. Wet coal enters the coal dryer at ambient temperature and flue gases leave at 280°F.

Calcium sulfide bearing slag from the combustor is sent to the desulfurization unit where it is contacted with steam and air at 2000°F to produce a sulfur rich gas. The sulfur is condensed and sent to storage. It is anticipated that slag from the combustor will undergo a heat loss and enter the desulfurization reactor at approximately 2300°F where it will be contacted with steam and air which will result in the following overall net reaction at 2000°F.

$$CaS + \tfrac{1}{2}O_2 \text{ (air)} \overset{H_2O}{=} CaO + S$$

Desulfurized slag leaving the desulfurization unit contains lime, magnesia, silica, and alumina. A portion of the desulfurized slag is recirculated to the dryer to utilize its valuable lime content as a fluxing agent in the combustor. The remaining slag is sent to storage for sale.

Important Process Parameters

The important process parameters and alternatives are AMW composition, coal composition (in particular its sulfur content), coal rate into the combustor, quantity of dolomitic limestone added to the process, basicity and sulfur content of combustor slag, economy factor of the distillation unit, and air preheat temperature required to maintain the combustor at 2700°F. Design and economic significance of these parameters will now be discussed.

The decision to partially neutralize the AMW depends upon its composition. The AMW compositions used in this study do not require neutralization. However, very acidic acid mine water will require partial neutralization to prevent excessive corrosion of expensive distillation plant materials of construction.

The AMW composition has a direct effect upon the basicity and sulfur content of the combustor slag and governs quantity of flux which must be used in the process and amount of spent slag recycled to the dryer to maintain the requisite slag basicity.

The higher the sulfate content, the more energy is required to convert calcium sulfate to calcium sulfide in the combustor. Consequently, additional coal must be used to supply additional energy requirements for the sulfate to sulfide reaction, increased quantity of solids requiring drying in the rotary kiln dryer, and increased energy requirements for air preheating and coal handling. Thus the AMW composition has an equally profound effect on process design and process economics which will be shown later.

The coal refuse composition and heating value is an equally important process variable. The heating value of the coal refuse determines the quantity of coal required in the combustor to satisfy the energy requirements of the entire process. The sulfur content of the coal refuse has a profound effect upon the composition of the combustor slag. Laboratory studies indicate the sulfur content of a usable fluid slag to be ten percent or less by weight, therefore, more flux and recycled spent slag will be required to maintain a sulfur content in the slag below ten percent. In addition, the sulfur content of the coal refuse has a profound effect upon the economics of the process because of by-product credits, and will be discussed later. Coal refuse also contains the ash constituents alumina and silica. The quantity of flux required to maintain the basicity of the combustor slag in the range of 0.8 to 1.2, depends in part on the quantity of the ash constituents in the coal refuse.

The quantity of coal refuse added to the combustor is directly related to the quantity of combustor offgas produced. In the discussion which follows, coal consumption will be measured by heat rate, which is defined as millions of BTU's (coal refuse) consumed per thousand gallons of AMW processed.

The combustor offgas is used to supply the energy requirements of the rotary kiln dryer, the air preheater, the coal dryer, and the waste heat boiler. As previously stated, the flash distillation unit can be designed to accommodate various economy factors (defined as the pounds of water distilled per pound of steam used). For conventional flash distillation installations the economy factor varies between a ratio of five to ten. Consequently, as long as there is sufficient combustor offgas available to the waste heat boiler to generate an economy factor of ten, the process is operable. This also means that the process is operable over a range of heat rates provided the economy factor is adjusted accordingly. Operation at a lower economy factor requires less heat transfer surface with a correspondingly lower capital investment cost. This can be economically attractive, provided the added operating costs associated with using larger quantities of coal do not offset the benefits of the lower capital investment.

As a process design consideration, the heat rate establishes the economy factor in the distillation unit, the air preheat temperature required to maintain the combustor at 2700°F (as more coal is combusted per gallon of AMW, a lower air temperature is required), and the heat requirements for coal drying which are directly related to the quantity of coal used in the combustor. Increasing the heat rate adds more ash to the combustor slag and increases the flux requirement to maintain an operable slag basicity in the combustor.

Basicity of the combustor slag is affected by AMW composition, the quantity and composition of the coal refuse and the quantity of flux added to the combustor. Because fluid slags are obtained when the slag basicity is in the range of 0.8 to 1.2 and contains less than ten percent sulfur, the process is considered operable when the various selected process parameters yield a combustor slag that meets these criteria.

The desulfurized slag recycled to the rotary kiln dryer for eventual use as a flux in the combustor is a variable which is inter-related with all other parameters. The primary purpose of recycling spent slag is to minimize the quantity of limestone required in the process. Desulfurized slag is normally sent to storage for sale, however, a fraction of this slag is directed to the rotary kiln dryer and is called the slag recycle fraction. The slag recycle fraction affects the size of the kiln and the composition of the combustor slag. The flux rate or the quantity of dolomitic limestone added to the process affects the kiln operation and the composition of the combustor slag. The dolomitic limestone entering the kiln is calcined to provide lime and magnesia for the combustor operation. Its primary purpose is to flux the ash constituent of the coal and to provide a source of calcium to react with sulfur to form calcium sulfide. The quantity of flux required is determined by combustor slag basicity and is inter-related with the slag recycle fraction. Increased flux requirements of the process increase the energy requirements of the kiln to perform the calcination reaction. Higher energy requirements for the kiln demand that more combustor offgas be produced which results in a higher heat rate for the process.

In summary, the important process parameters are the acid mine water composition, composition of the coal refuse, heat rate, desulfurized slag recycle fraction, flux rate, slag basicity and percent sulfur in the slag. Quantitative effects of these variables on process design and economics will be discussed in the following sections.

Process Design

The interrelationship and the operable ranges of the important process variables and their effect on process design will be discussed in this section. In this study, two concentrations of acid mine water are considered. The process design and economic analysis were based on dilute and moderately concentrated AMW of the compositions shown in Table I.

TABLE I
AMW Compositions Used in this Study

	Dilute ppm	Moderately Concentrated, ppm
Acidity (as ppm $CaCO_3$)	400	1200
Sulfate	1061	3183
Total Iron	200	600
Calcium (as Ca)	80	240
Aluminum (as Al)	5	15
Magnesium (as Mg)	24	72

The dilute acid mine water composition was suggested by the Environmental Protection Agency as an average composition of all AMW generated. Moderately concentrated acid mine water was selected to show the effect of acid mine water concentration on process design and economics. A coal refuse with a heating value of 6,000 BTUs per pound and the composition shown in Table II was selected as representative of a high-sulfur coal refuse.

TABLE II
Ultimate Analysis of Coal Refuse
(% by weight)

Carbon	40.6
Hydrogen	2.9
Oxygen	3.7
Nitrogen	.7
Sulfur	10.0
Moisture	3.0
Ash	39.3

Sulfur content of this coal refuse, in the form of organic sulfur and pyrites, is ten percent by weight. Once the compositions of the AMW and coal refuse are established, the remaining variables to be studied are the heat rate, spent slag recycle fraction, air preheat temperature, flux rate, slag basicity, and slag sulfur content. In regard to neutralization alternative, this study will evaluate the effects of utilizing partially neutralized and unneutralized AMW.

The energy and material balance computer program was used to generate quantities and temperatures of all process streams as functions of above variables. The operable range of the process is subject to the following constraints: 0.8 to 1.2 basicity, ten percent or less slag sulfur content, and 2000°F maximum air preheat temperatures based on the cost of materials of construction. These constraints are best illustrated using a Process Working Area Diagram (PWAD). The PWAD is a plot of slag basicity vs. the slag recycle fraction at various flux rates into the kiln. A particular PWAD pertains to one selected heat rate, acid mine water composition, and coal refuse composition. Located on this diagram are the constraints of basicity, sulfur content in the slag, and air preheat temperature.

The PWAD is generated by running the energy and material balance computer program over a wide range of process parameters. For a selected heat rate, AMW concentration, and coal refuse composition, the slag basicity is generated as a function of the slag recycle fraction and the flux rate into the combustor. These data are plotted as the slag basicity vs. slag recycle fraction at various flux rates. A plot is then made of the sulfur content in the slag as a function of slag recycle fraction at various flux rates. A line is drawn through this plot at the ten percent sulfur content level to pick out coordinates of the flux rate and the slag recycle fraction which yield a ten percent sulfur content in the slag. These points of ten percent sulfur content are then plotted on the PWAD to show the constraint of sulfur composition in the slag. In the same manner, slag recycle fraction--flux rate coordinates which yield a 2000°F air preheat temperature are determined and plotted on the PWAD. Two additional constraints are shown on the process working area diagram which are a minimum 0.8 and a maximum 1.2 slag basicity. In this manner the process working area (PWA) is established for which any point within the PWA yields an operable process. The technique used to generate a typical process working area diagram is explained in detail in Appendix B.

The PWAD's shown in Figures 2 and 3 were prepared to illustrate the effect of heat rate and AMW composition on the PWA for a two million gallon/day plant, using as fuel a coal refuse having a heating value of 6,000 BTU/lb and a sulfur content of ten percent. Figure 2 pertains to treatment of neutralized AMW, initially of the dilute composition shown in Table I. Figure 2a is based on a heat rate of two million BTU/1,000 gallons of AMW, while Figure 2b is based on a heat of 3.25 million BTU/1,000 gallons of AMW. The PWAD's are constrained at the top and bottom by 1.2 and 0.8 basicity limits respectively, on the left by the maximum ten percent sulfur in the slag and on the right by the maximum air preheat temperature of 2000°F. Any point selected within this area will yield an operable process. For example, in Figure 2a, if the point of intersection of the minimum basicity and maximum sulfur content is selected, the process operating parameters would be a flux rate of 230 tons per day and a slag recycle fraction of 0.26, (fraction of desulfurized slag that is reused in combustor). The same intersection in Figure 2b corresponds to a flux rate of 400 tons per day at a slag recycle fraction of 0.22. At the higher heat rate more flux is required because more coal is used. This results in more ash in the slag which must be offset by additional flux to obtain a basicity of 0.8. Also, more sulfur from the coal enters the process, therefore, more flux is required to dilute the sulfur in the slag to a level of ten percent.

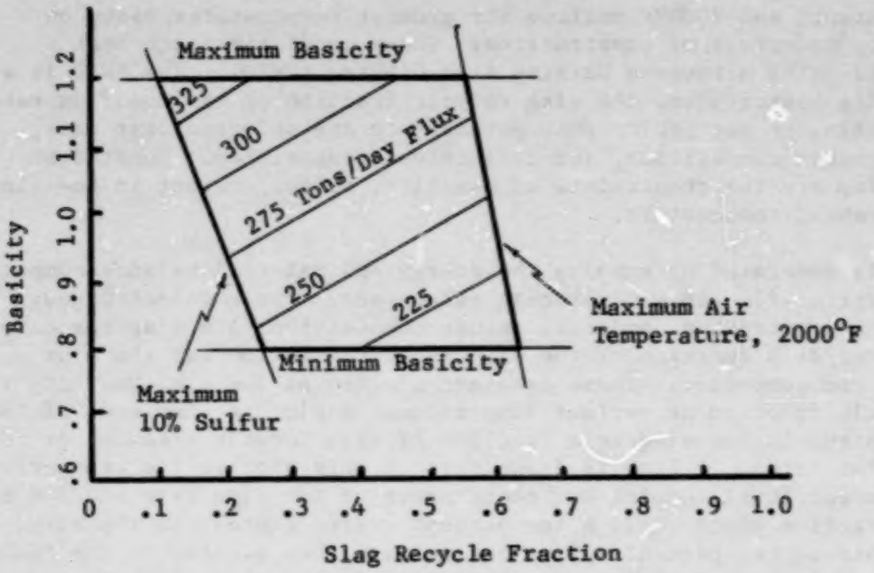

Figure 2 - a Conditions: Heat Rate 2 MM BTU/1,000 gal.
Partially Neutralized Dilute AMW

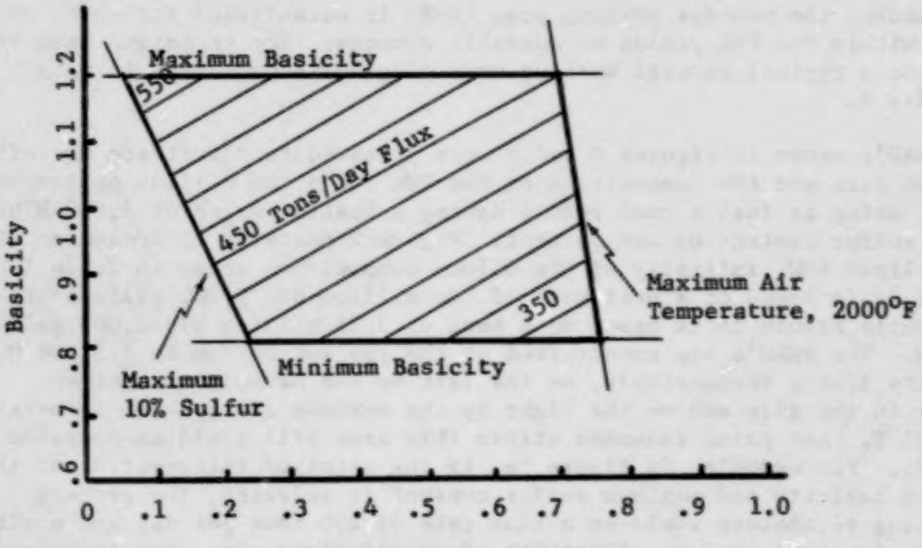

Figure 2 - b Conditions: Heat Rate 3.25 MM BTU/1,000 gal
Partially Neutralized Dilute AMW

FIGURE 2 - EFFECT OF HEAT RATE ON PROCESS OPERABILITY

Figures 2a and 2b which differ only in the heat rate represented, show that the PWA is larger at the higher heat rate. Since more coal energy is used at the higher heat rate, the required air preheat temperature is lower at a given slag recycle fraction. Consequently, the maximum air preheat temperature of 2000°F occurs at higher values of the slag recycle fraction.

Figure 3 is similar to Figure 2, except that it pertains to treatment of unneutralized AMW, of both the dilute and concentrated compositions shown in Table I. Figures 2b and 3a will be used to illustrate the effect of partial neutralization on the PWA. These figures were generated using a heat rate of 3.25 and a dilute acid mine water concentration. There is no significant difference in the PWA when partially neutralized or unneutralized acid mine water is used. This results from the fact that the limestone used to partially neutralized the AMW is eventually deposited and recovered in the combustor. Some small changes do exist because of redistribution of the heat requirements in the various unit operations but they are of no practical consequence.

To compare the effect of acid mine water concentration on the PWA, Figure 3b was prepared using a heat rate of 3.25 and the moderately concentrated acid mine water. Comparison of Figures 3b and 3a showed that the PWA is considerably smaller when a more concentrated acid mine water is used. This reduction in the PWA is due to the maximum air preheat temperature occurring at lower values of the slag recycle fraction. This is expected since the higher concentration acid mine water requires more energy in the combustor to convert the sulfates to sulfides. If the coal rate is held constant, then this additional energy must come from using higher air preheat temperatures. Consequently, under the same conditions of flux rate and slag recycle fraction the required air preheat temperature will be higher for a more concentrated acid mine water and the maximum air preheat constraint line will occur at lower values of the spent slag recycle fraction. Using the minimum basicity-maximum sulfur content point for comparison it is seen that for the moderately concentrated acid mine water, 410 tons per day of flux is required at a slag recycle fraction of 0.3 Both the dilute and moderately concentrated acid mine water process operations, require about the same quantity of flux. This is due to the effect of recycling more slag to the combustor for the more concentrated acid mine water (0.3 as compared to 0.2). The reason for recycling spent slag is to reduce the quantity of limestone required by the process.

In some situations it is possible that the maximum air preheat temperature constraint line will occur to the left of the maximum sulfur content line. This means that at the chosen heat rate the process is inoperable--there is insufficient energy to run the process. Making the process operable will require a higher heat rate. Similarly there may be situations where the maximum sulfur content constraint line will not appear on the PWA. For example, if a low sulfur coal refuse and an extremely dilute acid mine water were used, the slag composition within the basicity range of 0.8 to 1.2 will not yield a slag of more than ten

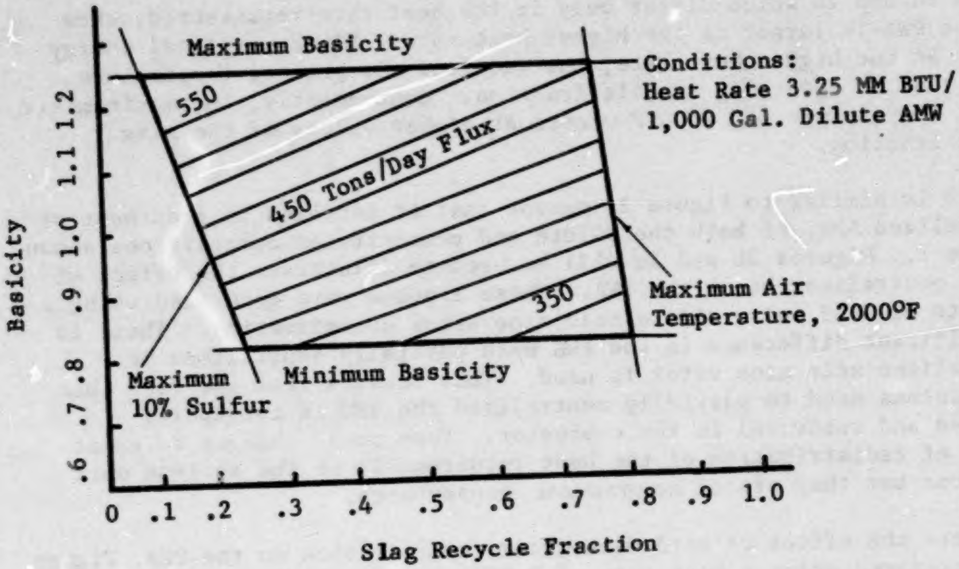

Figure 3 - a

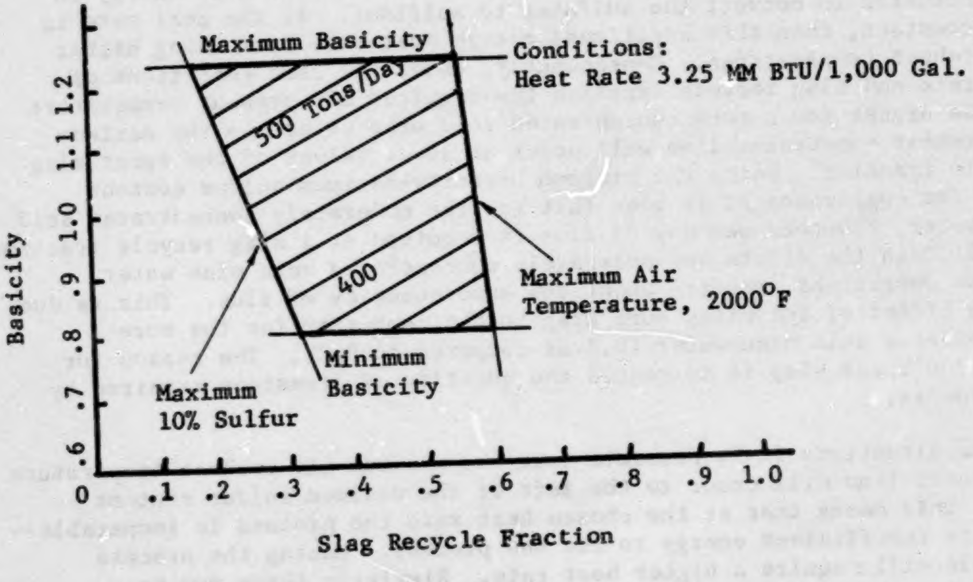

Figure 3 - b

FIGURE 3 - EFFECT OF AMW CONCENTRATION ON PROCESS OPERABILITY

percent sulfur. Under these conditions the heat rate should be decreased to yield a ten percent sulfur bearing slag provided there is sufficient energy to perform the distillation without using an economy factor higher than ten. Using economy factors higher than ten would result in excessive distillation capital investment costs.

It is of interest to note that the combustor can accommodate a wide range of variations in AMW concentrations and is evidenced by the rather broad PWA's shown on Figures 3a and 3b. Reasonably wide variations in AMW concentration can be accommodated rather easily by simply varying flux and/or slag recycle rates. These simple expedients provide substantial versatility to the process.

In summary, the interrelationship of heat rate, neutralization, slag recycle fraction, and acid mine water concentration on the process working area has been shown. Having established a means of determining operable ranges of the various process parameters, attention is now directed to determining the economic optimum point within the process working area.

ECONOMIC EVALUATION

Having established a technique (PWAD) to determine the operable ranges of the process parameters, the next logical step is to determine the point of operation within the process working area which maximizes profit. The profit or loss for the process will be a function of the process design parameters discussed previously, and process economic considerations such as plant capacity, capital investment requirements, raw material costs, product selling prices, capital interest charge, plant maintenance and labor requirements.

Determination of Equipment Costs

For convenience in determining the capital investment, the principal items of equipment have been grouped into nine complexes:

(1) Coal handling-for drying and pneumatic conveying of coal into the combustor.

(2) Neutralization of AMW.

(3) Steam turbine driven air compressors-to convey the coal and to supply compressed combustion air into the combustor.

(4) Direct fired heater-to preheat the air for the combustor.

(5) Waste heat boiler-to generate steam from combustor offgas for use in the distillation and steam turbine complex.

(6) Rotary kiln dryer-to calcine flux and dry the concentrated brine slurry from distillation.

(7) Combustor.

(8) Desulfurization-to recover sulfur from combustor slag.

(9) Distillation.

Figure 4 shows the major pieces of equipment comprising the Coal Handling Complex. Wet coal is pneumatically conveyed from a storage pile to a rotary dryer. Combustor offgas and offgas from the direct fired furnace serve as the energy source for drying. Dried coal is crushed in a hammermill and sent to a temporary storage tank. Coal from the storage tank is fed to a pneumatic feeder tank where air from the steam turbine-air compressors is used to transport the crushed coal into the combustor.

The Neutralization Complex is shown in Figure 5. A stainless steel pump is used to pump the acid mine water from its source to a neutralization tank. Limestone from a storage pile is pneumatically conveyed into the neutralization tank, which is a closed vessel containing agitators. Partially neutralized acid mine water plus suspended solids are pumped to the Distillation Complex.

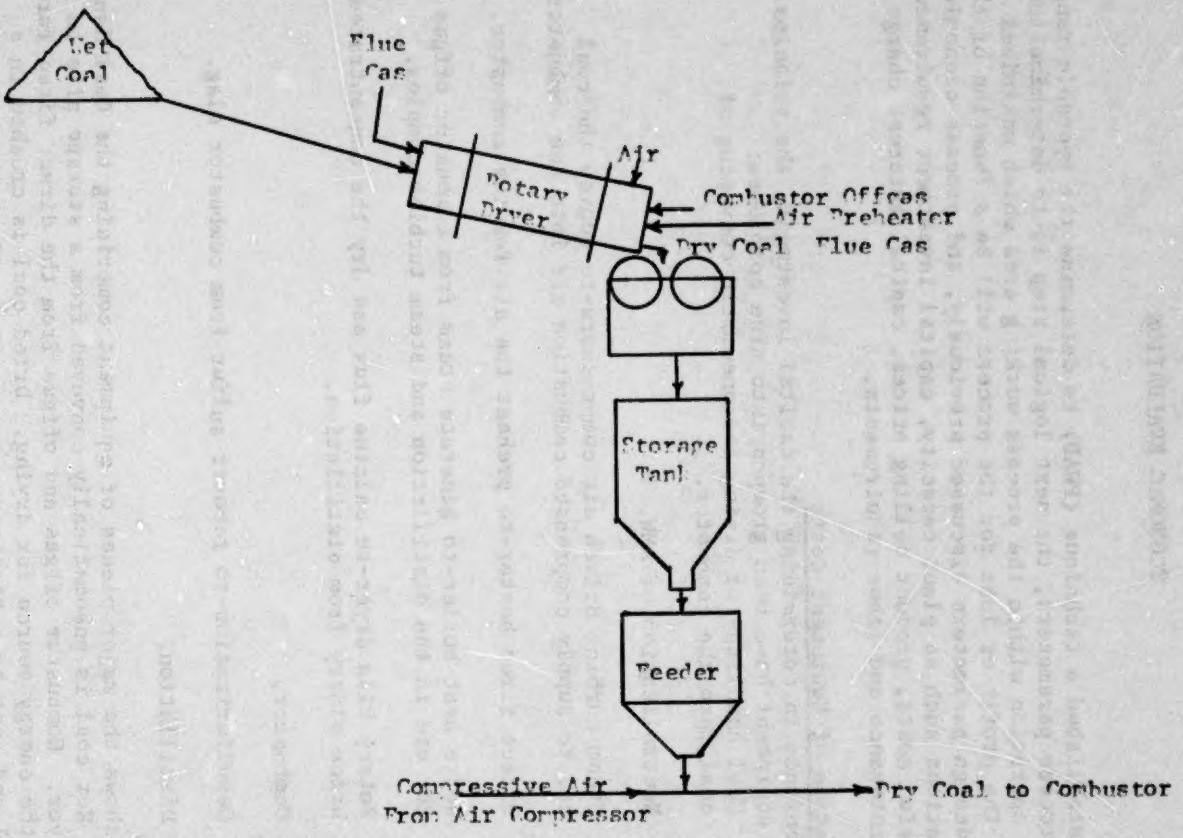

FIGURE 4 - COAL HANDLING COMPLEX

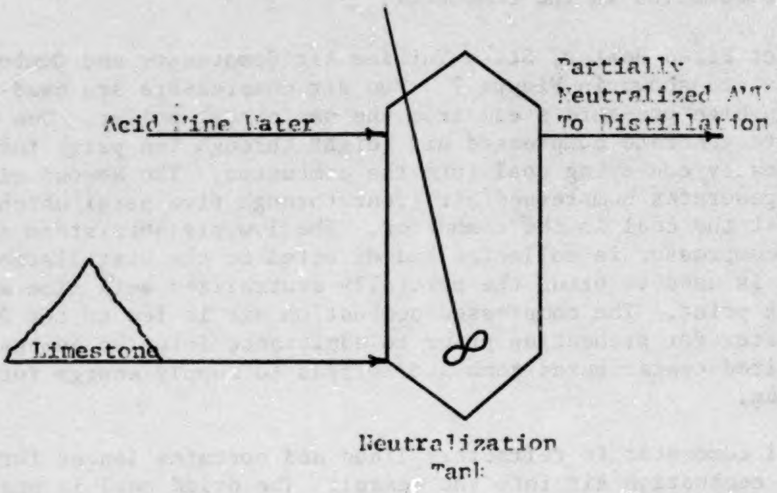

FIGURE 5 - NEUTRALIZATION CONTROL

Figure 6 shows the Distillation and Waste Heat Boiler Complexes. The Distillation Complex is a standard flash distillation scheme. Using a heat exchanger, the partially neutralized acid mine water is preheated with product steam from an evaporator and then proceeds through a series of evaporators where it is further heated by the steam produced in each evaporator. The preheated acid mine water then enters a heat exchanger where it is brought to its "flash" point. Low pressure steam exiting from the steam turbine-air compressors is flashed in the evaporators to produce steam. Concentrated brine slurry exiting the last evaporator is fed to the rotary kiln dryer. The steam product from the last evaporator is condensed as product water in the heat exchanger used to preheat the neutralized acid mine water. The water and uncondensed steam leaving the heat exchanger which brings the neutralized acid mine water to the flash point is recycled to the waste heat boiler. The waste heat boiler burns combustor offgas to generate high pressure steam from the condensed steam exiting the Distillation Complex. The high pressure steam is then used in the steam turbine air compressors to generate compressed air for pneumatically conveying coal into the combustor and air combustion in the combustor.

The Direct Fired Heater, Steam Turbine Air Compressor and Combustor Complexes are shown in Figure 7. Two air compressors are used--each requiring high pressure steam from the waste heat boiler. One compressor is used to generate compressed air (eight through ten psig) for pneumatically conveying coal into the combustor. The second air compressor generates compressed air (four through five psig) which is used to combust the coal in the combustor. The low pressure steam exiting at each compressor is collected and directed to the Distillation Complex where it is used to bring the partially neutralized acid mine water to the flash point. The compressed combustion air is fed to the direct fired heater for preheating prior to admittance into the combustor. The direct fired heater burns combustor offgas to supply energy for preheating.

The steel combustor is refractory lined and contains lances for admitting coal and combustion air into the vessel. The dried coal is pneumatically conveyed from the coal handling complex and the preheated combustion air is produced in the direct-fired heater. Dry solids from the rotary kiln dryer are metered and fed into the combustor using a gas tight star valve. The combustor offgas produced in the combustion of coal is collected and sent to various other equipment complexes. Slag is continually removed from the combustor and proceeds to the desulfurization complex. Iron is also continually removed from the combustor, granulated, and sent to storage.

One possible desulfurization scheme is shown in Figure 8. The slag exits the combustor via an enclosed conveyor and is immediately granulated by a water spray, and is brought to a crusher. The crushed slag is then fed to a refractory lined steel reaction vessel where it is contacted with water and air to produce a sulfur rich offgas. The sulfur rich offgas is

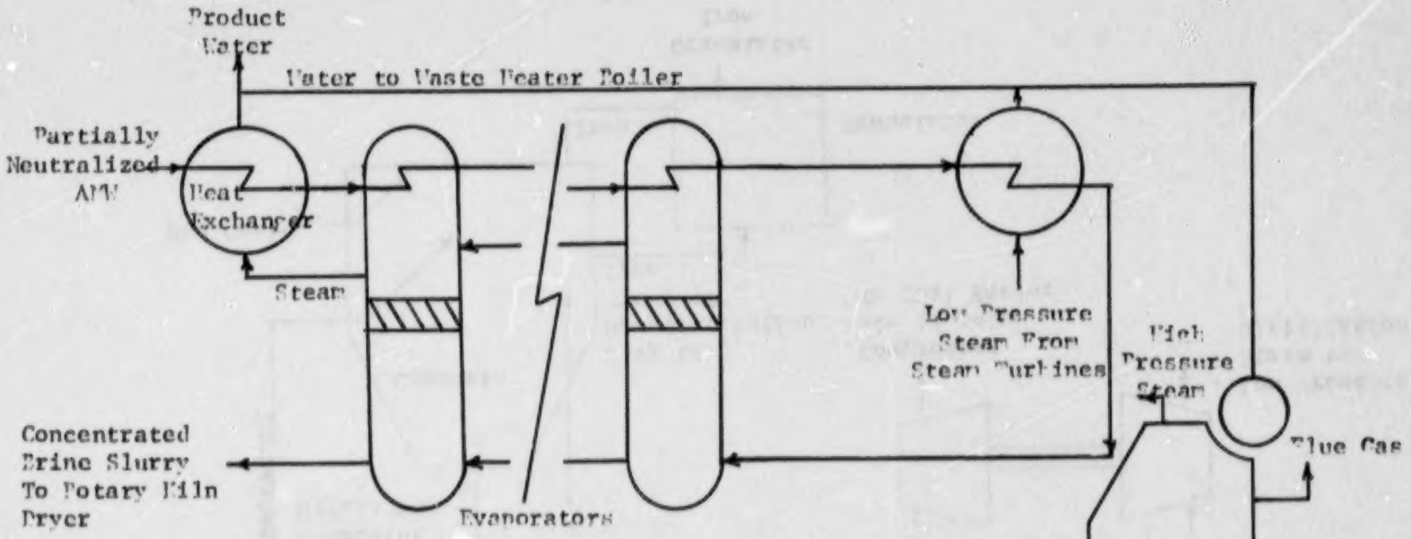

FIGURE 6 - DISTILLATION AND WASTE HEAT BOILER COMPLEXES

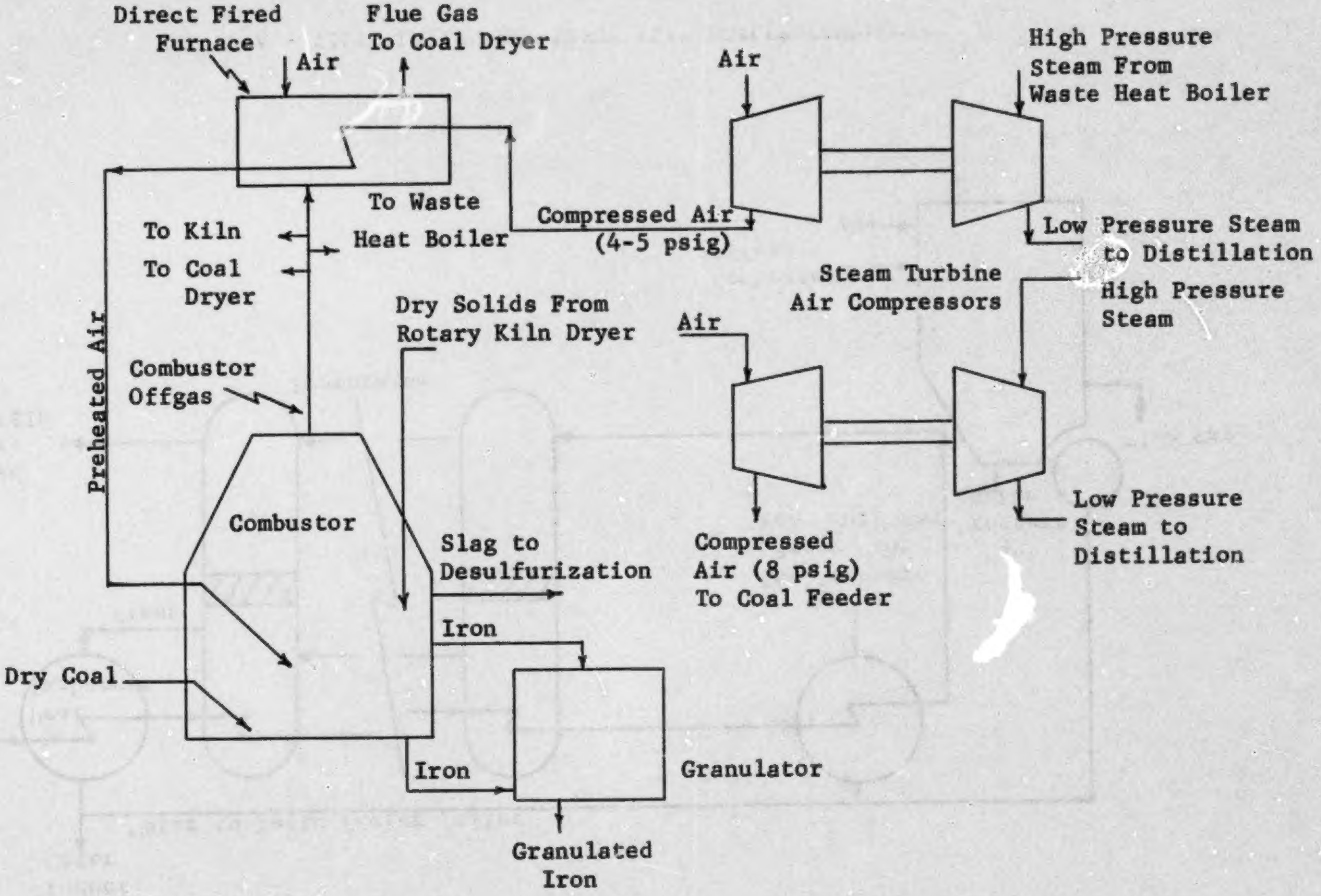
Direct Fired Furnace
Air
Flue Gas To Coal Dryer
To Waste Heat Boiler
To Kiln
To Coal Dryer
Preheated Air
Combustor Offgas
Combustor
Dry Solids From Rotary Kiln Dryer
Slag to Desulfurization
Iron
Iron
Dry Coal
Granulator
Granulated Iron
Compressed Air (4-5 psig)
Air
High Pressure Steam From Waste Heat Boiler
Low Pressure Steam to Distillation
Steam Turbine Air Compressors
High Pressure Steam
Air
Compressed Air (8 psig) To Coal Feeder
Low Pressure Steam to Distillation

FIGURE 7 - DIRECT FIRED FURNACE, STEAM TURBINE-AIR COMPRESSOR AND COMBUSTOR COMPLEXES

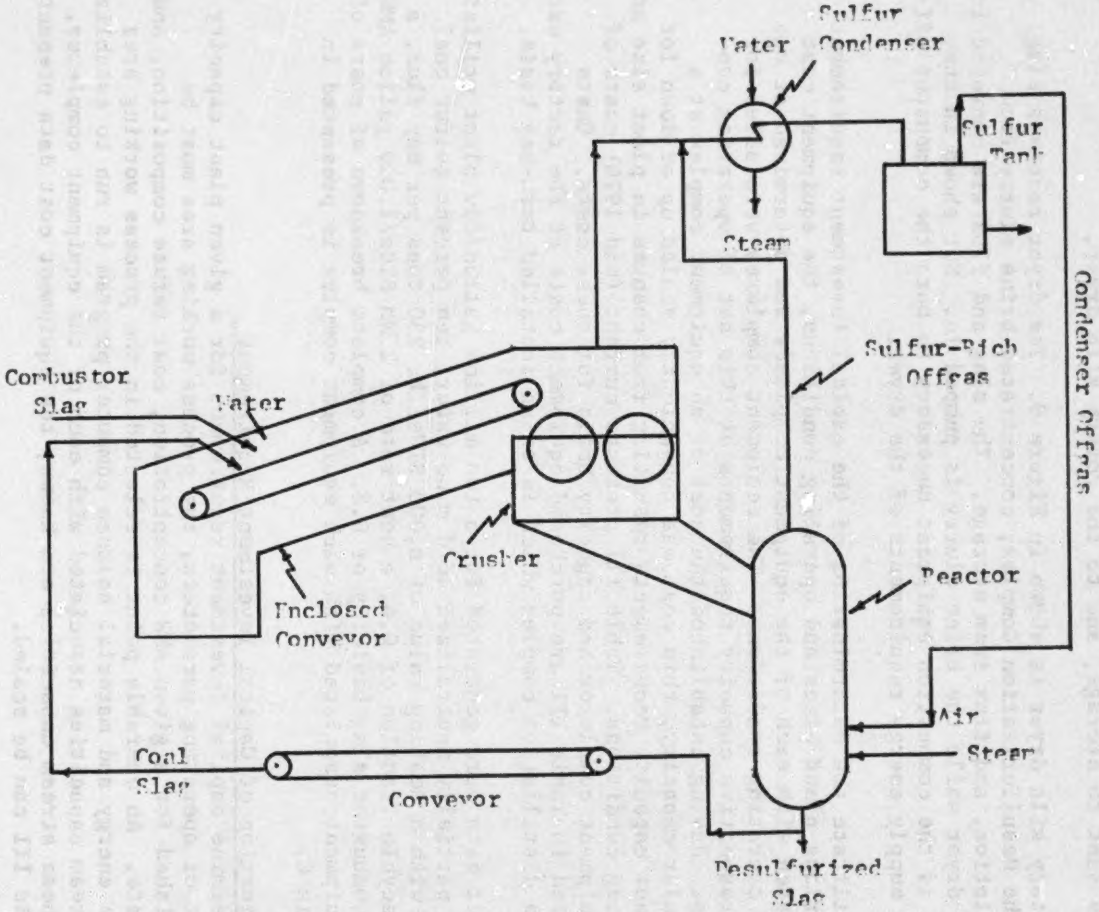

FIGURE [illegible] - DESULFURIZATION COMPLEX sent to a condenser where sulfur is condensed, using water as the cooling medium, and collected into a storage tank. The resulting condenser offgas is recycled for additional reaction in the desulfurizer. Part of the desulfurized slag leaving the reaction vessel is conveyed, via a belt conveyor, to the enclosed conveyor, to coat and protect the bucket belt from the molten slag leaving the combustor. The remaining slag is sent to storage, and to the rotary kiln dryer.

The rotary kiln dryer is shown in Figure 9. The dryer receives slag from the Desulfurization Complex, concentrated brine slurry from distillation, and flux from storage. The slag and flux are conveyed into the dryer while the brine slurry is pumped in. Not shown in the figure is the combustion equipment necessary to burn the combustor offgas to supply energy requirements of the dryer.

To facilitate the determination of the capital investment requirement for various plant sizes and operating conditions, the equipment cost associated with each of the equipment complexes was determined at one set of operating conditions. The equipment complexes were sized for their respective capacity requirements at this set of operating conditions. Having established the cost of an equipment complex at a particular capacity, this cost was conveniently scaled up or down for different capacity requirements resulting from changes in plant size and operating conditions. Table III presents current (mid 1970) costs of the equipment complexes and capacity basis for these costs. Costs presented in Table III are purchased equipment costs at the factory except for the distillation complex which is on an installed turn-key basis.

The cost data were generated for a two million gallon/day plant utilizing dilute partially neutralized acid mine water, ten percent sulfur coal refuse with a heating value of 6,000 BTUs/lb. 230 tons per day flux, a slag recycle fraction of 0.4, a heat rate of 2 MM BTUs/1,000 gallon AMW, and a combustor slag basicity of 0.8. A complete breakdown of costs of the equipment associated with each equipment complex is presented in Appendix C.

Determination of Capital Investment Requirement

To determine capital investment requirement for a given plant capacity and set of operating parameters, the process working area must be established for a given AMW concentration, coal refuse composition, and heat rate. An operable point is selected in the process working area and the energy and material balance computer program is run to establish the stream capacities associated with each of the equipment complexes. Once these stream capacities are known, the equipment cost data presented in Table III can be scaled.

The following procedure was used to determine the fixed capital investment requirement. Costs associated with the various equipment complexes, excepting distillation, are assumed to yield a total purchase equipment cost. Installation cost for this equipment was assumed to be 40 percent

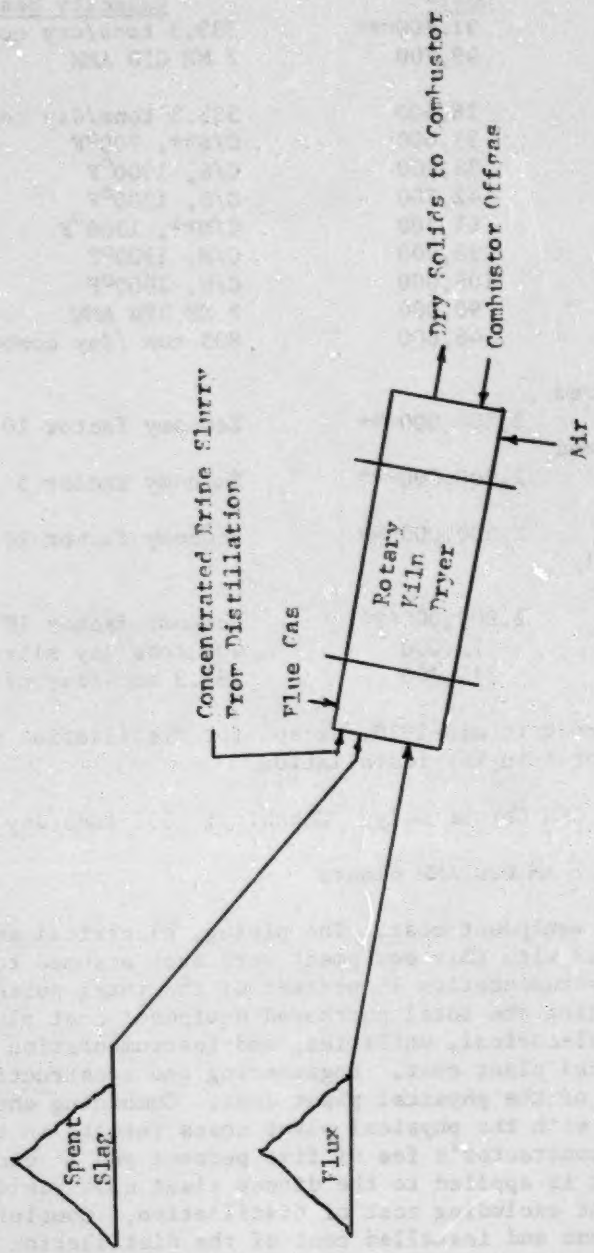

FIGURE 9 - ROTARY KILN DRYER

TABLE III
Equipment Complex Costs

Complex	Cost*	Capacity Basis
Coal Handling	91,300***	333.3 tons/day coal refuse
Neutralization	49,700	2 MM GPD AMW
Steam turbine Air Compressors	28,500	333.3 tons/day coal refuse
Direct fired furnace	33,000	C/S**, 700°F
	38,000	C/S, 1000°F
	42,700	C/S, 1300°F
	61,700	C/M**, 1300°F
	98,000	C/M, 1700°F
	108,000	C/M, 2000°F
Waste Heat Boiler	90,000	2 MM GPD AMW
Combustor	46,600	805 ton /day combustor offgas
Distillation, neutralized Acid mine water	2,500,000***	Economy factor 10
Distillation, neutralized Acid mine water	2,000,000***	Economy factor 5
Distillation, dilute Acid mine water	2,500,000***	Economy factor 10
Distillation, moderately Concentrated acid mine water	2,800,000***	Economy factor 10
Desulfurization	73,000	406 tons/day slag
Rotary kiln dryer	315,000	283.9 tons/day of solids

* Factory purchase cost in mid-1970, except for distillation plant which is priced for turn-key installation.

** C/S carbon steel; C/M Chrome moly. Capacity: 636 tons/day air

*** Installed cost of 2 MM GPD AMW plant.

of the total purchased equipment cost. The piping, electrical and utility costs associated with this equipment were each assumed to be ten percent and process instrumentation 15 percent of the total purchased equipment cost. Combining the total purchased equipment cost plus the installation, piping, electrical, utilities, and instrumentation cost yields the total physical plant cost. Engineering and construction costs were set at 30 percent of the physical plant cost. Combining engineering and construction costs with the physical plant costs results in the direct plant cost. A contractor's fee of five percent and a contingency of ten percent is applied to the direct plant cost yielding the fixed capital investment excluding cost of distillation. Combining the fixed capital investment and installed cost of the distillation plant yields the total fixed capital investment requirement for the given plant.

Determination of the Break-even Price of Water

The process utilizes acid mine water, coal refuse, and flux as raw materials and produces potable water, sulfur, iron and spent slag as products. In this study the acid mine water is considered to be available at no cost, the coal refuse cost is that associated with transporting the coal refuse to the plant site and assumed to be in the range of 0 to \$0.5/ton and the flux cost was set at \$2 per ton. Rather than consider the profit or loss of the process, the break-even price of water (BEPW) was used. Althought the selling price of water can vary considerably depending upon its marketability at the plant location, to simplify this presentation the selling price of the potable water is the price of water required to yield a no-profit-or-loss operation. The break-even price of water has the units of \$/1,000 gallons of potable water. Obviously, the lower the BEPW for a given process, the more desirable is that process. The selling price of sulfur was varied in the range of \$25 to \$40/ton to show its effect on process economics. Although the iron produced will contain less than 0.3 percent sulfur, the study assumes the iron contains one percent. The iron was conservatively valued at \$20 per ton. Unused spent slag from desulfurization can be briquetted to form a uniform road aggregate which was valued at \$0.5/ton. The cost of the briquetting press was not included in the overall plant cost because it was felt that utilization of spent slag should not be tied down to one specific application. Also, other slag desulfurization possibilities employing molten slag are possible for desulfurization which would preclude the need for an agglomeration operation (briquetting).

Determination of Operating Revenue

Once the fixed capital investment for a given plant capacity has been established, the daily capital interest charge can be determined. Knowing the costs and quantities of raw materials, assuming a three percent maintenance charge and a labor charge of \$300 per day enables the daily production cost to be determined. The daily production credits (not including the potable water credit) can be established since the quantity and selling price of the products are known. The difference between the daily production charge and the daily production credits is set equal to the potable water credit so that the operating revenue is zero. Knowing the potable water credit and the daily production of potable water enables the break-even price of water to be determined. A breakdown of the cost factors comprising the operating revenue and break-even price of water is presented in Table IV for a five million gallon per day plant, moderately concentrated AMW, eight percent sulfur refuse and a heat rate of 3.25 million BTU per 1,000 gallons of AMW.

Break-even Price of Water and Process and Economics Factors

In the discussion which follows, the break-even price of water will be determined as a function of plant size, acid mine water concentration, sulfur content of coal refuse, selling price of sulfur, capital interest charge, purchase cost of coal refuse, heat rate and whether neutralization is used.

To determine the optimum economic operating conditions (optimum operable point in the process working area), a series of process working areas were generated and the BEPW determined. In Table V the BEPW is shown

TABLE IV
Determination of Break-even Price of Water

Investment Cost	$	8,100,000
Potable Water Production		4,975,000 GPD
Daily Production Cost		
Capital Interest Charge*, (14%)		3,150
Flux, 1105 Tons @ $2/ton		2,210
Coal Refuse, 1427 Tons @ $0.25/ton		357
Labor		300
Maintenance, 3% of Investment		675
	$	6,692
Daily Production Credits (not including potable water credit)		
Sulfur, 126 tons @ $25/ton	$	3,150
Iron, 60 tons @ $20/ton		1,200
Slag, 1082 tons @ $.5/ton		541
	$	4,891
Operating Revenue (not including potable water credit)		(1,801)
Break-even Price of Water		$\frac{\$1{,}801 \times 1{,}000}{4{,}975{,}000}$ = $0.36/1000 of water
Potable Water Credit	$	1,801
Operating Revenue		0

* Capital Interest Charge = $8,100,000 x .14/360 days

as a function of various process parameters. Table V consists of six sets of results, which show the BEPW as a function of slag basicity, slag recycle fraction, heat rate, neutralization, AMW concentration, and the sulfur content of the coal refuse. Data of Table V was determined for a five million gallon per day plant, a 14 percent capital interest charge, and the following selling prices or purchase costs for the various raw materials or products; sulfur-$30 per ton, iron-$20 per ton, spent slag-$0.50 per ton, coal refuse-$0.25 per ton, and dolomitic limestone-$2 per ton.

Using the process working area generated for a heat rate of 3.25, operating conditions were selected which yielded slag basicities of 0.8, 1.0, and 1.2 at a maximum of ten percent sulfur in the slag. These operable points occur on the maximum ten percent sulfur line of the PWA. The BEPW was then determined for each of these operating conditions. As seen (Data Set 1) in Table V, the break-even price of water increased as the basicity increased. This means that the process should be run at the minimum operable basicity to yield the lowest break-even price of water.

TABLE V
BEPW for Process Operation Under Various Conditions

Data Set	Heat Rate MM BTU/ 1,000 gal	Flux Rate Tons/day	Slag Recycle Fraction	Slag Basicity	%S in Slag	Economy Factor	BEPW $/ 1000 gal	AMW conc	Neutral-ization	% sulfur in coal refuse
1	3.25	395	.24	0.8	10.0	5.0	.14	Dilute	Yes	10.0
	3.25	490	.15	1.0	10.0	5.6	.21	Dilute	Yes	10.0
	3.25	570	.05	1.2	10.0	6.3	.31	Dilute	Yes	10.0
2	2.00	242	.26	0.8	10.0	8.3	.35	Dilute	Yes	10.0
	2.00	230	.40	0.8	8.6	8.4	.37	Dilute	Yes	10.0
	2.00	200	.64	0.8	5.7	8.7	.41	Dilute	Yes	10.0
3	1.75	207	.31	0.8	10.0	9.8	.41	Dilute	Yes	10.0
	2.00	242	.26	0.8	10.0	8.3	.35	Dilute	Yes	10.0
	2.25	280	.22	0.8	10.0	7.3	.31	Dilute	Yes	10.0
	2.50	305	.25	0.8	10.0	6.6	.28	Dilute	Yes	10.0
	3.00	368	.25	0.8	10.0	5.4	.19	Dilute	Yes	10.0
	3.25	395	.24	0.8	10.0	5.0	.14	Dilute	Yes	10.0
4	3.25	395	.24	0.8	10.0	5.0	.14	Dilute	Yes	10.0
	3.25	415	.22	0.8	10.0	5.0	.09	Dilute	No	10.0
5	3.25	415	.22	0.8	10.0	5.0	.09	Dilute	No	10.0
	3.25	408	.30	0.8	10.0	5.3	.05	Med Conc	No	10.0
6	3.25	442	.08	0.8	10.0	5.3	.23	Med Conc	No	8.0
	3.25	408	.30	0.8	10.0	5.3	.05	Med Conc	No	10.0
	3.25	372	.45	0.8	10.0	5.3	-.14	Med Conc	No	12.0

In Data Set 2 the effect of spent slag recycle fraction on the BEPW is shown. These operating points were selected along the minimum basicity line on the PWA; therefore, the results yield a slag basicity of 0.8. The results indicate that the break-even price of water increases as the spent slag recycle fraction increases. Consequently, the process should be run using a minimum spent slag recycle fraction consistent with maintaining a maximum of ten percent sulfur in the slag.

These conclusions indicate that the optimum economic operating point occurs at the intersection of the minimum basicity line with the maximum (ten percent) sulfur line of the process working area. With this in mind, Data Set 3 was generated for heat rates of 1.75 to 3.25 and a slag basicity of 0.8 with ten percent sulfur in slag. Each of the selected heat rates yields an operable process. However, at a heat rate of 1.75 the economy factory is 9.5 whereas a heat rate of 3.25 yields an economy factor of five. Distillation units are normally designed for a maximum economy factor of ten and, since these economy factors are within the range of commercial distillation equipment design, the data represent the range of heat rates for which the process is operable. As shown in Table V the BEPW decreases as the heat rate increases. This is the result of using an inexpensive source of energy (coal refuse) for the process which allows a less efficient distillation unit to be built at a correspondingly lower price. These results show that optimum economic operation is achieved when using a distillation unit with an economy factor of five and operating the combustor with a ten percent sulfur slag of 0.8 basicity.

Data Set 4 presents a comparison of the BEPW for a process operating with and without neutralization. For this comparison the optimum economic point (0.8 basicity-ten percent sulfur in slag) was used. As seen, the BEPW decreased when the acid mine water is not neutralized. Specifically, the break-even price of water decreases from $0.14 to $0.09/1,000 gallons of water when neutralization is not employed.

Data Set 5 is used to show the effects of acid mine water concentration on the BEPW. The break-even price of water decreases from $0.09 to $0.05/1,000 gallons of water as the acid mine water concentration increases from dilute to moderately concentrated. Therefore, it is evident that unneutralized, concentrated (and still be compatible with the corrosion resistance of the distillation unit) acid mine water should be used in the process.

The effect of coal refuse sulfur content on the BEPW is shown in Data Set 6. The break-even price of water decreases as the sulfur content of the coal refuse increases.

In summary, the BEPW is minimized at a slag basicity of 0.8, a ten percent sulfur content in the slag, a heat rate which yields the minimum economy factor (5) and neutralization is not employed in the process. In addition, the BEPW decreases as the sulfur content of the coal refuse and the acid mine water sulfate concentration increases.

The effect of the selling price of sulfur and the purchase price of coal refuse on the break-even price of water will be illustrated for a process using moderately concentrated acid mine water, an eight percent sulfur coal refuse, a heat rate of 3.25 (economy factor equal to five), and a set of operating conditions which yield a basicity of 0.8 and ten percent sulfur in the slag. A 14 percent capital interest charge was used in this study. The BEPW, for a five million gallon per day plant operating at these conditions, as a function of the selling price of sulfur and the purchase price of coal refuse is shown in Figure 10. This figure shows that as the selling price of sulfur increases, the BEPW decreases. Also, as the coal refuse purchase price increases, the BEPW increases. Also shown in Figure 10 is an area of anticipated price ranges of sulfur and coal refuse.

The purchase price of coal refuse is difficult to ascertain. At present, coal refuse does not have a market and, consequently, has no market price. It is believed that the cost of coal refuse will be mainly the cost associated with transporting it to the AMW plant site. The price of coal refuse was assumed to range from 0 to $0.5 per ton. The zero cost number will probably apply to a coal producer operating the Acid Mine Water Process. Coal refuse produced from the coal washing operation can be brought directly to the AMW plant site at the same cost as transporting it to a coal refuse pile. The $0.25 per ton number is assumed to apply to a noncoal producer whose AMW plant is in close proximity to a coal washing facility. The $0.5 per ton number is believed to be a reasonable cost for coal refuse when the acid mine water plant is some distance away from the coal refuse source.

Selling price of sulfur is extremely variable. In the last four years, it has ranged from a high of approximately $40 per ton to a low of less than $20 per ton. Figure 10 shows that the selling price of sulfur is a prime consideration in the economics of the process. At a $25 per ton selling price, the BEPW is $0.29, whereas at $30 per ton the break-even price of water drops to $.16/1,000 gallons of water. The purchase price of coal refuse is an equally important economic consideration as can be seen from Figure 10 which shows a $0.14/1,000 gallons of water variance in the BEPW as the price of coal refuse varies from 0 to $0.5 per ton.

As of mid-1970 the selling price of sulfur has been approximately $25/ton. Assuming coal refuse is available at $0.25/ton, the BEPW for a five million gallon per day plant is $0.36/1,000 gallons of water.

The capital investment requirements and intermediate results necessary to calculate the capital investment for various sized acid mine water treatment plants are shown in Table VI. This table was prepared using moderately concentrated AMW, an eight percent sulfur coal refuse, a heat rate of 3.25, a set of operating conditions which yield a basicity of 0.8 and ten percent sulfur in the slag. The capital investment requirement increases as the plant size increases. Figure 11 indicates that the capital investment is not a linear function of plant capacity and economies can be realized by using higher plant capacities. This infers that the plant should be located

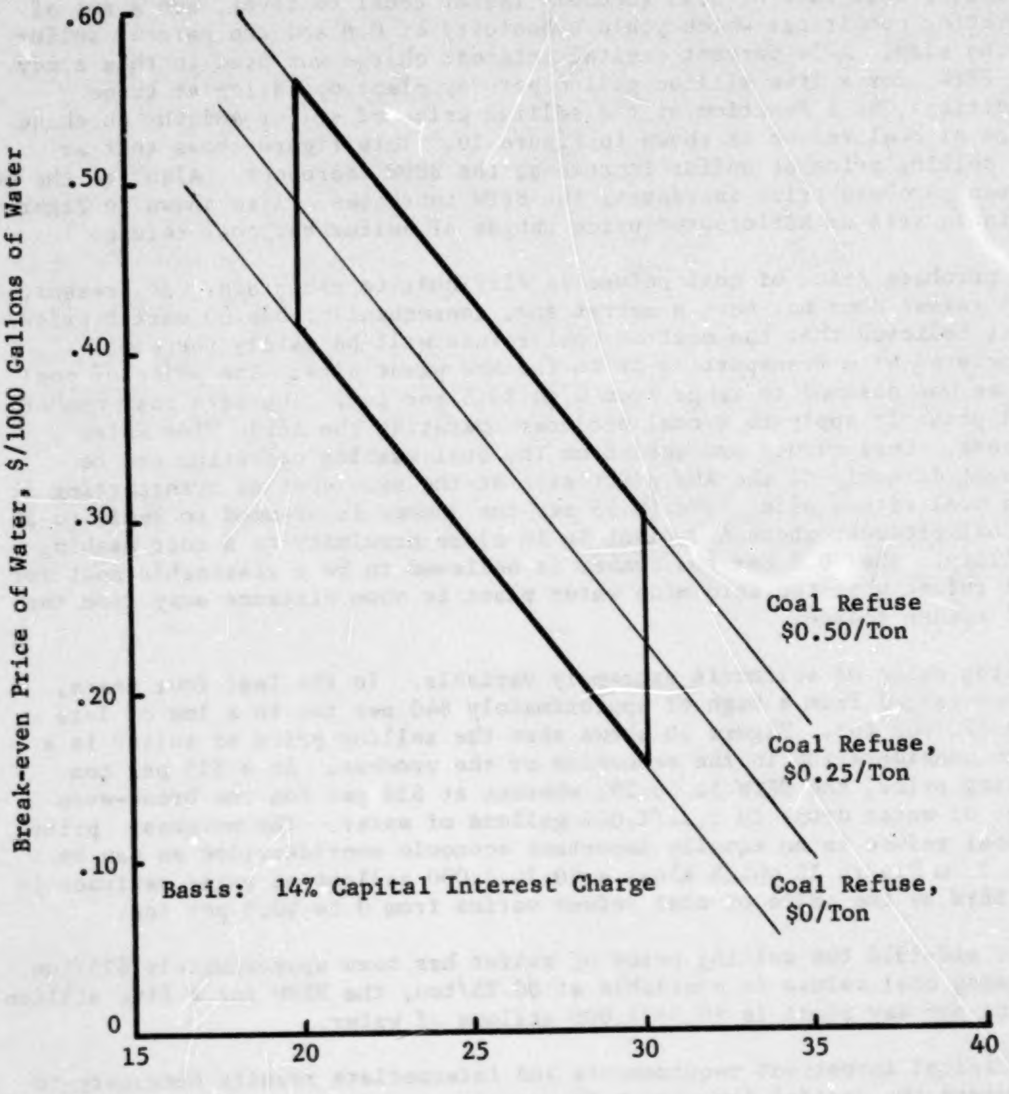

FIGURE 10 - EFFECT OF SULFUR PRICE ON BREAK-EVEN PRICE OF WATER

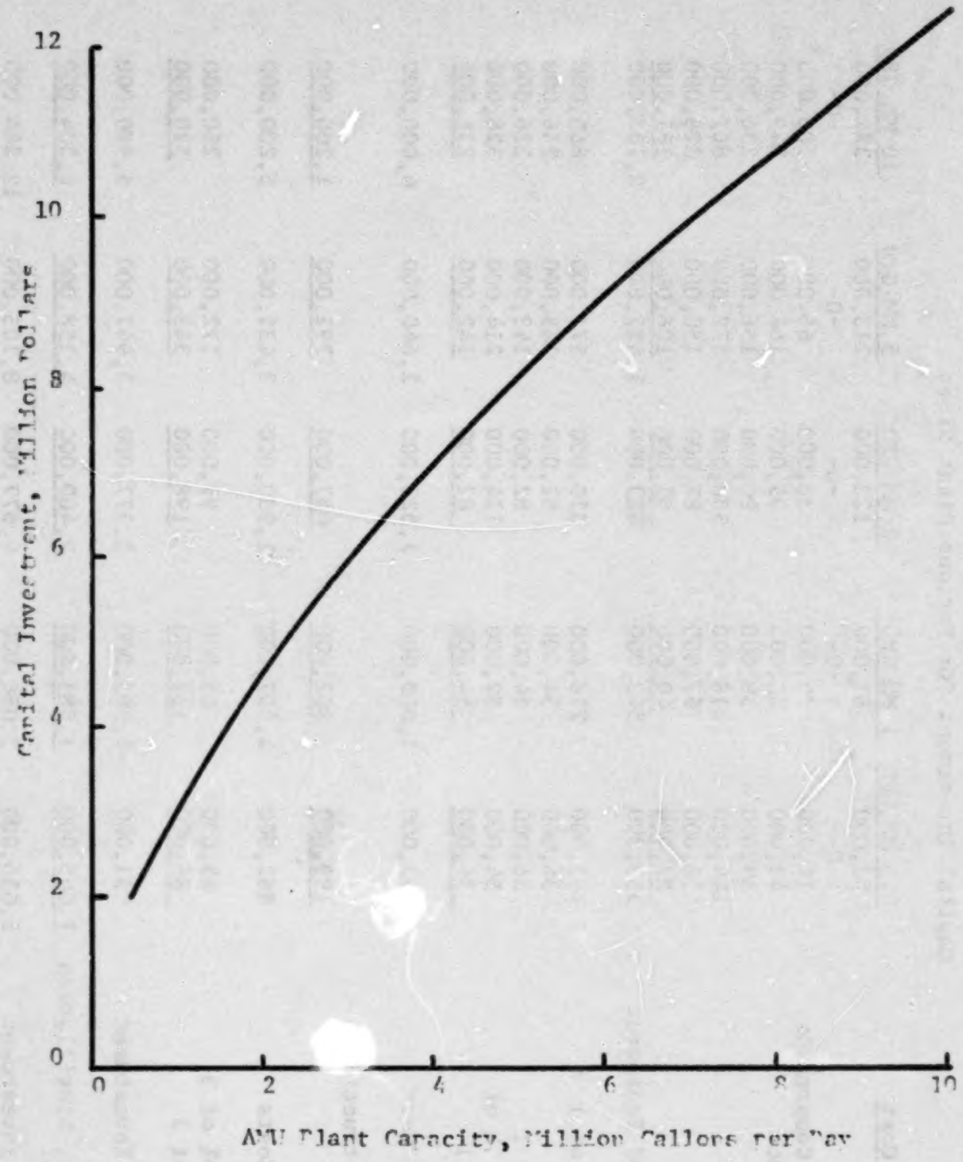

FIGURE 11 - EFFECT OF PLANT CAPACITY ON CAPITAL INVESTMENT

TABLE VI
Capital Investment for Various Plant Sizes

Equipment Complex Cost	0.5 MM GPD	1 MM GPD	2 MM GPD	5 MM GPD	10 MM GPD
Coal Handling	53,000	81,000	122,000	213,000	321,000
Neutralization	-0-	-0-	-0-	-0-	-0-
Steam Turbine Air Compressor	16,000	25,000	38,000	66,000	100,000
Direct Fired Furnace	41,000	63,000	95,000	164,000	249,000
Waste Heat Boiler	39,000	59,000	90,000	156,000	236,000
Rotary Kiln Dryer	144,000	218,000	330,000	572,000	867,000
Desulfurization	38,000	57,000	87,000	150,000	229,000
Combustor	27,000	40,000	61,000	106,000	161,000
1. Total Purchased Equipment	358,000	543,000	823,000	1,427,000	2,163,000
Installation, 40% of 1	143,000	218,000	330,000	571,000	865,000
Piping, 10% of 1	36,000	54,000	82,000	143,000	216,000
Electrical, 10% of 1	36,000	54,000	82,000	143,000	216,000
Instrumentation, 15% of 1	54,000	82,000	124,000	214,000	324,000
Utilities, 10% of 1	36,000	54,000	82,000	142,000	216,000
2. Physical Plant Cost	663,000	1,005,000	1,523,000	2,640,000	4,000,000
Engineering & Construction, 30% of 2	199,000	302,000	457,000	792,000	1,200,000
3. Direct Plant Costs	862,000	1,307,000	1,980,000	3,432,000	5,200,000
Contractor's fee 5% of 3	43,000	65,000	99,000	172,000	260,000
Contingency, 10% of 3	86,000	131,000	198,000	343,000	520,000
4. Fixed Capital Investment	991,000	1,503,000	2,277,000	3,947,000	5,980,000
5. Installed Cost, Distillation	1,045,000	1,583,000	2,400,000	4,158,000	6,304,000
Total Capital Investment	2,036,000	3,086,000	4,677,000	8,105,000	12,284,000

at a large source of acid mine water provided coal refuse is available in the vicinity.

Figure 12 shows the break-even price of water as a function of plant capacity and the capital interest rate, with coal refuse at $0.25/ton and sulfur at $25/ton. This figure indicates that both plant size and capital interest rate has a profound effect on the break-even price of water. For example, at a capital interest rate of 14 percent the BEPW decreases from $1.30 to $0.14/1,000 gallons of water when the plant size is increased from one to ten million GPD of AMW. For a five million GPD AMP plant, the BEPW decreases from $0.36 to $0/1,000 gallons of water when the capital interest charge is reduced from 14 percent to six percent.

Plant capacity has an important effect on the break-even price of water. The BEPW is considerably reduced as the plant capacity is increased from one to ten million GPD. Normally, the flow of most acid mine water streams is less than two million GPD. In heavily mined regions, several acid mine water streams can occur relatively close to each other; consequently, several streams could be combined to yield a five million GPD stream. Based on this reasoning, a five million gallon per day plant will be used to illustrate the capacity and temperature of the individual process streams and payback as a function of the selling and break-even price of water. Table VII presents the capacity and temperature of all process streams for a process utilizing moderately concentrated AMW, eight percent sulfur coal refuse, a heat rate of 3.25, a flux rate of 1,105 ton/day and a slag recycle fraction of 0.084. These values yield a slag basicity of 0.8 and a ten percent sulfur content in the slag. For convenience, the process flow chart is shown in Figure 13 with all streams labeled as in Table VII.

Figure 14 was prepared to illustrate the effect of water selling price on capital recovery. This figure shows a plot of payback versus the difference between selling price and break-even price of water. Payback is total investment divided by annual profit. For Figure 14, investment is $8.5 million for a five MM GPD plant, operating under the conditions of Table VII. The capital is higher than that of Table VI, because it includes cost of land, spare parts, and shakedown, plus working capital requirements during shakedown. Because the break-even price of water includes all direct and indirect costs, the difference between selling (at the plant) and break-even prices is used as profit in calculating payback. The selling price of water at the plant will depend on demand for water in nearby markets and cost of transporting water to these markets. The break-even price of water is a function of process parameters and capital interest charges.

A six percent capital interest charge is not unrealistic if municipal money in the form of tax-exempt six percent bonds is available. For a plant with an estimated life of 20 years and a one year construction and shakedown period, operating as indicated in Table VII the break-even

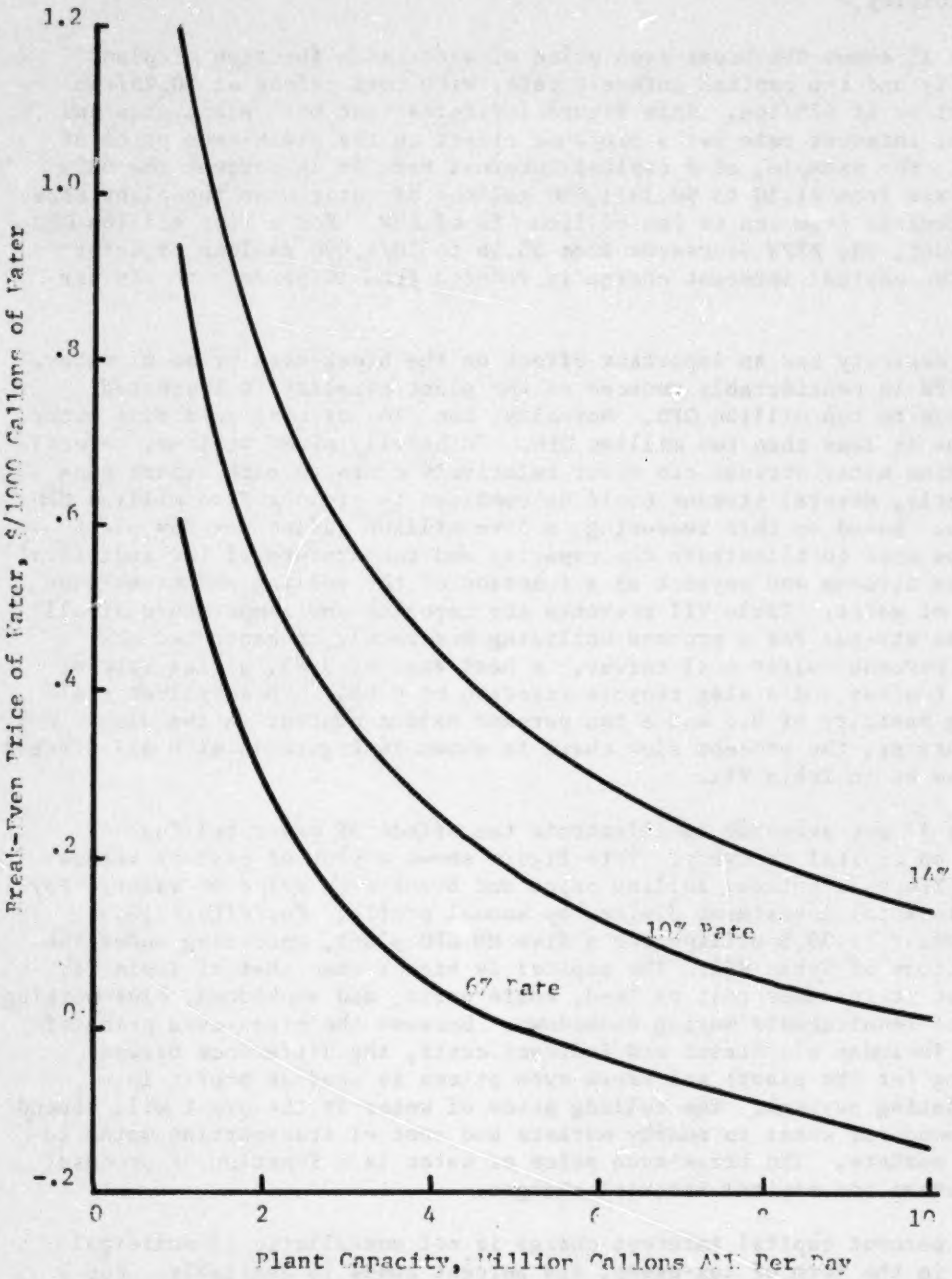

FIGURE 12 - EFFECT OF PLANT CAPACITY ON BREAK-EVEN PRICE OF WATER

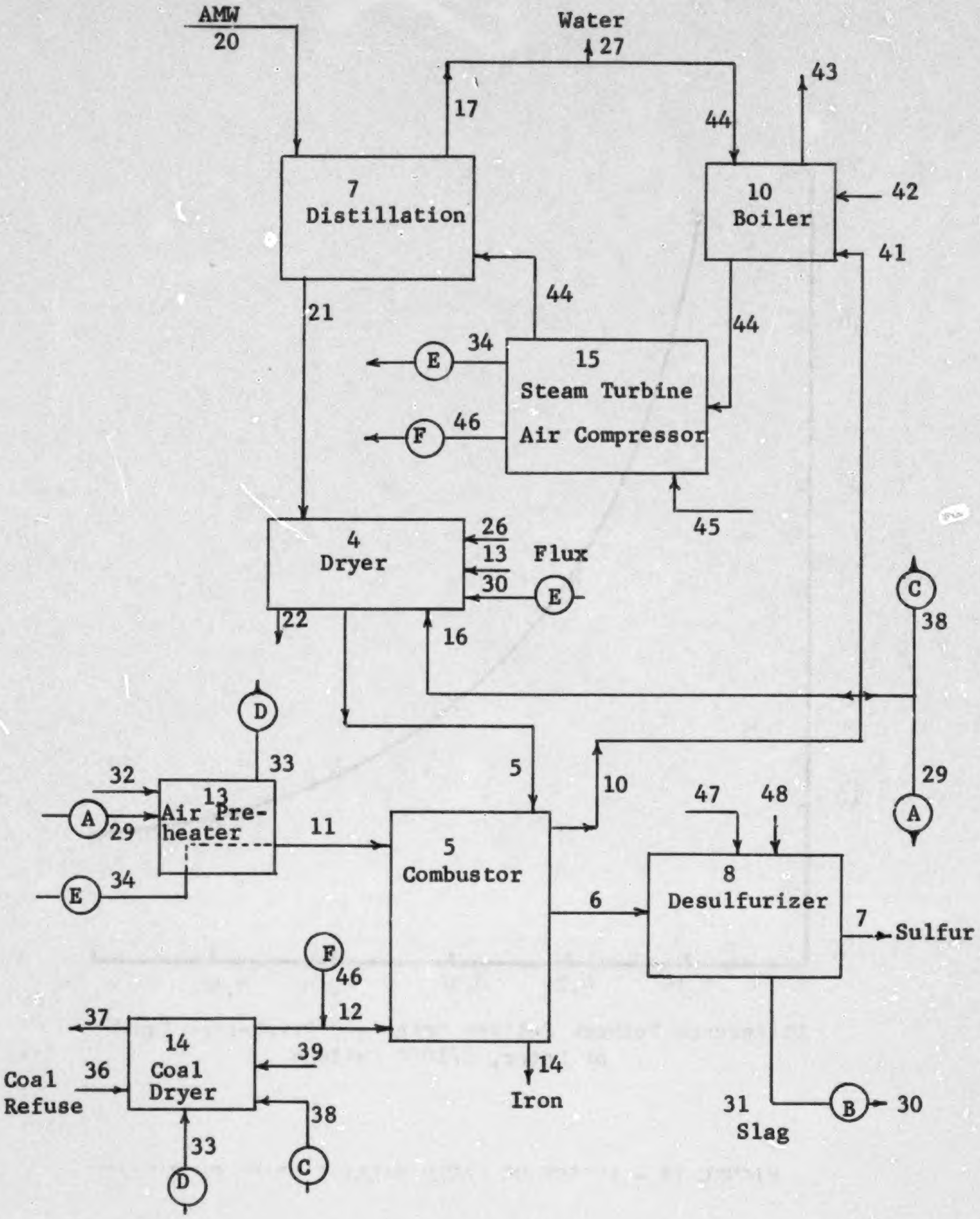

FIGURE 13 - PROCESS FLOW CHART OF AMW TREATMENT PLANT

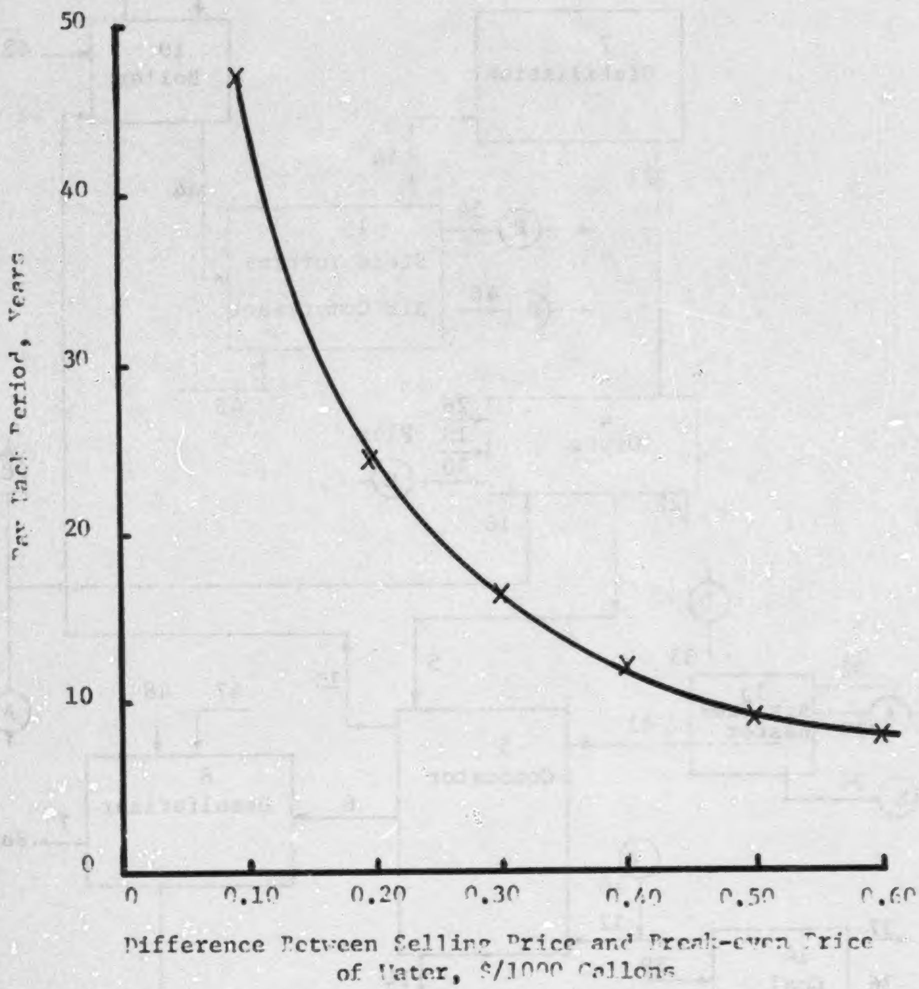

FIGURE 14 - EFFECT OF WATER SELLING PRICE ON PAYBACK

TABLE VII
Stream Capacities and Temperatures for 5 MM GPD Plant

Stream	Description	Capacity Tons/day	Temp. °F
5	Dryer solids	767	2200
6	Combustor slag	1245	2700
7	Sulfur product	126	200
8	Spent slag	1182	2000
10	Combustor offgas (assuming 10% heat loss)	3191	2430
11	Preheated air	2484	1332
12	Dry, crushed coal	1354	150
13	Flux	1105	70
14	Iron product	60	2700
16	Combustor offgas to dryer	700	2430
17	Potable water	22807	180
20	Acid mine water	20948	70
21	Concentrated brine slurry	214	180
22	Dryer flue gas	2307	250
26	Air	956	60
27	Water product	20734	212
29	Combustor offgas to air preheater	174	2430
30	Recycled spent slag	99	70
31	Spent slag product	1082	300
32	Air	2484	70
33	Air preheater flue gas	412	500
34	Air for preheating	238	60
36	Wet Coal	1427	70
37	Coal drying kiln flue gas	513	280
38	Combustor offgas to coal drying kiln	31	2430
39	Air	42	60
41	Combustor offgas to boiler	2286	2430
42	Air	3122	60
43	Boiler flue gas	5409	2280
44	Water to and steam from boiler	2103	300
45	Air into steam-turbine air compressors	2619	60
46	Air to convey coal into combustor	135	60
47	Water into desulfurizer	36	60
48	Air into desulfurizer	270	60

price of water is $0/1,000 gallons. If the plant sells water at $0.50/ 1,000 gallons (at the plant), Figure 14 shows that payback would be nine years from the initial date of the bond issued (beginning of construction). This is based on yearly profits of $900,000 which are set aside in a sinking fund which conservatively earns five percent interest per year. The sinking fund could, at the end of nine years, be used to retire the bonds. If this is done, then the profits become $1.4 million per year since the capital interest charge is now eliminated. If the profits generated in the 10th to 20th year are accumulated yearly in a construction fund earning five percent interest, the construction fund would be worth $17.8 million at the end of 20 years when the plant life is exhausted.

Assuming an average inflation rate of four percent, in 20 years the same plant would require $17.7 million to construct. The construction fund could then be used to totally finance a new plant and the profits would be $1.4 million per year. It is impossible to predict the future but the above figures indicate that the process can generate sufficient profits to be self-perpetuating.

The important conclusion is that if low cost money is available, the economics of the process are highly favorable and should stimulate municipalities to rid their communities of acid mine water pollution. An alternative manner in which to consider the economics of the process is to determine the selling price of water required to capitalize the plant over its life without any profit. Figure 14 shows that the difference between selling price and break-even price of water must be $0.235/1,000 gallons to yield a payback period of 20 years. This means that for the above plant, the selling price of water must be $0.235/1,000 gallons to eliminate five MM GPD of acid mine water at no cost (provided that capital is available at six percent).

As of this writing, (late 1970), the assumption of six percent tax-exempt municipal bond capital appears quite conservative. Distilled water prices in the range of $0.2/1,000 gallons to $0.5/1,000 gallons at the plant appear quite realistic for plants that are not too remote from consumers. Therefore, this process offers the incentive of profit or, at least, no cost for eliminating acid mine drainage from our streams.

It is difficult to make a cost comparison between AMW treatment processes because the literature data are based on AMW of different compositions for plants of various capacities or are estimated at different capital interest rates. In the following discussion, published cost data for lime neutralization and ion-exchange treatment of AMW were adjusted to a common basis for comparison with the new process. The common basis is a plant constructed at a six percent capital interest rate to treat five MM GPD of AMW of acidity of 500 (ppm $CaCO_3$). The current study has shown that the new process has a zero operating cost (no cost) when eight percent sulfur coal refuse at $0.25/ton is used in the base case plant.

A study of an ion-exchange AMW treatment process was reported by J. L. Rose at the Third Symposium on Coal Mine Drainage Research in May, 1970 (pages 267-278 of the Proceedings). Rose estimated costs of $0.73 and $0.45 per 1,000 gallons of AMW for plant capacities of one and ten MM GPD. These data were used to determine an ion-exchange AMW treatment cost of $0.55/1,000 gallons for the above-mentioned base case. Comparing the ion-exchange and new process treatment cost, it is seen that the ion-exchange process is substantially more costly.

At the Second Symposium on Coal Mine Drainage Research in May, 1962, (pages 274-290 of the Proceedings) Corsaro reported costs for lime neutralization plants treating up to 8.1 MM GPD of AMW of various concentrations. Using Corsaro's data, an operating cost of $0.20/1,000 gallons of AMW was obtained for the base case plant. In a report entitled "Operation Yellowboy" for the Pennsylvania Coal Research Board, Dorr-Oliver estimated lime neutralization treatment costs for various actual AMW sources. They estimated an operating cost of $0.22/1,000 gallons AMW at a four percent capital interest rate for the Blue Coal Corporation Loomis No. 4 site with a 5.7 MM GPD AMW source of 560 acidity. Adjusting these data for a six percent capital interest charge results in a $0.25/1,000 gallons operating cost. It is interesting to note that the operating costs determined by Dorr-Oliver for various AMW sources ranged from $0.10 to $1.23 per 1,000 gallons.

Even if it assumed that lime neutralization treatment costs only $0.20/1,000 gallons of AMW, the new process is the least expensive means to treat AMW because it has no operating cost for the base case.

There are other considerations which must be included in this discussion. Although operating costs for lime neutralization are high, the capital requirements are low enough to make lime neutralization attractive to small mine operators. On the other hand, both the ion-exchange and lime neutralization processes present by-product disposal problems. The new AMW treatment process does not produce any pollution-producing by-products and generates distilled water which can be sold to industry at a profit. Also the availability of distilled water in an area can bring in new industry and enhance the economic well-being of the community. In contrast, the lime neutralization treatment process does not produce water of any significant commercial value and the ion-exchange process produces a water whose quality is available in numerous locales throughout the nation and offers no particular inducement for industry. Accordingly, a meaningful comparison must be based on treatment of a specific stream, to include consideration of actual capital and operation cost.

ACKNOWLEDGEMENTS

The study described in this report was financed by a Federal Water Quality Administration (FWQA) contract to Black, Sivalls & Bryson, Inc., (BS&B). The Applied Technology Division of BS&B acknowledges the technical assistance of Messrs. R. D. Hill, and R. B. Scott of the EPA and of the Chemical Service Engineers, Inc., personnel who conducted the bench-scale laboratory work.

REFERENCES

1. Endell, K. and Ci Wens, Industrial Heating, 4, (2), 143, (1937).
2. Rait, J. R., Trans, Brit. Ceram. Soc., 40 157-204, 231-269, (1941).
3. Fehling, H. R., "Erosion of Refractories by Coal Slag", Institute of Fuel J. Vol. II No. 59, pp. 451-458, June (1938).
4. Herty, C. H. etal, Min. Met. Invest. Coop. Bull., No. 46 1, (1930).
5. McGannon, H. E., "The Making, Shaping & Treating of Steel," United States Steel Corporation, August (1964).
6. Herty, C. H., Blast Furnace & Steel Plant, 25, 1000 (1937).
7. Herty, C. H., Jr. Trans. Amer. Inst. Min & Met. Eng., Iron and Steel Div., pp. 284-299 (1929).
8. Gul'tyai, I. I. Iz Akad Nauk SSSR, Otd. Tekhn, Nauk. Met. Toplivo, No. 3, (1962).
9. F. Henen, G. R. etal, Acid Open Hearth Research Assn., Inc. Bull. No. 1, (1945).
10. Kozakevitch, P., Rev. de Metallurgie, Vol. 51. 569-587, (1954).
11. Machin, J. S., Lee T. B., Hanna, D. L., J. Am. Ceram. Soc, Vol. 35 pp. 322-25, (1952).
12. Cameron, J. Gibbons, T. B., and Taylor, J., Journal of the Iron and Steel Institute, pp. 223-28, December (1966).
13. Hatch, W. G., and Chipman, J., Metals Transactions, Vol. 49. pp. 479, 86 (1946).
14. Sharma, R. A., and Richardson, F. D., Journal of the Iron and Steel Institute, Vol. 198 p. 386, (1961).
15. Sharma, R. A., and Richardson, F. D., Journal of the Iron and Steel Institute, Vol. 200, p. 373, (1962).
16. Kozakevitch, P. "Physico-Chemical Measurements at High Temperatures," Butterworths Scientific Publications, pp. 212-221, (1959).
17. Dallavalle, J. M., "Micromeritics," Pitman Publishing Corp., New York, pp. 272, 334, (1948).
18. Gross, J., "Crushing & Grinding," U. S. Bur. Mines Bull. 402, (1938).

19. Brown, G. G., "Unit Operations," John Wiley & Sons, Inc. New York pp. 42-45 (1950).

20. Perry, J. H., "Chemical Engineers Handbook," McGraw Hill Book Company, Inc. p. 226 (1950).

21. Hougen, O. A., Watson, K. M., and Ragatz, R. A., "Chemical Process Principles," Part I, John Wiley & Sons, Inc. New York, pp. 262, (1954).

22. Boulanger, C. and Leroy, C., Fr. Patent 873, 093, June 29, 1942.

23. Smyers, W. H. and Manny, E. H., U. S. Patent 3,249, 402, October 2, 1962.

24. Gunterman, W. Fischer, F. and Kraus, H., Ger. Patent 1,184,895, January 7, 1965.

25. Franklin, R. L., Guseman, J., and Pelczarski, E. A., U. S. Patent 3,125,438, November 8, 1962.

26. Odeen G. A., etal, Norway Patent 83,374, March 22, 1954.

27. Rudweva A. V., and Panov, A. S., Iz., Akad, Nauk SSSR, Otd, Khim. Nauk, pp. 553-8 (1962).

28. Steyn, J. G. D., Mineraby, pp. 108-17, May 35 (269), (1965).

29. Squires, A. M., "Reaction Which Permits Cyclic Use of Calcined Dolomite to Desulfurized Fuels Undergoing Gasification," Am. Chem. Soc. Div., Fuel Chem. Vol. 10, No. 4, pp. 20-41, September 11-16, (1966).

30. Woehlbier, F. H., and Rengstorff, G. W. P., "Preliminary Study of Gas Formation During Blast Furnace Slag Granulation with Water", Preprint of paper presented at the annual meeting of the Air Pollution Control Association, June 26, 1968.

31. Wen, C. Y. Industrial and Engineering Chemistry, pp. 34-54, September (1968).

32. Olsson, R. G., Koump, V., and Penzak, T., "Rate of Solution of Carbon in Molten Iron-Carbon Alloys," Annual AIME meeting of February, 1965.

33. Leary, R. J., and Ostrowski, E. J., "Pneumatic Lance Injection of Carbonaceous Solids for Recarburizing Open-Hearth Melts," United States Bureau of Mines, Open File Report, 1963.

GLOSSARY

Basicity - Weight ratio, $(CaO + MgO)/(Al_2O_3 + SiO_2)$, of the components in a slag.

Desulfurized Slag - Slag in which all or most of the calcium sulfide has been removed.

Economy Factor - For a distillation plant, the weight ratio of the water distilled to the steam used for distillation.

Flux - Any agent which preferentially combines with the impurities of a molten metal and aids in the smelting operation.

Heat Rate - Millions of BTUs of fuel consumed per thousand gallons of acid mine water processed.

Partition Ratio - Percent of sulfur in a slag in contact with iron divided by percent of sulfur in the iron.

Process Working Area - The resulting operable range of process variables when certain constraints on slag basicity, sulfur content of slag and air preheat temperature are applied to the process working area diagram.

Process Working Area Diagram - Plot of slag basicity vs. slag recycle fraction at various flux rates into the process.

Slag - Product formed by the action of a flux upon the gangue of an ore or ash of a fuel. In this study, a mixture of silica, alumina, magnesium oxide, calcium oxide and calcium sulfide.

Slag Fluidity - Measure of the ability of a slag to flow. A qualitative term used interchangeably with apparent viscosity.

Spent Slag - Same as desulfurized slag.

Spent Slag Recycle Fraction - The fraction of the desulfurized slag exiting the desulfurization complex which is recycled back to the kiln dryer.

APPENDIX A
LABORATORY STUDIES

SLAG FLUIDITY

Introduction

Addition of limestone to control combustor slag properties contributes heavily to process costs. Limestone is added to the slag to increase its sulfur-retention capacity and to control its fluidity. A highly fluid slag is undersirable, because it increases costs by rapidly attacking combustor refractories[1,2,3]. On the other hand, the slag must be fluid enough to flow from the combustor. Accordingly, a search was made for viscous-but-pourable slags that could be derived from coal ash and AMW constituents with a minimum of additives.

An abundance of data is available for the effect of slag composition on the viscosity of blast furnace and steel making slags[4]. However, to minimize process operating costs, very low basicity high sulfur containing slags will be required. For these types of slags, literature data for the effect of high sulfur concentration on slag viscosity are scarce[5]. Since a large number of slag compositions are possible, a quick screening test was required to rank the various types of slags according to their relative fluidities so that more detailed measurements could be completed on those deemed suitable.

A simple test used in steelmaking operations has been developed by Herty[6] and has proven to be a valuable guide for a rough evaluation of slag fluidity. For this reason, the Herty method was modified and adopted for use in our screening experiments. The principle of the Herty test is quite simple: A known volume of molten slag is poured down an inclined plane. Contact with the cold inclined plane causes the slag to solidify. The thickness of the slag layer at any arbitrary specified point is a function of the fluidity (viscosity) of the material. Obviously a test as simple as this is influenced by a number of slag properties including heat transfer characteristics. However, as a relative guide for comparing differences in fluidity, the test has proved it can provide valuable information[2,6,4,7].

Experimental Procedure - General

Master batches of slag of a given composition were prepared in two-kilogram lots. Slags were prepared by adding reagent grade ingredients into a closed pyrolytic graphite crucible that was inserted within a high temperature furnace maintained at 2700°F. An argon purge was used in the interior of the furnace to eliminate air from the system. After a soaking time of six hours, the carbon crucible containing the molten slag was removed from the furnace, the slag was then quenched in argon and examined to determine if a homogeneous melt had been formed. It was found that to obtain a uniform slag, it was necessary to heat, melt, cool, and crush the slag three times before homogenity was observed.

The equipment used in the Herty Test is shown in Figure 15. With the exception of the orifice cup which was made of pyrolitic graphite, all other components were of carbon steel construction. The inclined plane (30 inches long) was maintained at an angle of 14 degrees from the horizontal. A departure was made from the recommended[4] angle of inclination of 30 degrees because the slag, upon solidifying, tended to break and slide down the inclined plane. Consequently, a 14 degree inclination angle was adopted to render the slag immobile after solidification.

The experimental procedure consisted of heating a 100 gram slag sample in the high temperature furnace until temperature equilibration was achieved. Variations in the test results during experimentation soon showed that a residence time at temperature of about three hours was required to assure temperature uniformity. Sulfur analysis of the slag before and after melting indicated no significant sulfur losses. The hot sample was withdrawn from the furnace and transferred to the orifice cup as quickly as possible and immediately poured down the inclined plane. Generally, the transfer of the slag from the furnace to the orifice cup was completed in 20 seconds or less. Measurements were made of the length, width, and thickness of the solidified slag lying on the inclined plane. These were used to correlate slag relative fluidity and, indirectly, viscosity with changes in composition.

Standardization of Experimental Techniques

A short study was conducted to determine the effect of slag time at temperature and position in the furnace on reproducibility of slag fluidity tests. Results of this work using a commercial blast furnace slag (slag No. 1, Table VIII) are presented in Figure 16. A slag residence time of at least three hours in the furnace is required to maintain reproducibility. Although not severe, a temperature gradient (as indicated by fluidity differences) appears to exist in the furnace since one sample position continually yielded lower fluidity values. In all subsequent work, a minimum time at temperature of three hours was established as a standard.

To evaluate the effect of the number of slag remelts required to obtain a uniform slag composition and to determine the effect of number of remelts on slag fluidity, a second series of tests was completed. In these tests, two slags (Table VIII, slags No. 2 and 3) were used in the fluidity tests, crushed to -20 mesh after cooling, remelted and used again in the fluidity test. This procedure was repeated three times for slag No. 2 and four times for slag No. 3. Results of this work are shown in Table IX and X. Data indicate fluidity increased with increasing number of remelts. Data in Tables IX and X indicate that three remelts per slag sample should be sufficient to obtain consistently reproducible fluidity test results. The fluidity increase can be attributed to increased compositional uniformity of the slag sample, which was observed upon remelting. This is consistent with the literature where similar results were obtained.

The time element involved in moving the slag sample from the heating furnace

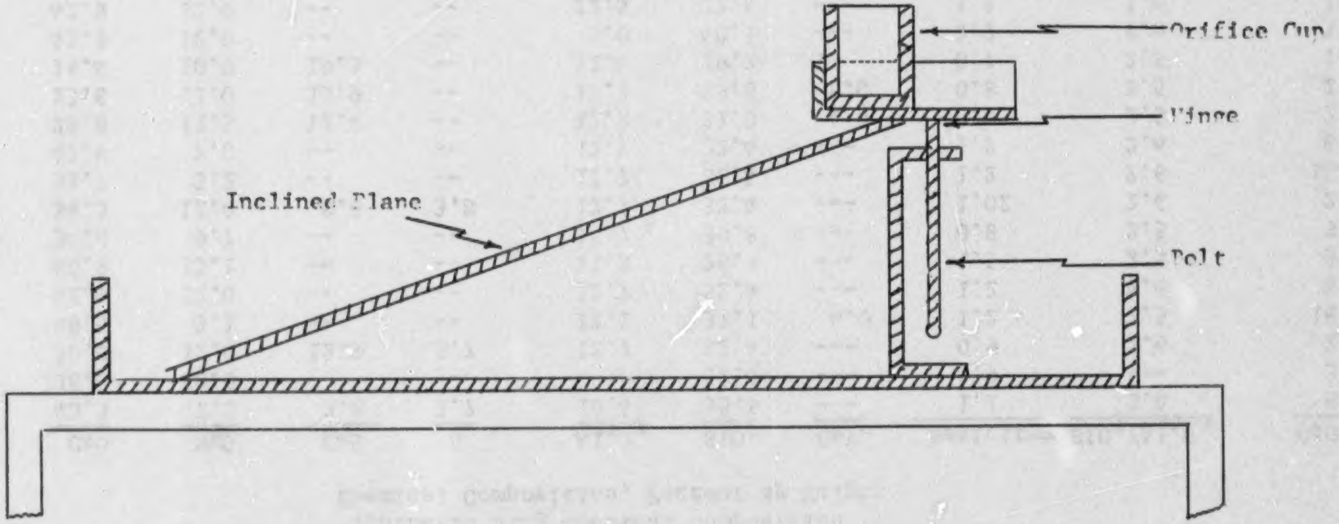

FIGURE 15 - FLUIDITY TEST APPARATUS

TABLE VIII
Synthetic Slag Chemical Composition
Chemical Composition, Percent by Weight

SLAG	CaO	MgO	CaS	S	Al_2O_3	SiO_2	CaF_2	Basicity*	SiO_2/Al_2O_3	CaO/MgO
1.	43.3	7.0	3.8	1.7	10.4	35.6	---	1.1	3.4	6.2
2.	38.0	10.0	--	--	--	52.0	---	0.9	---	3.8
3.	30.0	12.0	12.9	5.7	12.7	32.4	---	0.9	2.6	2.5
4.	49.6	3.1	--	--	12.2	31.1	4.0	1.2	2.5	16
5.	42.9	12.0	--	--	12.7	32.4	---	1.2	2.6	3.6
6.	46.9	13.1	--	--	11.3	28.7	---	1.5	2.5	3.6
7.	34.8	9.7	--	--	15.7	39.8	---	0.8	2.5	3.6
8.	34.3	12.0	8.6	3.8	12.7	32.4	---	1.02	2.6	2.9
9.	51.7	3.2	--	--	12.7	32.4	---	1.2	2.6	16.2
10.	47.9	7.0	--	--	12.7	32.4	---	1.2	2.6	6.8
11.	28.8	11.5	12.4	--	12.2	31.0	4.0	0.9	2.5	2.5
12.	23.6	11.0	15.9	--	11.7	29.8	8.0	0.8	2.5	2.1
13.	19.4	10.8	19.3	--	11.4	29.2	10	0.7	2.6	1.8
14.	42.9	12.0	--	--	5.0	40.1	---	1.2	8.0	3.6
15.	42.9	12.0	--	--	22.5	22.6	---	1.2	1.0	3.6

* Basicity is expressed as the weight ratio of basic oxides (CaO + MgO) to acid oxides ($SiO_2 + Al_2O_3$)

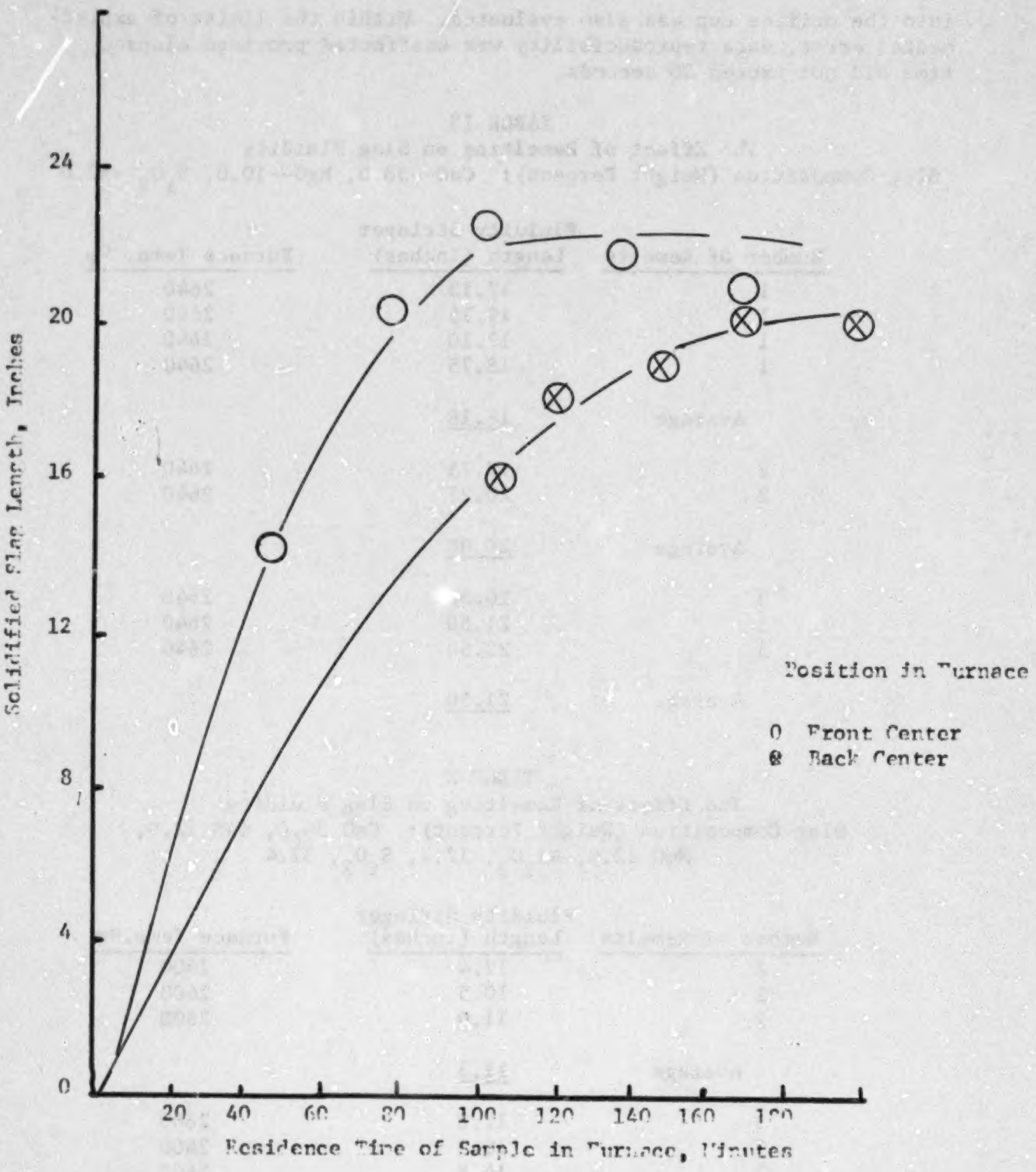

FIGURE 16 - RELATION BETWEEN FLUIDITY AND RESIDENCE TIME OF SAMPLE IN FURNACE

into the orifice cup was also evaluated. Within the limits of experimental error, data reproducibility was unaffected provided elapsed time did not exceed 20 seconds.

TABLE IX
The Effect of Remelting on Slag Fluidity
Slag Composition (Weight Percent): CaO--38.0, MgO--10.0, S_iO_2--52.0

Number of Remelts	Fluidity Stringer Length (Inches)	Furnace Temp. °F
1	17.13	2640
1	19.75	2640
1	17.10	2640
1	18.75	2640
Average	18.18	
2	19.75	2640
2	20.25	2640
Average	20.00	
3	20.50	2640
3	21.50	2640
3	22.50	2640
Average	21.50	

TABLE X
The Effect of Remelting on Slag Fluidity
Slag Composition (Weight Percent): CaO 30.0, CaS 12.9, MgO 12.0, Al_2O_3, 12.7, S_iO_2, 32.4

Number of Remelts	Fluidity Stringer Length (Inches)	Furnace Temp. °F
2	12.4	2600
2	10.5	2600
2	11.0	2600
Average	11.3	
3	12.8	2600
3	10.3	2600
3	14.8	2600
Average	12.7	
4	13.3	2600
4	13.4	2600
4	11.8	2600
Average	12.8	

Calibration of the Herty Fluidity Equipment

To establish a correlation between viscosity and the Herty fluidity of a given slag, the equipment was calibrated by use of a slag of known viscosity (see Table VIII, slag No. 4)[8]. A plot of the literature data for viscosity as a function of temperature is presented in Figure 17. Using the absolute viscosity shown in Figure 17 and Herty fluidity at the same temperature (Figure 18) it is possible to cross-correlate the two measurements so that an indication of viscosity can be obtained from the Herty fluidity results[9]. Such a correlation is shown in Figure 19. Because of the complexity of the physical phenomena involved during the cooling and flow of molten slag down the inclined plane it is not possible to claim great accuracy for the correlation. Nevertheless, it has a practical use in that a correlation of this nature permits a rough estimate of the viscosity of the slag.

Discussion of Results - The Effect of Basicity on Fluidity

To explore the lime requirements of the process, fluidity tests were completed on slags No. 5, 6, 7 (Table VIII) to determine the effect of basicity ratio on slag fluidity. Basicity ratio is the weight ratio of basic oxides (CaO and MgO) to acid oxides (SiO_2 and Al_2O_3) in the slag. In these tests, the weight ratio of silica to alumina was maintained constant at 2.5. This ratio was chosen to simulate the contribution of silica and alumina from the coal ash and limestone that will be used in operation of the combustor. Fluidity measurements were completed at a furnace temperature of 2600°F and related to apparent viscosities through the correlation of Figure 19. Figure 20 shows that the apparent viscosity exhibits a minimum at a basicity ratio of about 1.1. Viscosity at this ratio was approximately six poise.

Increasing the basicity ratio to 1.5 resulted in a viscous slag with an apparent viscosity greater than 22 poise. Decreasing the basicity to 0.8, also increased the viscosity but not at the same rate. At this basicity ratio, an apparent viscosity of approximately ten poise was observed.

A comparison of measured apparent viscosity and literature[8] values is shown in Figure 20. The comparison indicates a reasonable approximation to the actual viscosity.

Effect of Calcium Sulfide Content on Fluidity

Because the process operates with slags containing approximately ten times the sulfur content of the iron-making slags discussed in the literature, the effect of calcium sulfide content on slag fluidity was evaluated. In these tests, calcium sulfide replaced calcium oxide starting with the slag composition given in Table VIII for slag No. 5 (see Table VIII, slags No. 3, 5, 8 for slag composition used in this work). The results of this work are shown in Figure 21 which presents the effect of calcium sulfide addition on the apparent viscosity of the slag having an initial basicity of 1.2. Figure 21 shows the apparent viscosity of the slag was relatively unchanged provided that calcium sulfide addition

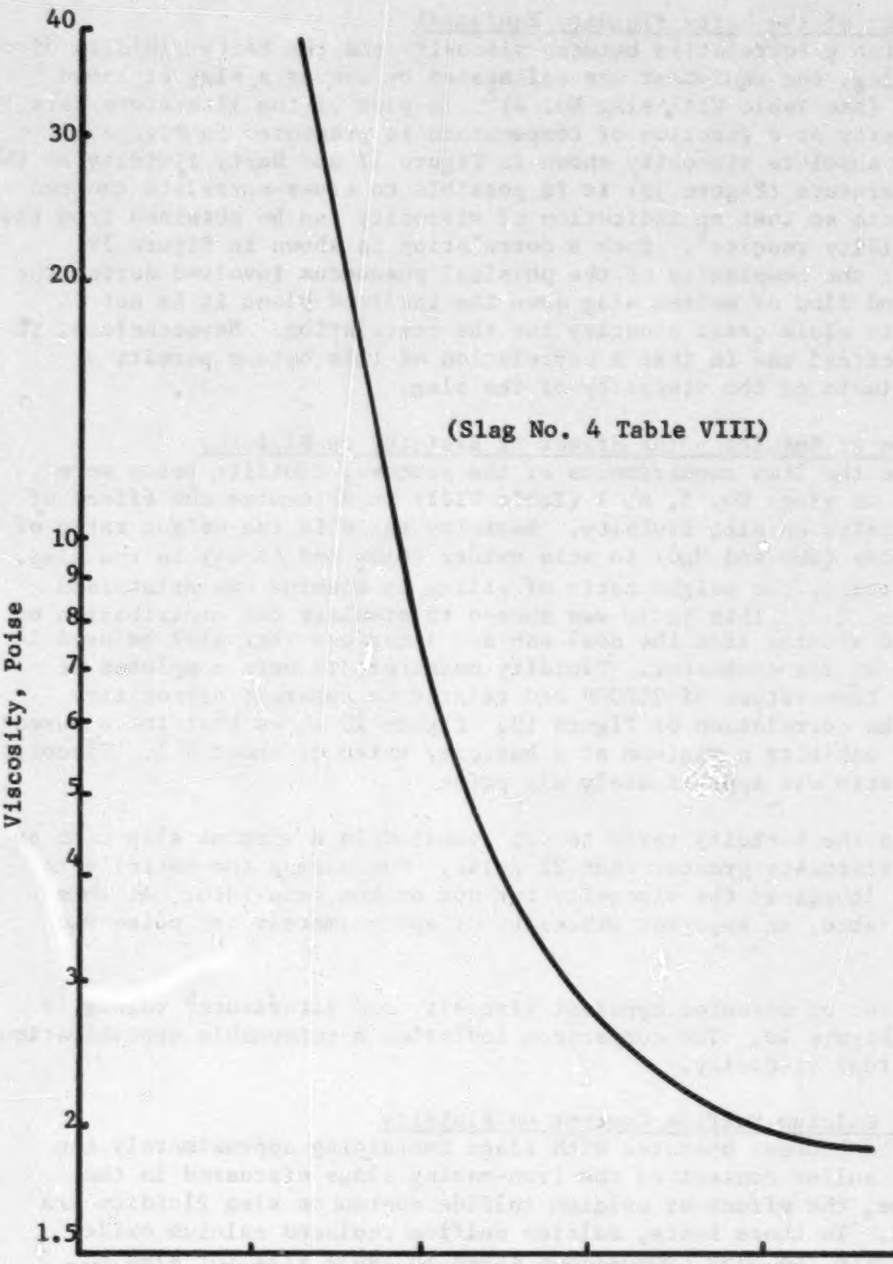

FIGURE 17 - EFFECT OF TEMPERATURE ON VISCOSITY OF A SYNTHETIC SLAG

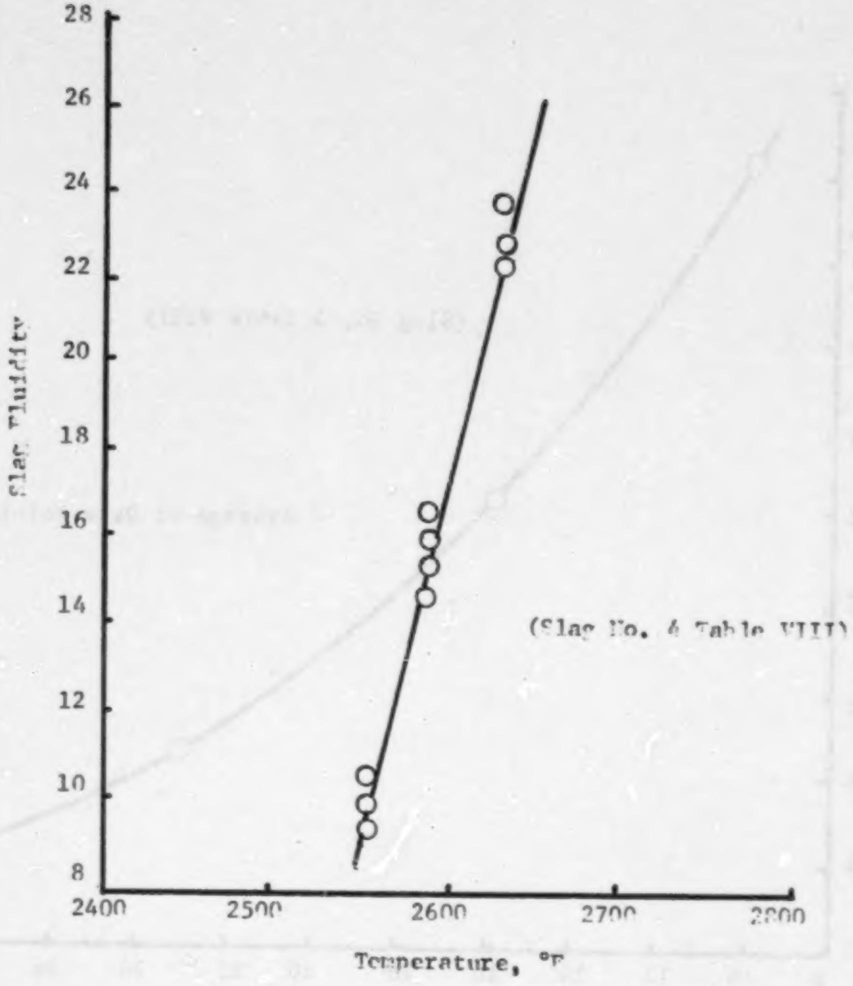

FIGURE 18 - EFFECT OF TEMPERATURE ON SLAG FLUIDITY

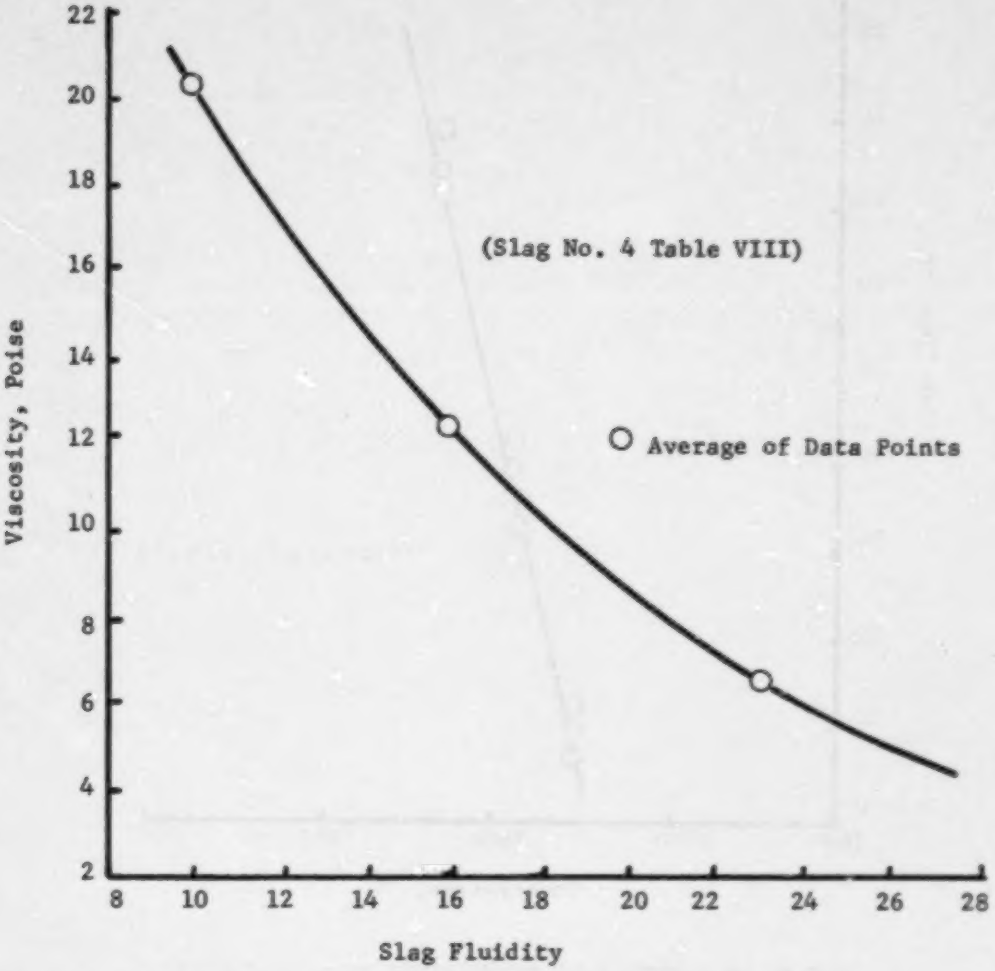

FIGURE 19 - RELATIONSHIP OF SLAG FLUIDITY AND SLAG VISCOSITY

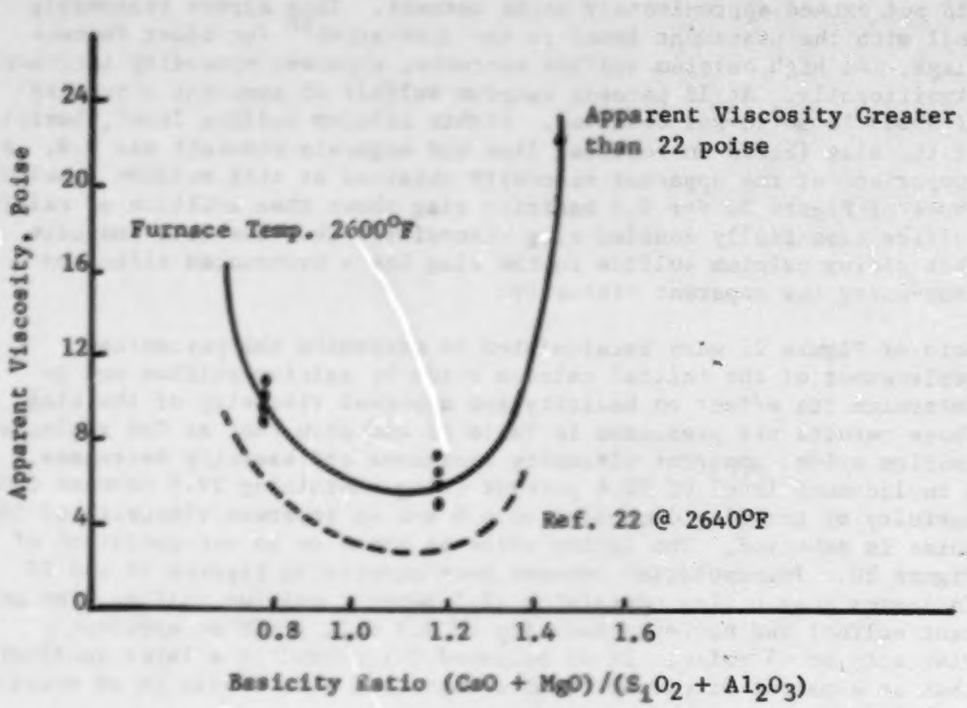

FIGURE 20 - EFFECT OF BASICITY ON APPARENT VISCOSITY OF SULFUR-FREE SLAGS

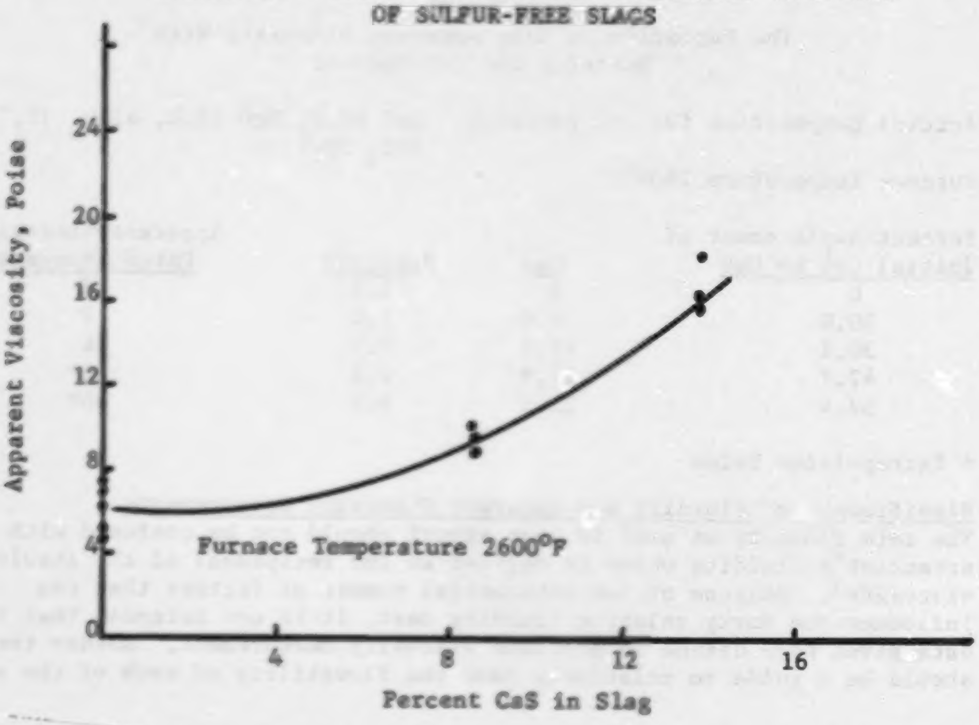

FIGURE 21 - THE EFFECT OF CaS ADDITION ON APPARENT VISCOSITY

did not exceed approximately eight percent. This agrees reasonably well with the statement found in the literature[10] for blast furnace slags. At high calcium sulfide contents, apparent viscosity increased significantly. At 13 percent calcium sulfide an apparent viscosity of about 16 poise was observed. At this calcium sulfide level, basicity of the slag (based on residual lime and magnesia content) was 0.9. A comparison of the apparent viscosity obtained at this sulfide level with those of Figure 20 for 0.9 basicity slag shows that addition of calcium sulfide essentially doubled slag viscosity. Thus the data indicate that adding calcium sulfide to the slag has a pronounced effect on increasing its apparent viscosity.

Data of Figure 21 were recalculated to determine the percentage replacement of the initial calcium oxide by calcium sulfide and to determine its effect on basicity and apparent viscosity of the slag. These results are presented in Table XI and show that as CaS replaces calcium oxide, apparent viscosity increases and basicity decreases. At a replacement level of 52.4 percent (slag containing 22.5 percent CaS) basicity of the slag decreases to 0.6 and an apparent viscosity of 56 poise is expected. The latter value is based on an extrapolation of Figure 20. Interpolation between data comprising Figures 19 and 20 indicates that a slag containing 22.5 percent calcium sulfide (ten percent sulfur) and having a basicity of 0.8 will yield an apparent viscosity of 44 poise. It is believed (discussed in a later section) that an apparent viscosity of this magnitude will result in an operable combustor.

TABLE XI
The Variation of Slag Apparent Viscosity With
Basicity and CaS Content

Initial Composition (Weight Percent): CaO 42.9, MgO 12.0, Al_2O_3 12.7, SiO_2 32.4

Furnace Temperature 2600°F

Percent Replacement of Initial CaO by CaS	Cas	Basicity	Apparent Viscosity Poise (Average)
0	0	1.2	6
20.0	8.6	1.0	9
30.1	12.9	0.9	16
47.7	17.9	0.8	36*
52.4	22.5	0.6	56*

* Extrapolated Value

Significance of Fluidity and Apparent Viscosity Measurements

The term fluidity as used in this report should not be confused with the scientist's fluidity which is defined as the reciprocal of the absolute viscosity[3]. Because of the substantial number of factors that can influence the Herty relative fluidity test, it is not intended that the data given here define an absolute viscosity measurement. Rather they should be a guide to relatively rank the flowability of each of the slags studied. For expediency's sake, fluidity has been converted via the correlations presented earlier to an apparent viscosity which is more generally understood.

In operation of the combustor, it is extremely important that the slag be maintained in a fluid condition to facilitate removal from the combustor and to minimize slag expansion due to entrainment of rising gas bubbles. At the same time, sufficiently high viscosity must be maintained in the slag layer to minimize corrosive attack by the slag material on the refractory lining of the vessel. Consequently, an optimum slag viscosity should be between the extreme low and high.

A blast furnace can operate over a wide range of slag viscosities up to 30 poise. The fluid slag percolates down through a packed bed of solids which implies that flow at these high viscosity levels is not a severe problem. Also this slag desulfurizes pig iron located in the hearth of the furnace. In the combustor, slag need not pass through the interstices of a bed of solid particles, as in the blast furnace. Therefore, it is reasonable to assume that viscosities higher than the limits used in the blast furnace operation can be effectively employed provided that the slag can be poured from the combustor.

In the open hearth, slag viscosities are maintained at a level not much in excess of two poise. The reason for that is that removal of sulfur from steel is normally controlled by diffusion of sulfur through the slag layer. Consequently, to minimize residence time in the open hearth and increase production, low viscosity slags are employed. In the combustor, the kinetics of desulfurizing the iron contained in the vessel are not as critical since (1) a much longer slag residence time can be employed in the combustor, and (2) the iron sulfur content will be approximately 50 times that found in steel making operations. Accordingly, sulfur recovery by the slag does not have the critical dependence on viscosity found in open hearth practice.

For these reasons, the combustor probably will be operable with slags with apparent viscosities of 50 poise or less. The upper limit is on the apparent viscosity for an operable combustor is not precisely known. Effect of high-viscosity fluid slags on slag expansion, corrosion rate and capacity for entrapment of solid particles can only be positively established during operation of the combustor. However, we believe that if the combustor is operated under the guidelines specified in the Engineering Design Recommendations, satisfactory combustor operation will ensue.

Effect of MgO Additions on Slag Fluidity

To determine effect of magnesia on apparent slag viscosity, a series of fluidity measurements were completed at a furnace temperature of 2600°F. In these experiments, basicity and silica to alumina weight ratio were maintained at 1.2 and 2.6 respectively. Magnesium oxide content was varied over the range of 3.2 percent to 12 percent (see slags 5, 9, 10, Table VIII). Results of this work are shown in Figure 22 .

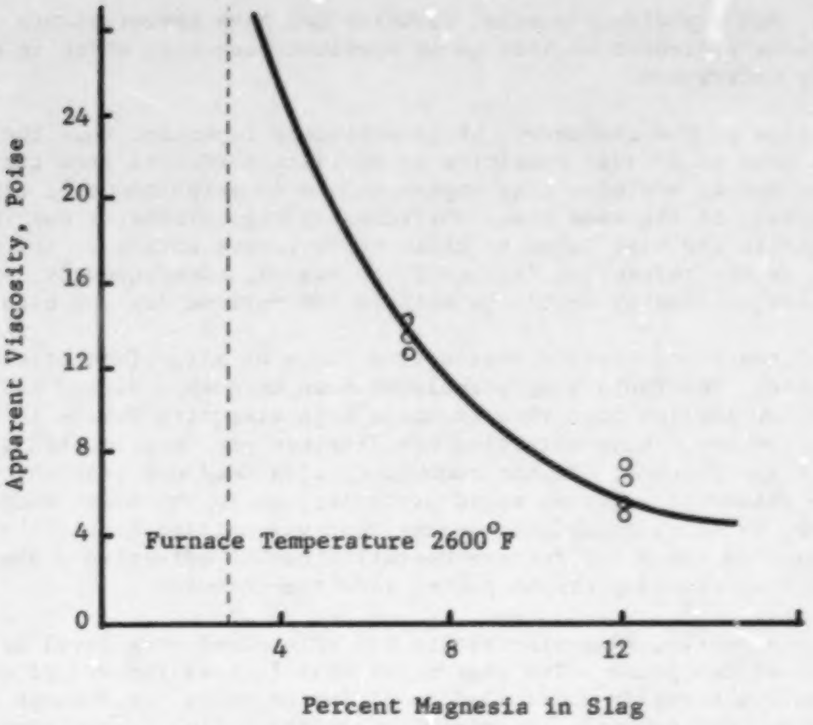

FIGURE 22 - THE EFFECT OF MAGNESIA CONTENT ON APPARENT SLAG VISCOSITY

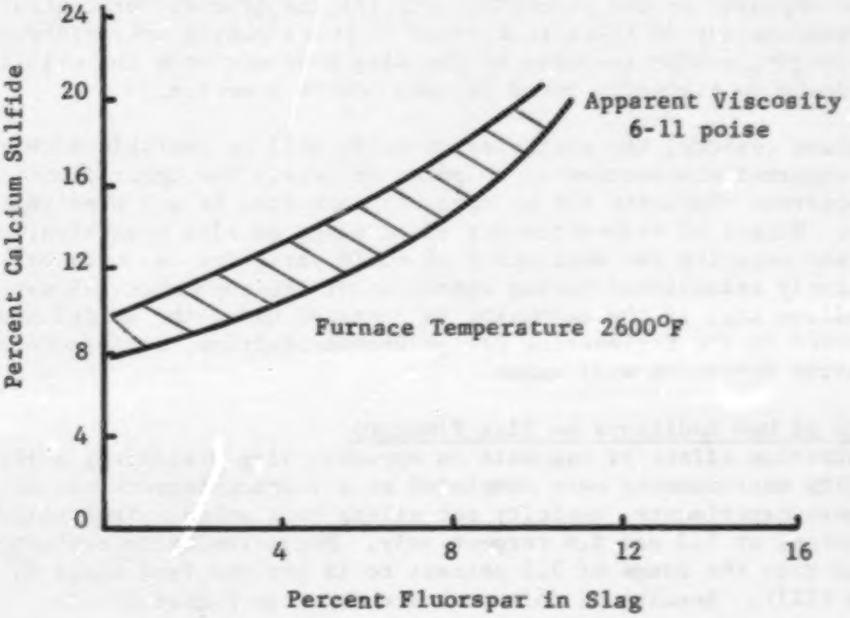

FIGURE 23 - THE EFFECT OF FLUORSPAR ON APPARENT SLAG VISCOSITY

Data reveal that apparent viscosity of the slag decreases with increasing magnesia content. This is consistent with the literature[5], and indicates that magnesium oxide or dolomitic limestones can be used to decrease the overall viscosity of the slag. At an MgO content of 3.2 percent by weight, a fluid slag was not obtained at a furnace temperature of 2600°F. This point, although not shown in Figure 22, is represented by the asymptote for the curve drawn through the liquid slag points. References to the literature[11] indicates that this slag composition borderlines the liquidatus point for the slag.

The results thus indicate that slag apparent viscosity can be decreased by increasing magnesium oxide content. From an economic viewpoint, the MgO concentration should be maintained as low as possible and still maintain good slag fluidity characteristics because MgO is not effective for reaction with sulfur. Selection of the optimum MgO content will be discussed later in the conclusions portion of this section.

Effect of Fluorspar on Slag Fluidity

It is well known[10] that calcium floride (fluorspar, CaF_2) has a dramatic effect on slag viscosity. In general, as the CaF_2 content increases slag viscosity greatly decreases. Because it is desirable to have available a strong fluidity control additive, a series of experiments were completed to determine the effect of CaF_2 on the apparent viscosity of slags containing both high magnesia and high sulfur.

In this work, the percentage of CaS and CaF_2 was varied, but the silica to alumina weight ratio was maintained at 2.5 and the calcium oxide to magnesium oxide weight ratio was maintained at 1.8. Slag basicities covered the range of 0.7 to 1.2 (see slags 5, 11, 12 and 13, Table VIII). Fluidity data were obtained at a furnace temperature 2600°F.

Figure 23 presents results of this work in the form of a plot of percent CaS versus percent CaF_2 with a correlating iso-viscosity curve covering the range of experimental apparent viscosities of six to eleven poises. The pronounced effect of calcium fluoride addition in lowering apparent viscosity of high sulfur bearing slags is readily observed. A comparison of Figures 21 and 23 verifies this. For example, at a 16 percent calcium sulfide content in the slag, apparent viscosity (Figure 20) is approximately 27 poises. By the addition of eight percent calcium fluoride to the same slag, apparent viscosity was decreased to the range of six to eleven poise (Figure 23).

In general, the data show that if a more fluid slag is required, calcium fluoride additions can easily compensate for the deleterious effect of calcium sulfide on apparent slag viscosity. Calcium fluoride will probably not be required to decrease slag viscosity in the operation of the combustor. However, its effect is encouraging as it offers a means of control when required.

Effect of SiO_2/Al_2O_3 Ratio on Fluidity

Effect of coal ash chemistry (particularly the major constituents, silica and alumina, on apparent slag viscosity was investigated. In this study 1.2 basicity slag (Table VIII, slag Nos. 5, 14, 15) having a constant CaO/MgO weight ratio of 3.6 was tested at a furnace temperature of 2600°F. The silica to alumina ratio was varied over the range of one to eight. Results are presented in Figure 24 and show that apparent viscosity of the slag decreases as the silica to alumina ratio increases and asymptotically approaches a minimum value of about four poise. This effect is in agreement with general trends reported by Machin et al. The data are of particular interest since they indicate that variations in coal ash chemistry will not significantly affect the overall viscosity of the slag. It is expected that the typical coal ash will have a silica to alumina ratio varying in the range of about two to three. Consequently, a change of this magnitude in the silica to alumina ratio should present no more than a one poise variation in slag viscosity.

Engineering Design Recommendations

Experimental work completed on the fluidity of various slags for use in the combustor has yielded significant operating guideline parameters. Conclusions and recommendations which should serve as the design criteria for an engineering and economic analysis of the process are as follows:

1. Slag used in operation of the combustor should contain ten to twelve percent MgO and have a lime to magnesia weight ratio of about 1.8 to 2.1.

2. Silica to alumina weight ratio should be maintained as high as possible, preferably above three.

3. Using these ratios, a calcium sulfide content of 22.5 percent (ten percent sulfur) will result in a slag having an apparent viscosity of 44 poise at 2600°F.

4. A typical slag composition meeting these requirements is: CaO 21.5 percent, MgO 12.0 percent, CaS 22.5 percent, Al_2O_3 12.7 percent, SiO_2 31.3 percent.

5. Effects of slag composition on slag expansion due to gas entrapment and ability of the slag to entrap solid particles resulting from the coal and coal ash are not known. These effects must be determined during actual operation of the experimental combustor.

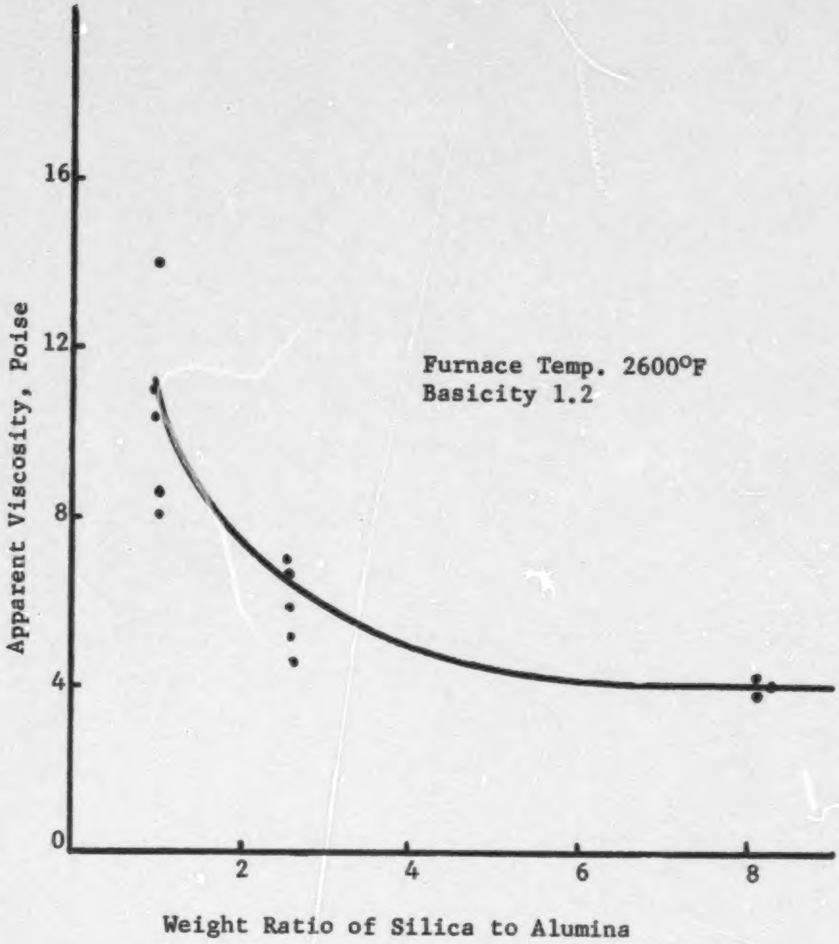

FIGURE 24 - THE EFFECT OF SILICA TO ALUMINA WEIGHT RATIO ON APPARENT SLAG VISCOSITY

SULFUR RETENTION BY SLAG

Introduction

Sulfur is introduced into the combustor via two streams of solids. The first is the stream of sulfates recovered from the acid mine water through the distillation and drying units. These sulfate-bearing solids will be deposited into the combustor slag layer. The second source of sulfur is coal that is injected beneath the surface of the molten iron bath. The coal sulfur exists as pyrite and as organic sulfur bound within high carbon content molecules. From an economic point of view, it is desirable that all of the input sulfur be recovered as calcium sulfide in the molten slag. Of particular importance, both from a technical and economic viewpoint, is the distribution of sulfur between the liquid slag and molten iron at steady state or equilibrium. This distribution, termed the partition ratio, is defined as the percentage of sulfur in the slag divided by the percentage of sulfur in the iron. To maximize the operating credits associated with the combustor, it is necessary that the partition ratio be as high as possible. This is to say that the bulk of the sulfur should exist in the slag with very little in the iron phase. If high partition ratios (20 or more) can be obtained at relatively low excess lime, lime consumption will be low and operating costs will be reduced. Additionally, as the partition ratio increases, sulfur content in the iron will decrease which should improve the by-product value of the iron produced in the process.

A considerable amount of literature is available concerning the partition ratio and desulfurizing power of blast furnace and steelmaking slags[5,12]. In general, high partition ratios are associated with increasing temperature, reducing atmospheres, low slag viscosities and high slag basicities. However, the literature data are generally confined to slags containing less than two percent sulfur. Unlike steelmaking practice, the combustor will operate with a slag containing large amounts (about ten percent) of sulfur. For such slags, no literature data are available to estimate expected partition ratios.

Calcium sulfide solubility for a $CaO-Al_2O_3-SiO_2$ system has been evaluated over a fairly broad range of compositions[13]. Depending upon the region of the slag system, sulfur solubility varied from about two to six percent. For a $CaO-SiO_2$ system, saturation sulfur concentration increased from about three to six percent with increasing concentration of silica in melts liquid at 1550°C [14,15]. No data were available for determining the effect of undissolved CaS on partition ratio. Accordingly, a laboratory investigation was completed to determine the partition ratio and expected sulfur contents for both iron and slag when a high sulfur bearing slag ($CaO-MgO-SiO_2-Al_2O_3$ system) was placed in contact with molten iron. No attempt was made to measure the maximum solubility of CaS in these slags. Rather, the work was directed to an applied research effort to evaluate the overall effect of high sulfur slag (regardless of solution state) on combustor operating parameters.

Experimental Procedure

Two separate experimental procedures were used in the sulfur partition ratio studies. The first procedure consisted of measuring equilibrium partition ratios for a system employing sulfur-free slags and high-sulfur molten iron. In these studies, a $CaO-MgO-SiO_2-Al_2O_3$ slag of the composition given for slag G in Table XII was employed. Master batches of this slag were prepared from reagent grade materials. The well blended mixture was placed in graphite crucibles and heated to 2600°F for five hours. The slag was then removed from the furnace, cooled, crushed, and reheated to 2600°F. This procedure was repeated three times[4,6] to provide a slag of uniform composition. After three remelts, the slags were ready for use in the partition ratio test. In these tests, the molten iron bath was prepared by melting reagent grade iron powder which was then saturated with graphite. Once the iron was saturated, iron sulfide was added to the melt in varying proportions to produce high sulfur pig iron. In later experimentation, the iron powder was replaced with a four percent carbon pig iron to avoid the necessity of saturating the melt with carbon.

TABLE XII

Slag Compositions Used in Partition Ratio Studies

Slag Identification	Weight Percent of Component CaO	MgO	SiO_2	Al_2O_3	CaS	Basicity
A	29.0	8.0	26.3	10.2	26.6	1.01
B	27.2	7.8	27.5	10.7	26.8	0.91
C	26.0	7.2	29.0	11.2	26.6	0.82
D	31.7	8.8	23.7	9.4	26.5	1.22
E	37.3	10.4	28.1	11.0	13.2	1.22
F	25.9	7.2	19.4	7.7	39.8	1.22
G	42.9	12.0	32.4	12.7	0.0	1.20

To obtain partition ratio data, a known weight of molten slag (previously melted in a graphite crucible) was added to a graphite crucible containing the molten iron. The ratio of slag weight to iron weight was maintained at 0.3. The crucible containing the molten iron-slag mixture was then covered with a graphite lid and maintained at a furnace temperature of 2600°F. Furnace temperature was controlled to ± 25°F of the set point temperature. The furnace chamber was purged with argon for duration of the run. At the end of the designated test time, the graphite crucible was removed from the furnace and cooled to room temperature in an argon atmosphere. The iron and slag samples were then removed from the crucible and prepared for analysis. The slag was crushed to -100 mesh to free entrained particles of iron which were removed by dry magnetic separation. Representative samples of both the slag and iron were taken for carbon and sulfur analysis.

The second series of partition ratio tests differed from the first in that sulfur-free iron was used. In these tests, sulfur in the form of calcium sulfide was added to the slag. In this manner, the effect of sulfur transfer from the slag to the iron could be established. Otherwise, the experimental procedure was identical to that outlined above.

Results and Discussions

Results of this work are presented in Figure 25 which shows the effect of time-at-temperature on the approach to partition ratio equilibrium. A partition ratio of about 35 was achieved after 50 hours in the furnace. In general, the equilibrium partition ratio obtained from melts in which the sulfur was initially contained within the iron are about ten percent lower than that obtained from the reverse or high sulfur slag condition. This is due to the difficulty of maintaining a four percent carbon level in the molten iron. Sulfur removal from the iron is accompanied by carbon consumption which in turn decreases the equilibrium partition ratio that may be achieved. At time zero, when all of the sulfur is in the slag, the partition ratio is infinite. Consequently, as soon as sulfur is transferred from the slag to the sulfur-free metal, the ratio drops extremely rapidly as shown by the upper curve of Figure 25. On the other hand, when all of the sulfur is initially contained in the metal, the partition ratio is zero and gradually builds as sulfur is transferred to the slag (see lower curve of Figure 25). In either case, both methods yield essentially the same equilibrium results.

Figure 26 presents the effect of contact time on the sulfur content of iron (initially containing no sulfur) exposed to slags (Table XII, slags D, E, F) containing about six to eighteen percent sulfur. At equilibrium (about 50 hours) the small sulfur loss by the slag results in relatively low iron sulfur content. In general, the sulfur content in the iron tends to increase as the initial slag sulfur increases. However, even at an initial slag sulfur content of 17.7 percent, the equilibrium percent sulfur in the metal was only 0.25 percent.

Consequently, it can be conservatively estimated that in the commercial operation of the combustor the iron produced will contain less than 0.3 percent sulfur.

Data on Figures 25 and 26 also present some interesting insight into the slag and metal sulfur reactions that may be expected to occur in the commercial combustor. Because the steady state sulfur content in the metal is relatively low, it is unlikely that any of the sulfur introduced into the slag by the solids recovered from the distillation unit will enter the molten metal phase. Under commercial conditions there should be sufficient sulfur and pyrites in the coal so that the bulk of the transfer will occur from the metal to the slag. This would imply that reduction of sulfate to sulfur will occur primarily in the slag phase or at the slag-iron interface.

Because the combustor will operate commercially with a slag having a basicity of about 0.8 to 1.0, a series of tests were completed to determine effect of slag basicity on equilibrium partition ratio. For this work, slags A, B, C, D, whose compositions are given in Table XII were used. Results of this work are presented in Figure 27. Data indicate that the partition ratio decreases slightly with decreasing basicity. This is consistent with the literature[5] which indicates that

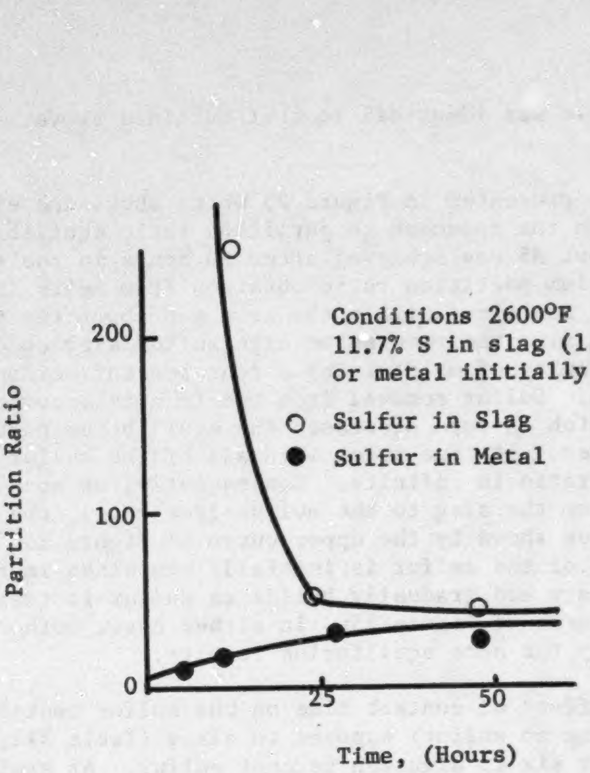

FIGURE 25 - THE EFFECT OF TIME ON THE APPROACH TO PARTITION RATIO EQUILIBRIUM

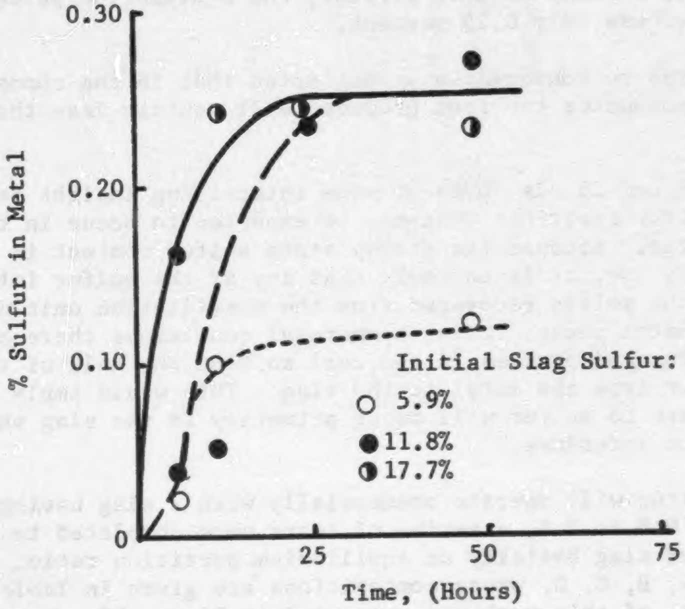

FIGURE 26 - THE EFFECT OF CONTACT TIME ON THE SULFUR CONTENT OF IRON

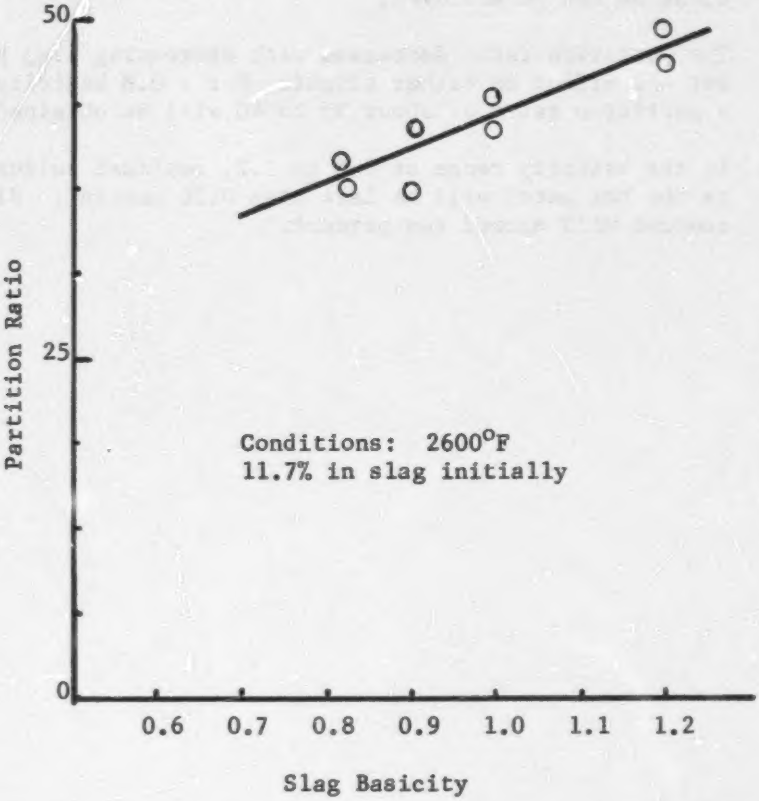

FIGURE 27 - THE EFFECT OF SLAG BASICITY ON EQUILIBRIUM PARTITION RATIO

better partition ratios are obtained at high slag basicities. For a 1.2 basicity slag, a partition ratio of about 45 was obtained. The partition ratio decreased linearly with decreasing slag basicity until at 0.8 basicity a partition ratio of about 38 was achieved. The decrease in partition ratio was rather slight.

Engineering Designs Specifications

Based on the results of the partition ratio study, the following recommendations are given:

1. At a slag to iron weight ratio of 0.3 partition ratios of about 50 can be achieved.
2. The partition ratio decreases with decreasing slag basicity but the effect is rather slight. For a 0.8 basicity slag, a partition ratio of about 35 to 40 will be obtained.
3. In the basicity range of 0.8 to 1.2, residual sulfur content in the hot metal will be less than 0.30 percent. Slag sulfur content will exceed ten percent.

DETAILED SLAG CHARACTERIZATION

Based on the fluidity measurements of various types of slags, three slags were chosen covering the range of basicities of 0.83 to 1.01 as suitable for use in the operation of the combustor. In the slags, the silica to alumina ratio and the lime to magnesia ratio were maintained constant at about two. The slags contained sulfur in the form of calcium sulfide (16.9 to 18.0 weight percent). Composition of these slags is presented in Table XIII.

These three slags were chosen as the basic slags for detailed study and were used throughout the course of this work as described in the following sections.

APPARENT DENSITY OF HIGH SULFUR BEARING SLAGS

Experimental Equipment and Procedure

Two techniques were employed to measure apparent density of slags as a function of particle diameter. Standard pychnometer and burette methods were employed. Of the two, the bulk of the measurements were conducted using the burette method. Within the limits of sample composition variations, the latter method was considered as reliable as the pychnometer technique, but much faster.

The experimental procedure consisted of filling a 25 ml burette to a known level with carbon tetrachloride. The burette was graduated in 0.1 ml increments and was capable of being read to ± 0.05 ml. Carbon tetrachloride was used as the displacement medium to prevent any reaction with the sulfur constituents in the slag. Once the burette was filled to some level with liquid, a known weight of solids was introduced into the fluid. From the solids' weight and volume change read from the burette, the apparent solids' density was calculated.

Discussion of Results

The effect of particle diameter on apparent density of 0.82, 0.90, and 1.01 basicity slags shown in Table XIII is presented in Figure 28. All slags show the same effect in that particle apparent density increases as the average diameter decreases. Within the limits of experimental error, the two lower basicity slags (0.82 and 0.90) yield a common curve. However, the higher 1.01 basicity slags yield a significantly lower apparent density. Although the reason for such behavior is not known conclusively, the difference is attributed to variations in the crystal structure upon solidification[5]. In the relatively narrow range of basicities 0.82 and 0.90, the crystal structure of the solid phases would tend to resemble each other. However, as the basicity was increased to 1.0 and beyond, the crystal characteristics would shift as estimated from phase diagrams for analogous systems[5].

TABLE XIII
Slag Compositions Used in Characterization Studies

	Composition, weight percent					Ratios	
Basicity	SiO_2	Al_2O_3	MgO	CaO	CaS	SiO_2/Al_2O_3	CaO/MgO
0.82	30.0	15.0	12.3	24.7	18.0	2.00	2.01
0.90	28.6	14.4	13.0	26.0	18.0	1.99	2.00
1.01	27.6	13.8	13.9	27.8	16.9	2.00	2.00

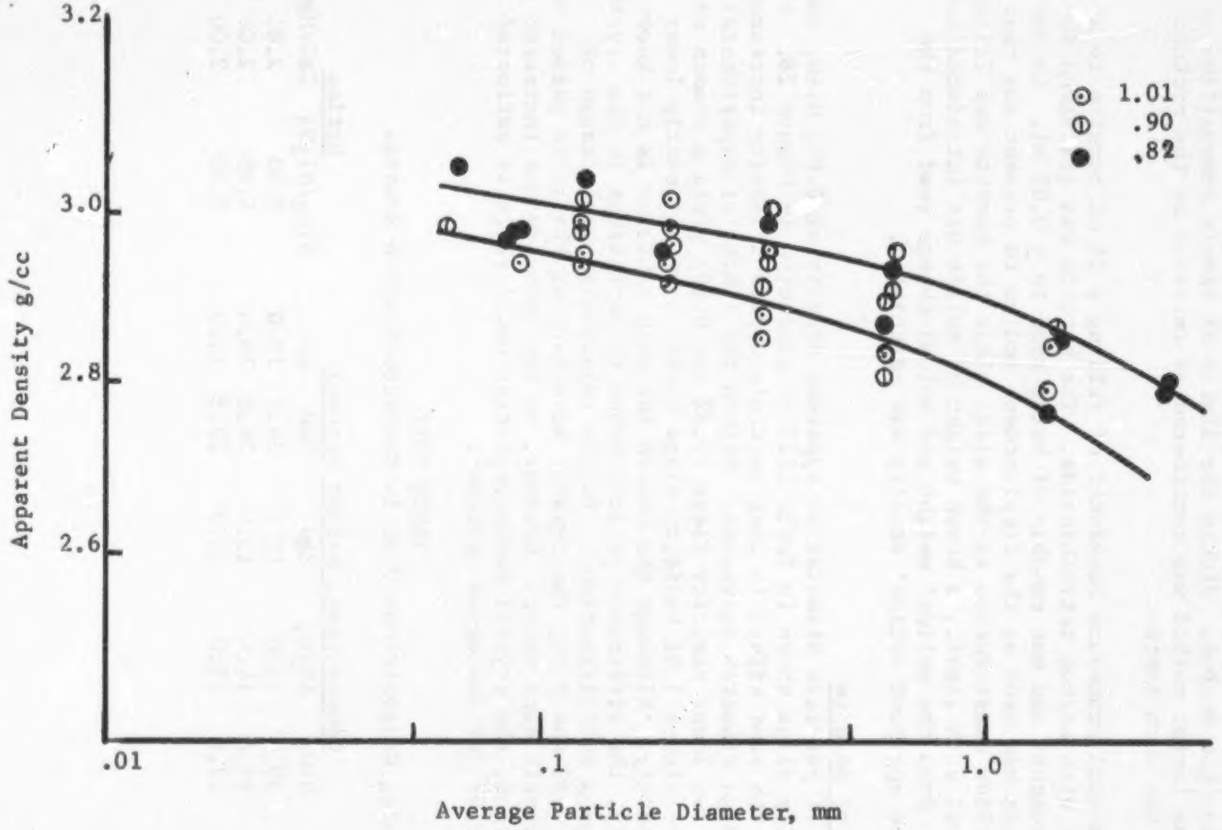

FIGURE 28 - THE EFFECT OF PARTICLE DIAMETER ON APPARENT DENSITY

VISCOSITY MEASUREMENTS

Introduction

Surface tension and viscosity data are not available for the high sulfur bearing slags that will be used in the combustor. To reasonably estimate the heat and mass transfer that occurs within the combustor, an experimental program was initiated to measure these physical properties. For these measurements, an oscillating-bob viscometer[2,11] was constructed and a maximum bubble-pressure device[16] for surface tension measurements was designed.

The theory and technique for determining viscosity and surface tension values will not be discussed in this report, as detailed explanations can be found in the literature[2,11,16]. Briefly, the viscosity measurement is obtained by the logarithmic decrement method[2]. In this technique, an initial torque is given to a wire from which a platinum bob is suspended and immersed in the fluid whose viscosity is to be measured. Depending upon the magnitude of the viscous forces resisting the rotation of the bob, a characteristic dampened oscillation frequency is obtained. The decrement, or the ratio of two successive dampened oscillation amplitudes, is a function of the fluid viscosity.

In the maximum bubble pressure surface tension measurement, a platinum tube is immersed vertically into the molten slag. Argon is forced down the tube and the maximum pressure achieved prior to release of a gas bubble is recorded. The surface tension of the fluid is a function of the gas pressure reading and the depth of immersion of the tube in the fluid[16].

Experimental Procedure

Equipment (see Figure 29) used for the viscosity measurements was similar to that employed by Machin and Hanna[11]. It was of the oscillating or torsion pendulum type. One major modification was made to the assembly which related to the method by which the angular displacement or oscillation was measured. Machin and Hanna used a mirror that reflected light to measure the angular displacement. In this study, angular displacement was measured by the interruption of a photocell whose output was made to be proportional to the radial deflection of the suspension torque wire. Except for this and some minor modifications with regard to the length of the torsion wires and more convenient means for setting the vibrating system in motion, other features were comparable.

The oscillating bob and crucible were made from platinum. The equipment dampening constant which is a function of the shape and dimensions of the bob and crucible was evaluated by calibrating the equipment in an oil of known viscosity, which covered the range of 0.6 to 81 poises as a function of temperature. The calibration work showed that the assembled apparatus used in this work could effectively cover the range of eight to 40 poise.

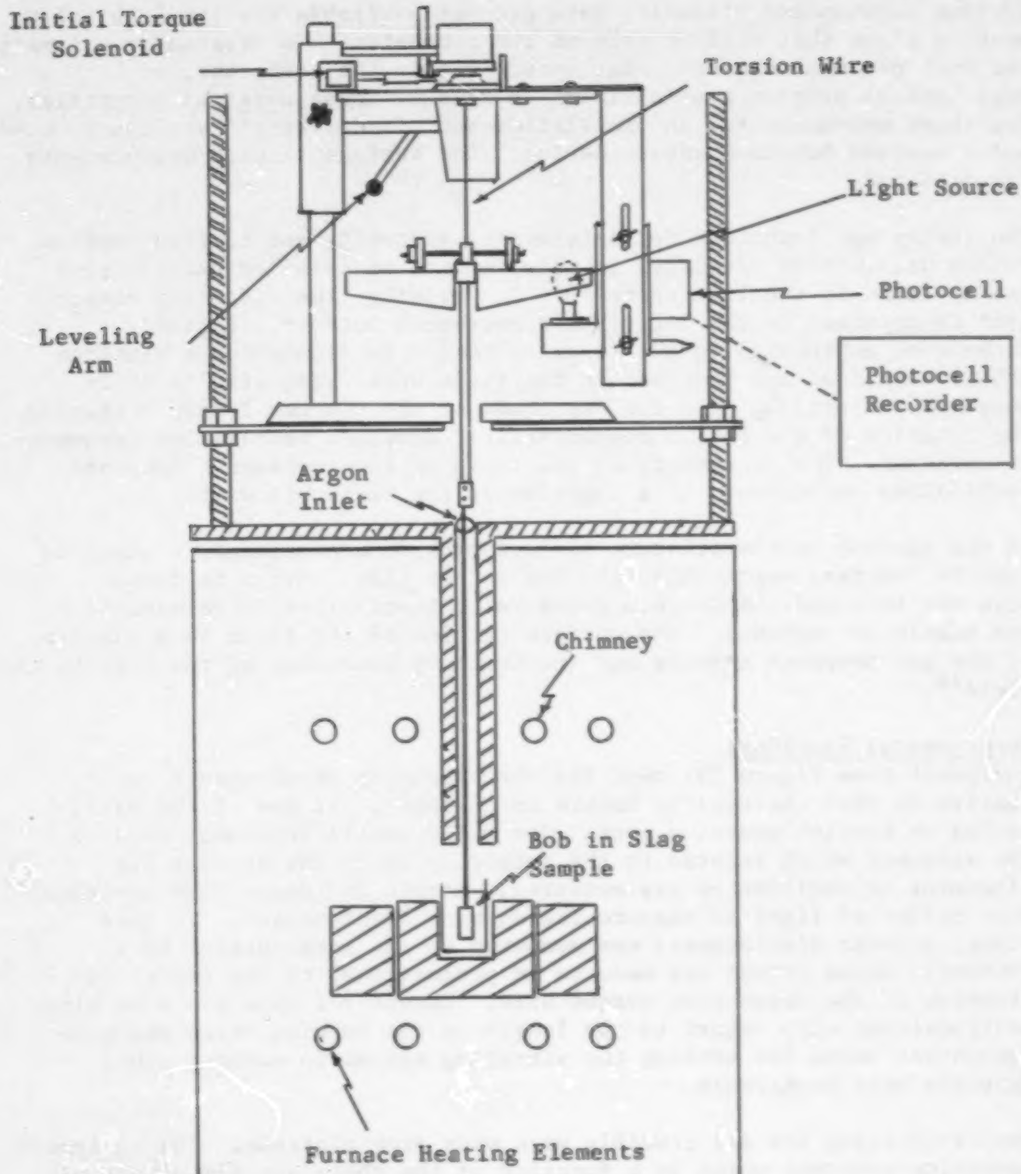

FIGURE 29 - VISCOSIMETER

Discussion of Results

During the first experiments to determine viscosity of high sulfur content slags (slag No. 3 Table VIII) a severe operating problem was encountered. The platinum crucible and bob were severely attacked by the molten high sulfur bearing slag and resulted in total failure of the equipment. The severe corrosive attack of the slag on the platinum caused holes in the crucible walls. The platinum bob was equally damaged and was of no further use in the experiments.

New crucibles and osciallating bobs were constructed from pyrolitic graphite rods. Viscosity tests depend on the liquid wetting the walls of the container and the bob to cause the liquid to shear upon itself. Since slag does not wet graphite, the internal surface of the crucibles and the external surface of the oscillating bob were corrugated. The corrugations were made parallel to the longitudinal axis of both the crucibles and the bob in the form of deep grooves, approximately ¼-inch deep by 3/16-inch wide. When slag filled the grooves of the bob and crucible, the rotation of the bob caused the slag to shear upon itself.

To determine whether this method was feasible, the equipment was recalibrated using the oil mentioned previously. Tests were then completed on molten slags of known viscosity[8] (slag No. 7, Table VIII). These measurements were conducted at a furnace temperature of 2650°F. Actual slag temperatures, as measured by the immersion of the platinum rhodium thermocouple into the slag, indicated a slag temperature of 2570°F, approximately 80 degrees lower than the furnace temperature. A number of viscosity measurements were made at this temperature to determine the effect of time on slag viscosity. It was known that significant air infiltration existed in the furnace and was oxidizing the graphite rods. Consequently, the time measurement was taken to determine the effective length of time that a graphite rod would be employed without severely influencing the viscosity measurements.

These results are shown in Figure 30. The initial viscosity measurement was the highest (approximately 16) when the graphite bob was first inserted into the furnace. This agrees reasonably well with the literature[8] for sulfur free slags of this composition, where the reported viscosity at 2552°F is 14 poise. As time increased, viscosity decreased rather rapidly. This was primarily attributed to the oxidation of the graphite rod which had the effect of lowering the equipment constant. It should be mentioned that the furnace was continually purged with argon to minimize air infiltration but air entry could not be prevented entirely. Because of the expense and work required to machine the rods and crucibles, the argon purge was increased in an effort to minimize oxidation.

High sulfur bearing slags were then evaluated to determine the effect of sulfur content on slag viscosity. In these measurements, and at the argon flow employed, a maximum furnace temperature of 2650°F was achieved. Attempts to measure the actual slag temperature were of no avail as the thermocouple was immediately attacked and destroyed by the high sulfur bearing slags. Based on work with sulfur-free slags, it is estimated that the slag temperatures were approximately 100°F lower than the indicated

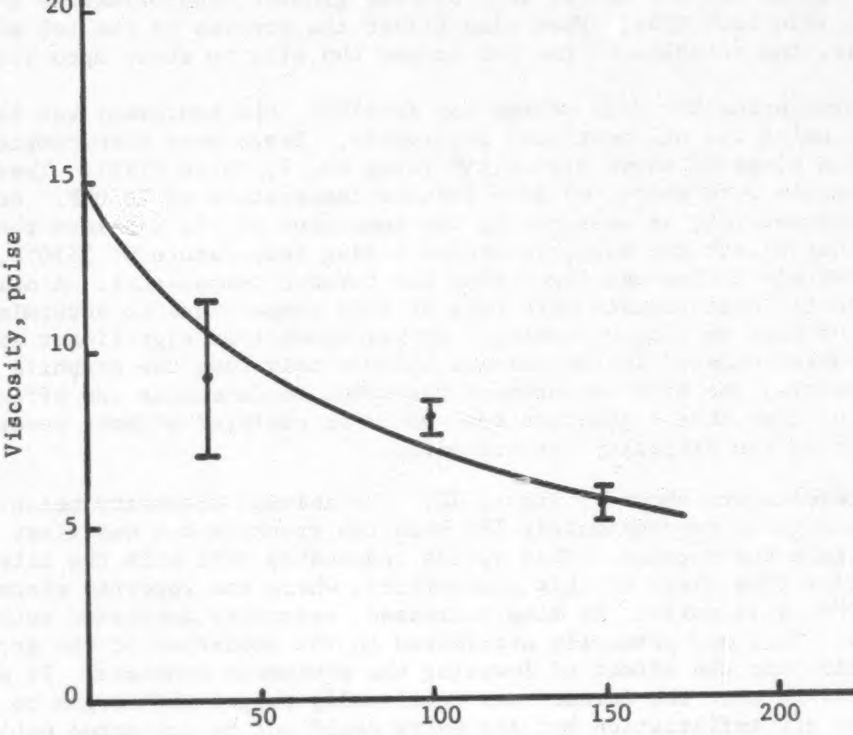

FIGURE 30 - EFFECT OF CARBON BOB RESIDENCE TIME IN FURNACE ON MEASURED VISCOSITY

furnace temperature. At these low temperatures, the bulk of the viscosity measurements was outside the range of the instrument. However, measurements of 0.82 basicity slag show that viscosity increases with increasing calcium sulfide content. At an estimated slag temperature 2550°, viscosities of 16, 22 and 40 poise were obtained at calcium sulfide concentrations of zero, six and twelve percent respectively. At higher calcium sulfide contents, viscosity was outside the range of the viscometer.

At the higher argon gas flow rates employed in this latter work, a crust was observed on the surface of ths slag in the crucible. When the oscillating bob was introduced in the crucible, force had to be exerted to break through the top of the slag. Consequently, it is highly probable that the surface of the slag was receiving some cooling from argon introduction. After considerable stirring, a fluid surface was maintained and viscosity measurements were completed. However, it is probable that some solid particles did exist in the slag. Since this method of measurement is subject to severe perturbations in a two-phase system, viscosity measurements can be only estimates. Based upon freezing point data, an estimate of the actual slag temperature can be made. Freezing points of 0.82, 0.9 and 1.01 basicity slag were found to be 2450, 2340, and 2447°F respectively. Based on this knowledge and the temperature difference measured by thermocouples inserted in sulfur-free slag, it is probably true that the slag temperature was in the neighborhood of 2550°F. Because slags of this nature will experience a halving of the viscosity for 100°F rise in temperature[8] it is reasonable to expect that slag viscosity at an actual temperature of 2600°F will be about 40 to 50 poise, at a calcium sulfide content of about 20 percent.

Because of the sulfur attack on the platinum equipment, no surface tension measurements were attempted.

Engineering Design Recommendations

Because of the experimental difficulties encountered in measuring the viscosity and surface tension of high sulfur bearing slags, no reliable absolute measurements were possible. However, the viscosity data tend to support conclusions and recommendations derived from fluidity measurements reported in an earlier section.

EXTERNAL SURFACE AREA

Introduction

As a part of the detailed slag characterization study, external specific surface area was determined for each of the three slags of Table XIV as a function of particle size. The external surface area measurements were a useful correlating factor in kinetic studies for desulfurization and neutralization of acid mine water. This section presents the results obtained from the experimental investigation of the external surface areas of high-sulfur bearing slags.

TABLE XIV
Comparison of Surface Areas for Glass Beads
Determined by Air Permeability and Micrometer Methods

Glass Bead	Specific Surface, sq cm/gram	
Diameter, mm	Air Permeability	Micrometer
3.15	7.9, 7.7, 7.4	7.6
4.06	5.5, 5.8, 6.1	5.9
5.95	3.9, 4.1, 4.4	4.1

Theory

The theory relating the specific surface of solids to the pressure drop obtained in the laminar flow of fluids through packed beds of granular materials was first formulated by Kozeny[17]. His equation relates the volumetric flow of fluid to the pressure drop established per unit length of bed, the specific surface of the solids, the porosity of the bed, the viscosity of the fluid, and the cross-sectional area of the packed column. Since all quantities are easily measured, the specific surface of the materials is readily obtained by measuring the appropriate variables and calculating the specific surface from the equation:

$$S = \frac{14}{d}\left(\frac{E^3}{Pv\,(1 - E)^2}\right)^{\frac{1}{2}}$$

where, d = apparent density of the solids, grams/cu cm
E = porosity
v = kinematic viscosity of fluid, cm^2/sec sq cm/sec
S = specific surface, sq cm/gram
P = permeability of packed bed, cm/$(sec)^2$

The above equation is valid provided laminar flow exists through the packed bed.

Equipment and Experimental Procedure

Equipment used to measure the external specific surface area by air permeability methods is well known and will not be presented here[17]. Essentially, the apparatus consists of a flow meter, an inclined manometer and a graduated (volumetrically) sample holder of known cross-sectional area.

The experimental procedure was as follows. A known weight of solids (whose apparent density is known) was poured into the graduated glass sample tube holder and slightly vibrated to maximize packing of the solids. Sample volume and height was determined from the graduation and cross-sectional area of the sample tube holder. Bed porosity was calculated from known weight, density and volume of the packed bed. A known volume of air was then caused to flow downward through the packed bed. Pressure drop was measured across the bed once flow reached a steady state. In general, pressure drop measurements were obtained for five different flow rates. For the equipment used in this work, laminar flow occurred when the air flow rate was maintained at less than five cc per second. From the pressure drop and flow rate data, the permeability constant for the system was calculated. Using this value along with the kinematic viscosity of air, porosity and apparent density of the solids the specific surface was calculated using the equation presented earlier.

Discussion of Results

Before conducting surface measurements on the synthetic slag, equipment was standardized by measuring the surface areas of glass beads. In this work, glass beads having nominal diameters of 3, 4 and 6 were employed. Specific surface of the glass beads was determined initially by micrometer measurements of the diameter and by obtaining a particle count per unit weight for each size of glass bead. In this manner, it was possible to calculate their specific surfaces in terms of square centimeters surface area per gram of sample. A comparison of the specific surface obtained by micrometer measurement and air permeability methods is presented in Table XIV. Agreement between the two methods was excellent.

The effect of slag basicity and particle size on external specific surface for the synthetic slags is presented in Figure 31. The data show that a difference exists in the external surface areas for each of the slags provided that the particle diameter is greater than 0.2 mm. At the smaller particle sizes (within the limits of the experimental error) the data are adequately defined by one common curve.

It is not clear why there should be a divergence in the specific surface area measurement at the larger particle sizes. Based on the apparent density data presented earlier, it would be expected that the lower basicity slags would have the least specific surface since they were heavier. However, this density variation is not sufficient by itself to account for the spread in the data. Differences are probably the result of significant variations in fracture characteristics of the materials.

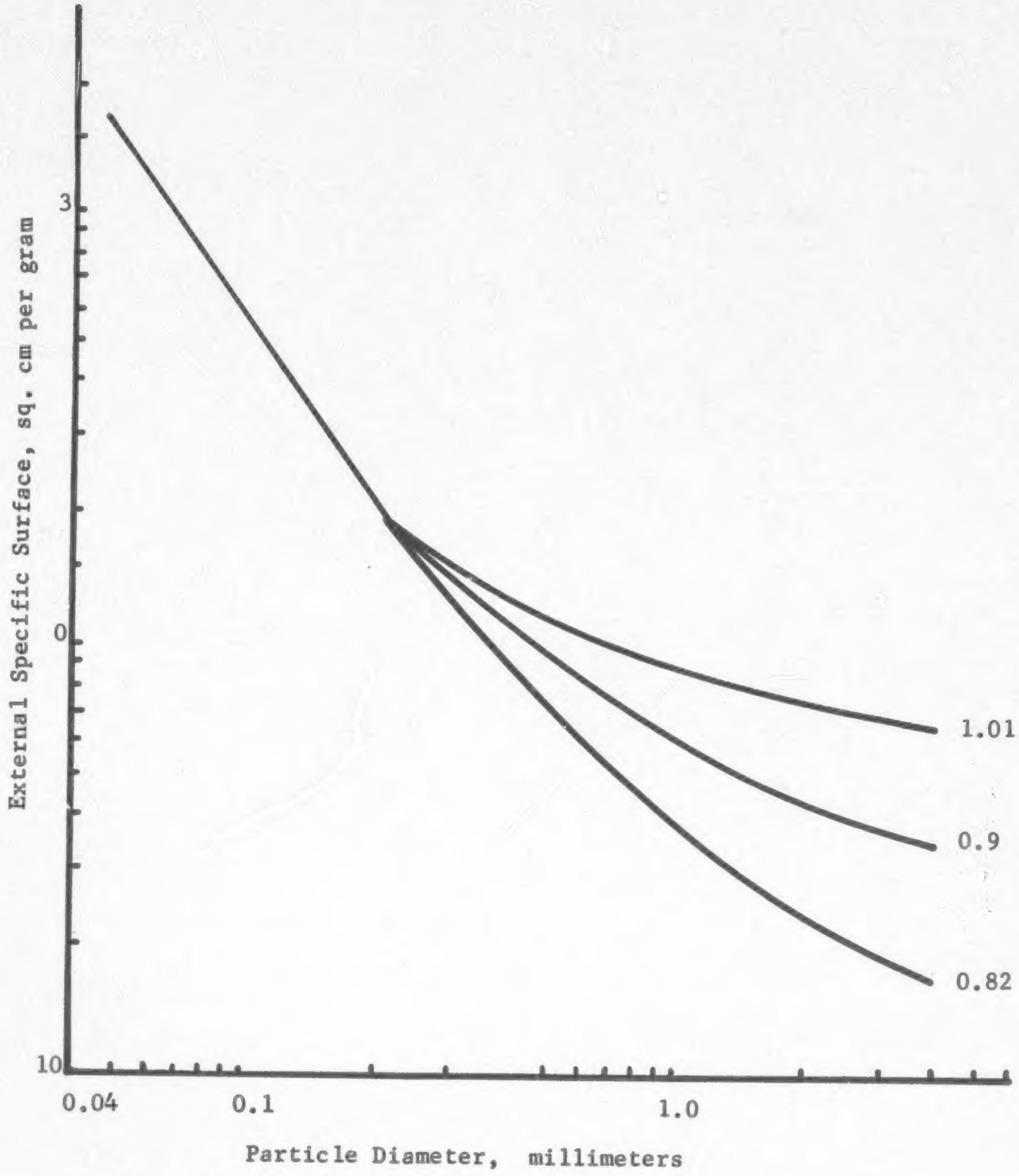

FIGURE 31 - THE EFFECT OF SLAG BASICITY AND PARTICLE SIZE ON EXTERNAL SPECIFIC SURFACE

TOTAL SPECIFIC SURFACE AREA

Introduction

As part of the detailed characterization work, total specific surface area for each of the synthetic slags shown in Table XIII was determined. Surface area measurements were obtained with a Perkin Elmer Shell Model 212 D Sorptometer.

The principle of the surface area measurement is based on measurement of an amount of gas adsorbed by the solid sample. In this method a known mixture of nitrogen and helium is passed over the sample in a sample tube and the effluent is monitored by a thermal conductivity detector. While the gas is flowing to the sample, the sample tube is cooled by immersion in a bath of liquid nitrogen. The cooled sample adsorbs a certain amount of nitrogen from the gas stream which is indicated on a recorder chart as a peak. The area of this peak is proportional to the volume of nitrogen adsorbed. After equilibrium is established, the recorder pen returns to its original position and the liquid nitrogen gas is removed from the sample tube. As the sample tube warms, the adsorbed gas is released and enriches the effluent gas passing through the sample tube. A desorption peak is then obtained which is in the reverse direction of the adsorption peak. When desorption is complete, a known volume of nitrogen is added to the nitrogen helium stream and the resulting (calibration) peak is recorded. By comparing the areas of the desorption and calibration peaks, the volume of nitrogen adsorbed by the sample can be calculated.

Discussion of Results

Effect of slag basicity on the total specific surface area is presented in Figure 32. The specific surface decreases from about 5.4 square meters per gram for the 0.82 basicity slag to a low of about 1.5 square meters per gram for the 1.01 basicity slag. It appears that the higher basicity slags, because they are more fluid in the liquid conditions, tend to yield more glass-like solids with low porosity. Attempts were made to measure pore size distribution of the slags but to no avail. Discussions with the manufacturer of the Sorptometer indicated that at these low surface areas and porosities, the equipment was being operated at its minimum reliability levels. To overcome this problem, different cells would have to be purchased to accommodate our materials. Inasmuch as the total surface area measurements did not appear to be a good correlating variable for other work, purchase of additional equipment was not made. Consequently, pore size distributions were not made.

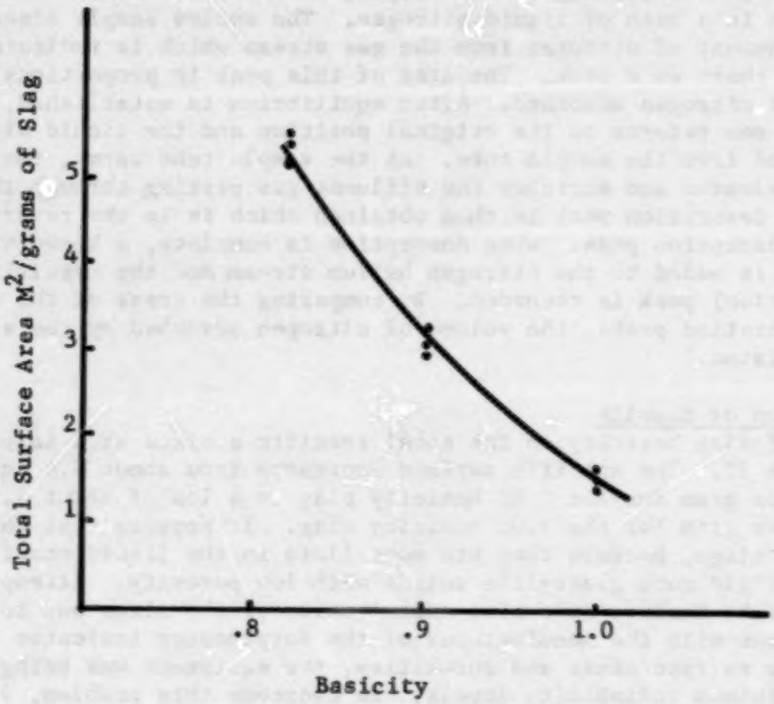

FIGURE 32 - THE EFFECT OF BASICITY ON TOTAL SPECIFIC SURFACE AREA

CRUSHING ENERGY REQUIREMENTS

Introduction

Sulfur recovery from slag and acid mine water neutralization with slag can both be accelerated by crushing the slag to a smaller size. Therefore, the economies of these operations can be affected by cost of crushing or grinding slag. Because both the capital cost and the operating cost for crushing equipment depend on the crushing energy required, a study of crushing energy requirements for slag was undertaken.

Experimental Equipment and Procedure

A modified version of the drop weight machine used by Gross[25] was adopted for this work. A schematic diagram of the apparatus is presented in Figure 33. The crushing chamber was housed in a cylindrical die made of stainless steel construction. The crushing chamber consisted of a cavity located within the die and was 6.1 centimeters in diameter. A smooth-fit stainless steel plunger was used to transmit the energy derived from the falling 2.62 kg drop weight to the sample contained between the plunger and the base plate. Walls between the plunger and the die were lubricated with graphite to minimize plunger friction.

The test procedure was relatively straightforward. Before beginning a crushing energy test the external specific surface area of the test solids was determined by the air permeability method. From this sample, a known weight of material was taken and introduced into the die. The plunger was inserted within the die and rested on top of the bed of solids. Once the die was assembled, the entire apparatus was placed on a circular piece of aluminum wire (0.0640 inches thick) that had been previously centered directly beneath the drop weight. The aluminum wire had previously been calibrated to determine the energy absorbed by the wire as function of wire diameter after deformation. In this manner, it was possible to determine the energy absorbed by the solids and the energy transmitted to the wire. In practice, the drop weight was raised by means of a string mounted on an overhead pulley to a known height above the plunger resting on the test solids. Once the elevated drop weight had finished oscillating and was stationary, the string was cut to permit the hemispherical drop weight to impact on the center of the plunger. After impact, the aluminum wire was removed from beneath the die and measured at seven positions to determine deformation of the wire. Knowing the kilogram-centimeters of energy input by the drop weight and amount of energy absorbed by the wire, it was then possible to calculate the energy absorbed by the impacted solids. If additional work was required to crush the solids still further, a new aluminum ring was positioned under the die and the drop weight was once again raised and released.

Crushed solids were removed from the die and weighed to determine weight loss, if any (usually less than 0.5 percent). A new external specific surface measurement was then conducted to determine increase in surface area after crushing. Knowing the new surface area generated and the energy

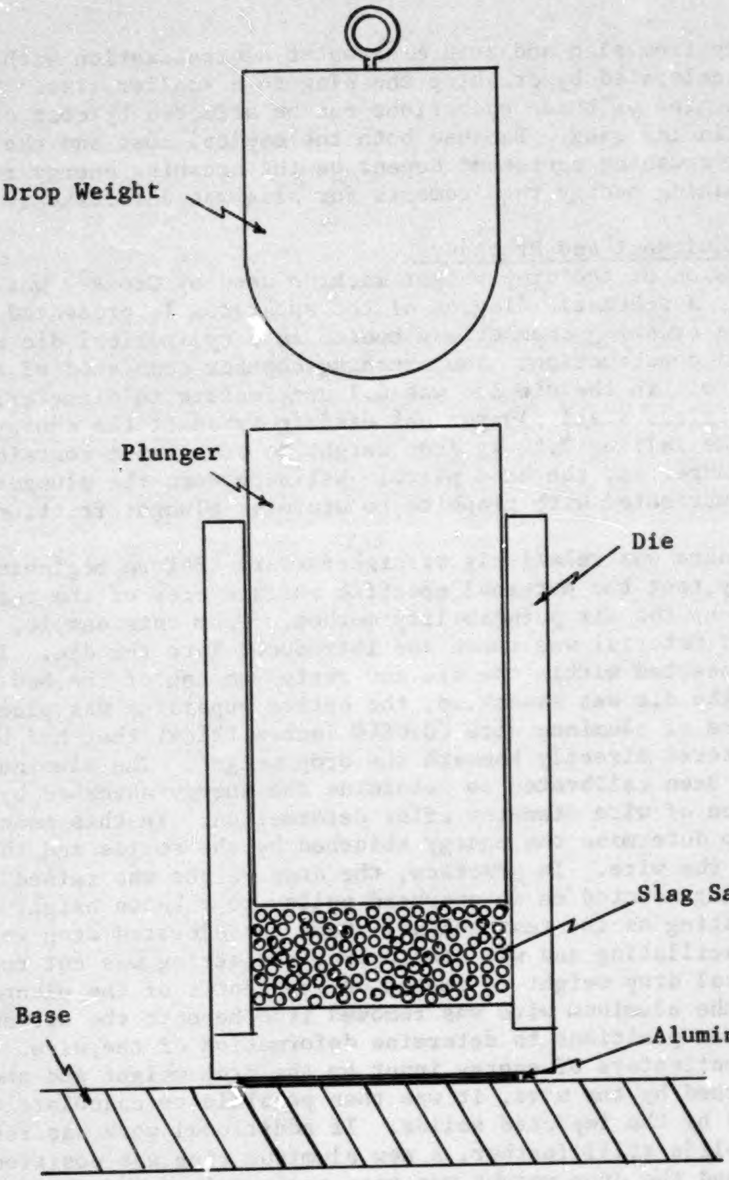

FIGURE 33 - CRUSHING ENERGY APPARATUS

input, it is then possible to calculate the crushing energy or Rittinger's number.

Calibration of Crushing Energy Equipment

The thickness of the aluminum wire used to measure the transmission of energy from the die to the floor upon which the die rested was measured at seven different equally spaced positions before and after each test. Consequently, hundreds of measurements were obtained on the average diameter of the wire before deformation. The average diameter of the wire was 0.0640 plus or minus 0.0002. Less than one half of one percent of the data fell outside of this range (within plus or minus 0.0005). Uniformity of the initial starting diameter of the wire resulted in excellent reproducibility of the calibration curve data. In these calibration experiments, no solids were introduced into the die. To obtain deformation data, the drop weight was elevated to varying heights above the plunger and released. The height from which the drop weight was released was varied over the interval of two to twenty centimeters. In the event that the aluminum wire was not evenly deformed after releasing the drop weight, the test was discarded with the assumption that a direct on-center high of the drop weight was not achieved. Consequently, it was likely that some binding of the plunger occurred with a resulting non-measureable energy loss attributed to friction. Results of this work are presented in Figure 34.

The figure shows a linear relationship between deformation and energy input up to about 40 kilograms-centimeters. Because of alignment difficulties between the plunger and drop weight at higher energy inputs, data reproducibility became poorer. Accordingly, in all subsequent experimentation the weight was not raised to an elevation greater than 15 centimeters.

Discussion of Results

Effect of slag basicity on grinding energy requirements is presented in Figure 35. In this work, slags having basicities of 0.82, 0.90 and 1.01 were used. In each of the crushing tests initial particle size of the slag was -10, + 20 mesh. Results show that the new surface area produced per unit of energy absorbed increases with increasing slag basicity. This would indicate that higher basicity slags are more readily crushed and can be accommodated in smaller sized equipment.

To obtain a relative ranking and a reference point on the grindability of the slag as compared to a standard material for which equipment has already been sized, the grinding energy requirements were determined for a silica sand (Ottawa sand). The results of this work along with the comparative values obtained from the slags is presented in Table XV. It is evident from the higher new surface area generated per unit energy absorbed for the silica sand, the slags produced in this work are slightly more difficult to grind. However, as the synthetic slags produced in this work were very dense and since it is expected that the slag produced during the actual operation of the combustor will be more porous, the sizing of crushing and grinding equipment can be safely

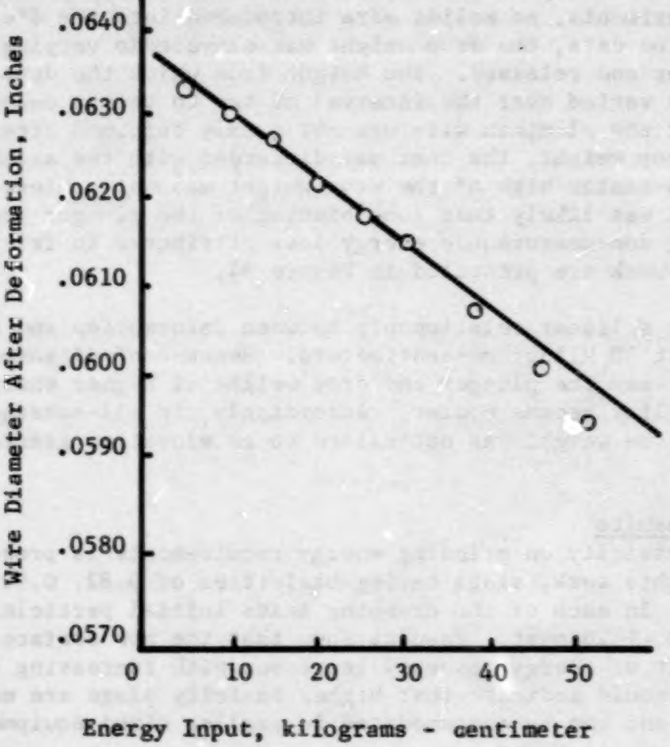

FIGURE 34 - CALIBRATION CURVE FOR ALUMINUM WIRE USED IN CRUSHING ENERGY TEST

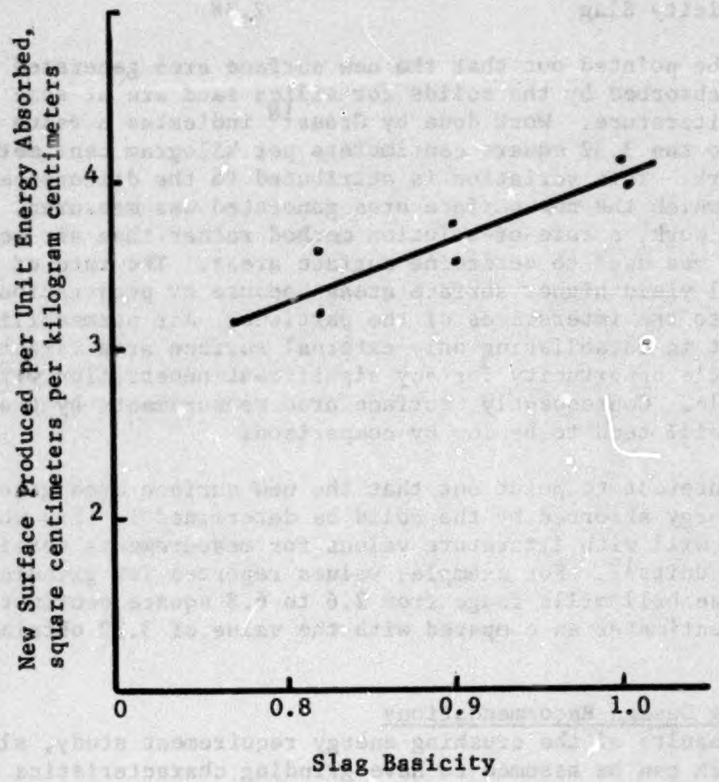

FIGURE 35 - THE EFFECT OF SLAG BASICITY ON GRINDING ENERGY REQUIREMENTS

based on silica sand characteristics. This assumption should facilitate the selection of suitable commercial grinding equipment.

TABLE XV

A Comparison of Crushing Energy Requirements for Silica and Slags

Material	Average Crushing Energy sq cm/Kg-cm
Silica	3.32
1.01 Basicity Slag	2.99
0.90 Basicity Slag	2.60
0.82 Basicity Slag	2.38

It should be pointed out that the new surface area generated per unit of energy absorbed by the solids for silica sand are at some variance with the literature. Work done by Gross[18] indicates a value of 17.56 as compared to the 3.32 square centimeters per kilogram centimeter obtained in this work. This variation is attributed to the difference in the method by which the new surface area generated was measured. In the literature work, a rate-of-solution method rather than air permeability techniques was used to determine surface areas. The rate of solution method will yield higher surface areas because of penetration of the solvent into the interstices of the particle. Air permeability techniques will result in establishing only external surface area variations and afford little opportunity for any significant penetration within the particle. Consequently, surface area measurements by the latter technique will tend to be low by comparison.

It is of interest to point out that the new surface area generated per unit of energy absorbed by the solid as determined in this work agree reasonably will with literature values for measurements obtained on commercial units[19]. For example, values reported for grinding quartz in various size ball mills range from 2.6 to 6.8 square centimeters per kilogram centimeter as compared with the value of 3.32 obtained in this work.

Engineering Design Recommendations

Based on results of the crushing energy requirement study, slag produced in this work can be assumed to have grinding characteristics comparable to silica. This criterion should facilitate the selection of commercial crushing and grinding equipment for use in the process.

HEAT CAPACITY

Introduction

To adequately define the heat balances in the process, it is necessary to have reliable data on the heat capacity (specific heat) of the slag at the temperature at which slag is used. This section presents the experimental work conducted on the three slags (Table XIII) selected as typical of those that may be employed in the operation of the combustor.

Experimental Equipment and Procedure

Standard calorimetry equipment and procedures were used to determine specific heat of the solids. The calorimeter was a one-liter capacity vacuum bottle. To preclude the possibility of slag reaction with water, ethylene glycol was used as the heat absorption liquid. A laboratory C.P. grade of glycol was used. Specific heat data on the ethylene glycol were obtained from the literature[20]. A Beckmann differential thermometer graduated to 0.01°C and capable of interpolation to 0.005°C was used to measure the temperature rise of glycol. A standard laboratory thermometer used to measure the end point temperature of glycol and the cooled solids was accurate to within 0.5°C.

Heat Capacity

Before beginning the experiments, the heat absorption value for the calorimeter, Beckmann thermometer and stirer were determined. This was done by use of the method of mixtures whereby hot and cold water were mixed in the calorimeter to determine the steady state temperature. From the results, heat absorption and losses were determined. Once the calorimeter constant was evaluated, the method was standardized by determining the specific heat of alumina of temperatures up to 1100°C. A comparison of the experimental and literature values for the specific heat of alumina over the temperature range studied permitted an estimate to be made of the heat losses experienced during the transfer of the hot alumina sample from the furnace of the calorimeter. The alumina was a thin disc of 1 inch diameter by approximately 1/8 inch thick. Since the slag samples were available in the form of thin discs of comparable size and shape, a reasonable estimate of transfer heat losses for the slag could be obtained from the alumina studies. Alumina data show that radiant heat transfer losses and vaporization of glycol will introduce no more than a seven percent error in the specific heat measurement. At a temperature of 1100°C the measured heat content of the alumina disc was seven percent lower than that calculated from literature values. The major proportion of heat losses were associated with vaporization of the ethylene glycol.

Experimental procedure for the slag samples consisted of briquetting a known weight of slag into a cylindrical disc of one inch diameter and about 1/8 inch thickness. The slag disc was then inserted within a ceramic combustion thimble. The weight of the thimble varied between 60 and 70 grams and the ratio of thimble weight to slag sample weight ranged from four to eight. Relatively massive thimbles were employed to minimize heat losses during the transfer of the disc from the muffle furnace to the calorimeter. Before the heated solids were placed in the calorimeter, a known volume of ethylene glycol (500 grams) was introduced into the vacuum bottle and allowed to temperature equilibrate. The Beckmann differential thermometer was then adjusted to read near the bottom of the scale so that a maximum temperature increase in the ethylene glycol of 5.2°C could be obtained. In the event the temperature rise of the glycol exceeded the range of the thermometer, the test was discarded. Once the solids were transferred from the thimble to the calorimeter, fluid agitation was maintained by means of a glass stirrer. To establish an absolute value for the final temperature of the fluid and solids, a standard laboratory thermometer was employed.

The heat content per gram of slag as the function of furnace temperature was calculated from the initial and final temperatures of the slag, the calorimeter constant, and the temperature increase of the ethylene glycol along with the weights of materials involved. Heat content was measured above the final slag temperature in the calorimeter. A polynomial fit was then developed for the experimental data and the resulting equation was differentiated with respect to temperature to obtain a second equation defining specific heat of the slag as a function of temperature.

Discussion of Results

Effect of slag basicity and temperature on the heat content (calories per gram above 28°C) of the solid materials is presented in Figure 36A. Variations in heat content between slags of different basicities were not observed. Within the limits of experimental error all three slags yield the same values. Data were then correlated by means of the polynomial curve shown in Figure 36B. The data correlate reasonably well. The resulting polynominal was differentiated to arrive at the specific heat capacity of the slags as a function of furnace temperature. This result is presented in Figure 36B. For comparative purposes, literature values[21], two types of compounds comparable to those that may be formed in the slags are also presented. The literature values effectively bracket the range of specific heat capacities obtained in this work. At temperatures of 900°C, the slope of the experimental curve tends to approach zero. This is attributed to radiation and glycol vaporization losses experienced at the higher temperature levels which would tend to offset the heat capacity increase with increasing temperatures. The experimental heat capacity data should prove to be adequate for design purposes.

Engineering Design Recommendations

The specific heat capacity of high-sulfur bearing slags covering a range of basicities of 0.8 to 1.0 is adequately defined by the curve of Figure 36A. These data cover the temperature range of 200 to 1000°C. Values obtained at temperatures in excess of 600°C may be on the conservative (low) side.

The equation correlating the heat capacity as a function of temperature is as follows:

$$Cp = 0.196 + 2.02 \times 10^{-4}T - 9.33 \times 10^{-8}T^2$$

where Cp is in calories/degree C/gram, T is in degrees C.

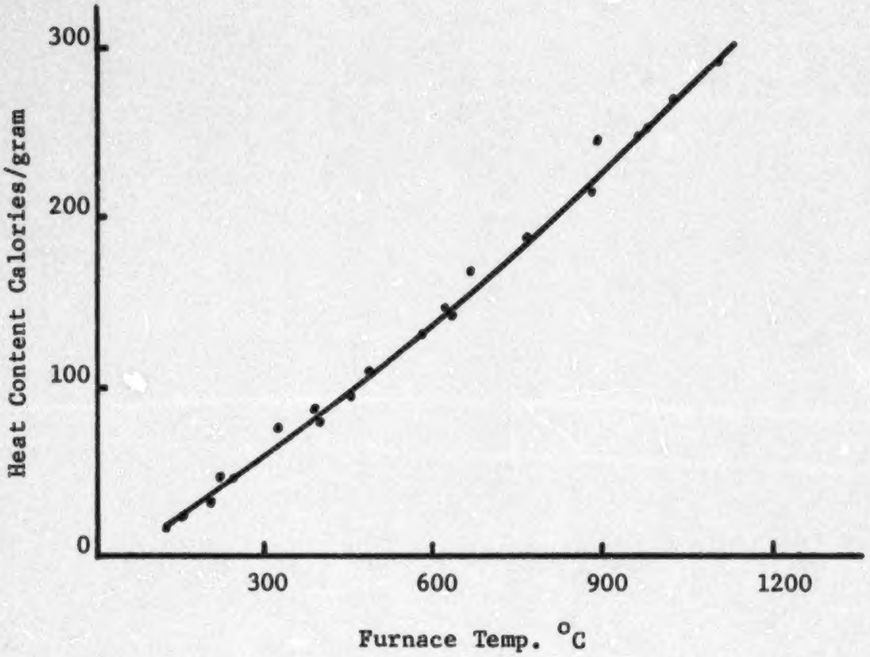

FIGURE 36A - THE EFFECT OF TEMPERATURE ON HEAT CONTENT OF SLAG

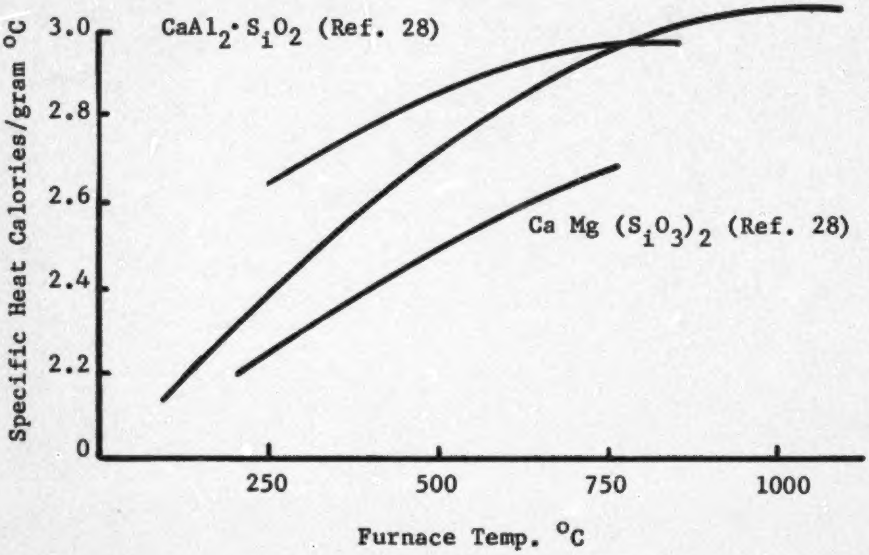

FIGURE 36B - THE EFFECT OF BASICITY AND TEMPERATURE ON SPECIFIC HEAT CAPACITY

ACID MINE WATER NEUTRALIZATION WITH SLAG

Introduction

Neutralization of acid mine water is usually not recommended prior to distillation or reverse osmosis treatment. However, the process generates a neutralizer at no additional cost. This neutralizer is the slag generated in the combustor, which has a high lime content after processing for sulfur recovery.

Depending upon neutralization characteristics of desulfurized slags, it is possible that neutralization of acid mine water prior to distillation could lower the overall process capital and operating costs. For this reason, continuous and batch neutralization tests were carried out on various types of slags to determine their effectiveness in neutralizing acid mine water. This section presents results of this work.

Experimental

Experimental equipment used in the continuous neutralization studies is presented in Figure 37. The packed bed reactor containing slag particles was made of 3.06 cm I.D. plexiglass tube flanged on both ends. The flanges contained fritted glass discs. The packed bed rested on the bottom disc and the top disc was used to prevent the elutriation of solids with the effluent stream. Fresh acid mine water was caused to flow upward through the bed of solids by means of a variable speed pump. Samples of the liquid leaving the fixed bed were obtained by inserting five ml pipette through the top flange of the reactor. Samples were obtained at two minute intervals over the entire run and back-titrated with sodium hydroxide to determine equivalent calcium oxide consumption in the slag. Samples were also obtained from the effluent stream to determine pH as a function of time.

In addition to the continuous neutralization test, batch neutralization studies were also completed. In the batch test program, a standard procedure using 200 ml of acid mine water and approximately 0.40 grams of slag was adopted. In these tests a slag sample of known weight and particle size was placed within a 400 ml beaker along with 200 cc of acid mine water and agitated by means of a magnetic stirer. Measurements of pH were obtained as a function of time over the entire test.

In this work a standard acid mine water composition was adopted as proposed by the Environmental Protection Agency. This composition is presented in Table XVI.

To determine the percentage of slag alkali content that is effectively utilized for neutralizing acid mine water, the following test procedure has been employed to rank the various slags. A slag sample (about 2.5 grams) was weighed on an analytical balance and transferred to a 250 ml beaker containing 15 ml of water. The beaker was covered and the water heated to boiling. The hot mixture was allowed to stand for several minutes to slake any free lime that may be contained within the slag.

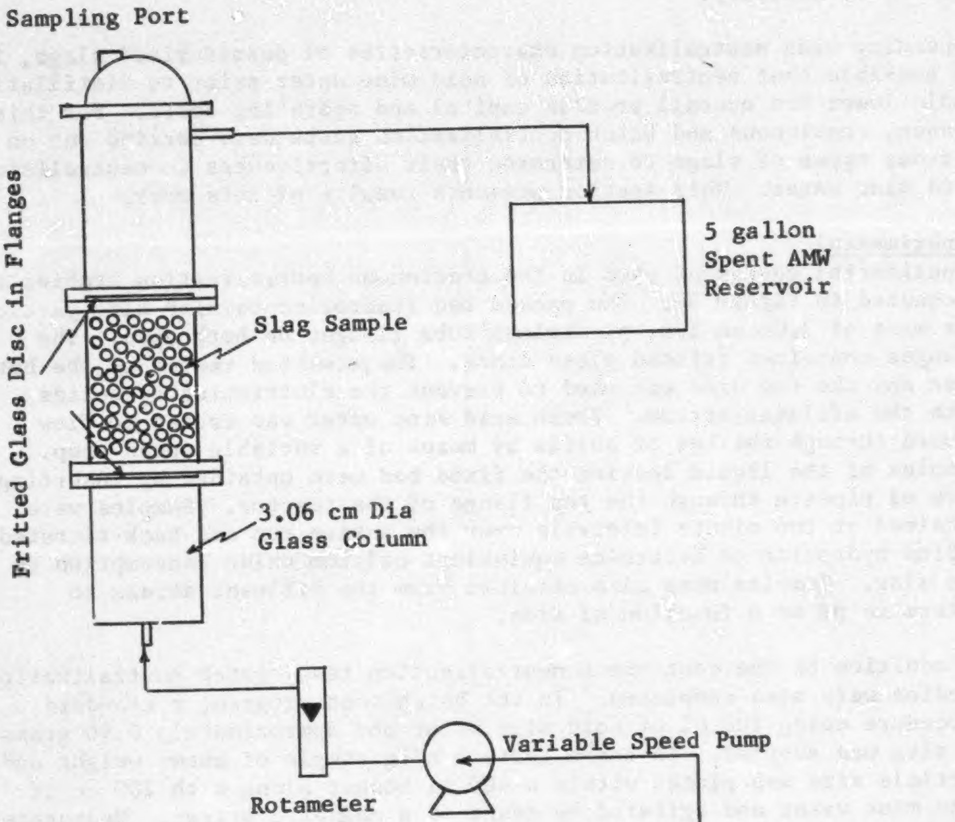

FIGURE 37 - CONTINUOUS NEUTRALIZATION APPARATUS

A burette was then used to add a quantity of 0.5 N sulfuric acid to react with the lime. Once the end-point had been reached, 100 ml of sulfuric acid was added in excess. The mixture was then washed into an erlenmeyer flask, boiled for 15 minutes, cooled to room temperature and titrated with 0.5 N sodium hydroxide to the phenolphthalein end point. Knowing the amount of sulfuric acid, sodium hydroxide and the weight of the sample used in the test the weight of equivalent CaO per gram of sample was calculated. Both CaO and MgO contained within the slag were expressed on a CaO basis.

TABLE XVI

Standard Acid Mine Water Composition

Component	Concentration (Mg/1)
Ca (as Ca)	80
SO_4	1061
Mn	2
Al	5
Fe (Total)	200
Mg (as Mg)	24
Acidity ($CaCO_3$)	400

Effectiveness of Slag Alkali for Neutralization

Using the alkali effectiveness test procedure described above, an alkali utilization factor was defined. This factor (percent alkali utilization) measures the percentage of total slag alkali that is effective for neutralizing sulfuric acid in the specified test procedure. Thus a 100 percent alkali utilization indicates that all of the calcium oxide and magnesium oxide contained within the slag is effective for neutralization.

The effect of basicity ratio and slag particle size on the percent alkali utilization factor is presented in Figure 38. The data indicate that, as the basicity ratio increases for any given particle size of slag, the efficiency of alkali utilization increases. For a 1.5 basicity slag, 100 percent of the alkali (CaO + MgO) contained within the slag enters into the neutralization reaction provided the particle size of the slag is smaller than 60 mesh. As the particle size increases, the utilization factor decreases rapidly. For a given particle size, the alkali contained in the lowest basicity slags (0.8) is least effective for neutralization

Rather strong neutralization test conditions were employed in these experiments. Consequently, the effect of basicity ratio on the alkali utilization factor tends to be somewhat diminished. Under milder neutralization conditions it can be expected that the effect of basicity and particle size on alkali utilization factor will be more pronounced. Nevertheless, the test is indicative of the relative ease with which different slags can react with acids.

In the commercial operation of the combustor, it is probable that the slag will contain silica and alumina in the ratio of two to one. However,

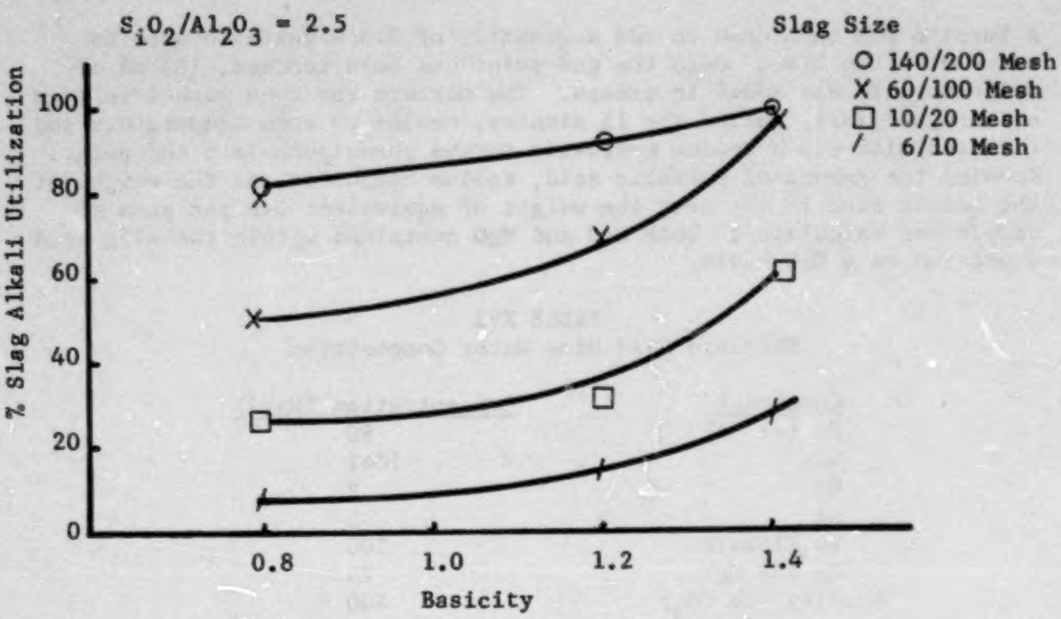

FIGURE 38 - THE EFFECT OF SLAG PARTICLE SIZE AND BASICITY RATIO ON SLAG ALKALI UTILIZATION IN NEUTRALIZATION

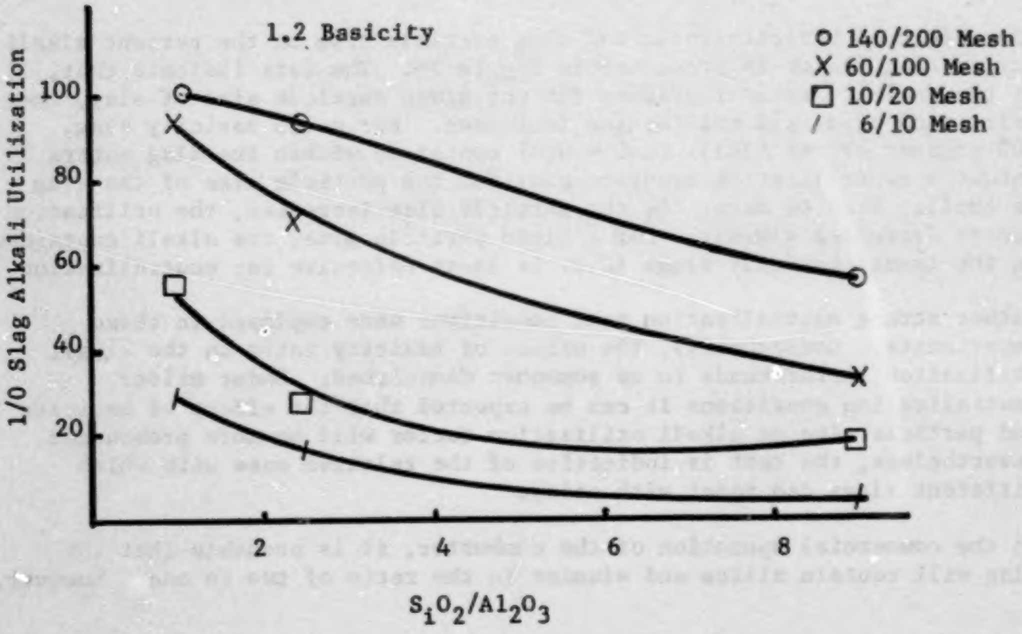

FIGURE 39 - EFFECT OF SLAG PARTICLE SIZE AND S_iO_2/Al_2O_3RATIO ON THE SLAG ALKALI UTILIZATION FACTOR

because of the flux characteristics and variations in coal ash, this ratio may vary substantially. Accordingly, a brief study was completed using a 1.2 basicity slag to determine effect of particle size and silica-to-alumina ratio on the alkali utilization factor. Results of this work are presented in Figure 39. Higher alkali utilization is obtained as particle size decreases. The silica to alumina effect is somewhat analagous in that alkali utilization increases with decreasing SiO_2/Al_2O_3 ratio. This is probably due to an occlusion factor resulting from the formation of more glass at the higher SiO_2 concentrations. Inasmuch as commercial slag will contain a ratio of about two, alkali utilization will not be severely impeded.

Continuous Neutralization Tests

For the continuous neutralization studies, synthetic sulfur-free slags were employed in the equipment shown in Figure 37. Because of the relatively high capital and operating costs associated with grinding hard, abrasive materials to fine sizes, comparatively coarse particles were used in this work. It was reasoned that since a wide particle size distribution would be obtained in crushing the slag, it is only necessary to study the neutralization rate for the top size, or coarse particles. In this manner, if the neutralization reactor design were based on the top size, a safe and conservative approach to the engineering design would be possible because smaller particles will be consumed quite rapidly.

In this work, two particle sizes were employed: -¼ + 10 mesh and -10 + 20 mesh. A slag of 1.2 basicity (slag No. 5 Table VIII) was used for the reacting material. Results of the neutralization study are presented in Figure 40 which shows the effect of particle size, acid mine water flow rate, and throughput on slag consumption. Slag consumption is expressed in terms of equivalent moles of calcium oxide consumed per second per square centimeter of slag external surface. The data show that depending upon flow rate, the neutralization reaction is controlled by diffusion either through the liquid phase surrounding the slag particle or by diffusion of the acidic constituents through the slag particle itself. In Figure 40, the rate of equivalent lime consumed per unit time per unit of external surface area is independent of flow rate provided that the acid mine water flow was maintained in excess of 370cc per minute. This implies that the liquid diffusion of acidic constituents through the liquid medium surrounding the slag particle is not the controlling mechanism. Instead, the data show that neutralization rate is controlled by diffusion through the interior of the slag particle. It is evident from the decreasing rate of equivalent lime consumption with increasing throughput, the resistance due to internal diffusion within the slag particle effectively diminishes the neutralization rate. Observation of large, partially neutralized, slag particles revealed that a clear topochemical reaction had occurred. Consequently, equivalent lime consumption rates were normalized by basing the reaction on the external surface area of the slag particle. If the equivalent lime consumution were expressed as a function of time only, distinctly different curves are obtained for each of the different acid mine water flow rates

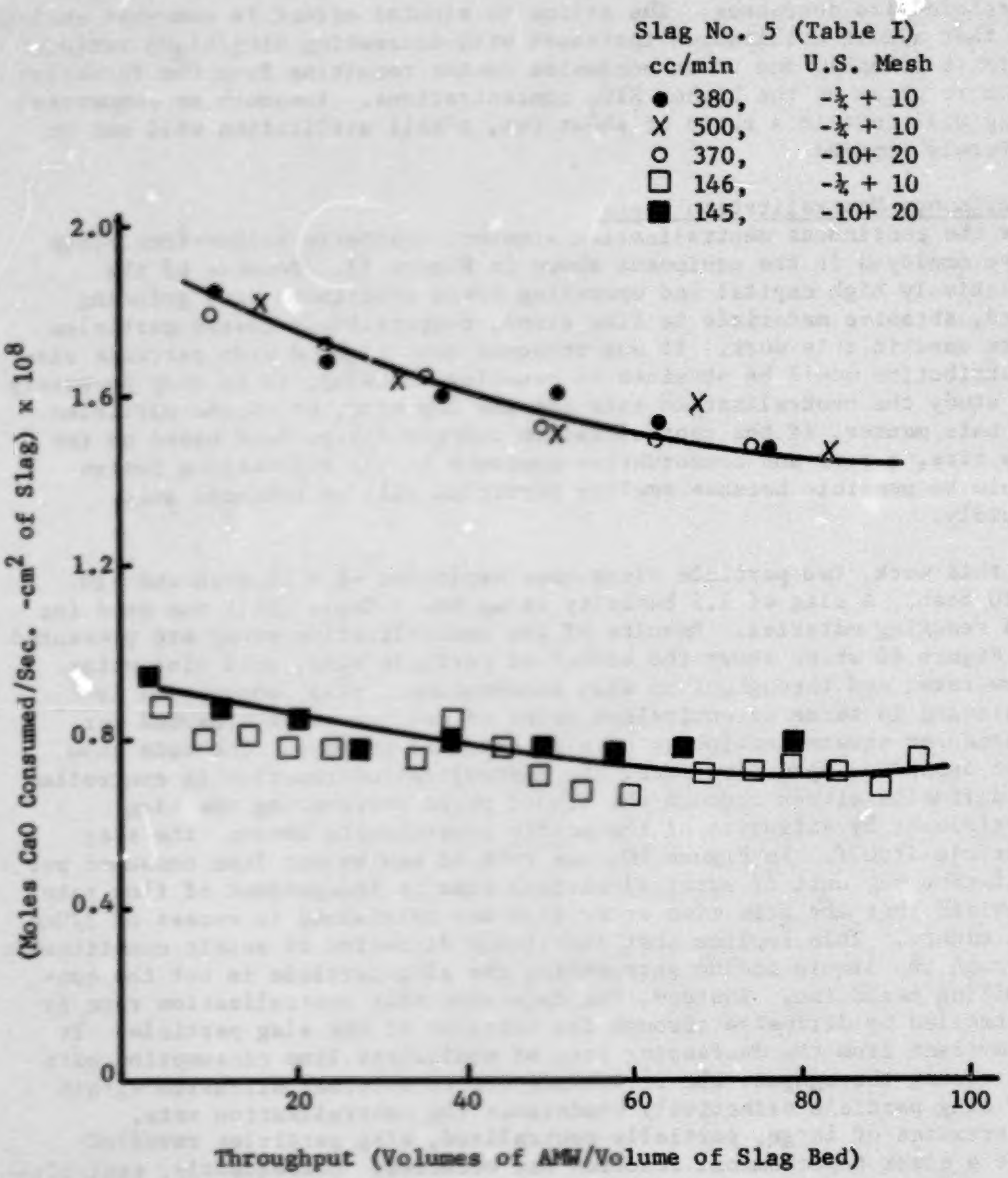

FIGURE 40 - EFFECT OF OPERATING PARAMETERS ON THE NEUTRALIZATION OF ACID MINE WATER WITH SULFUR FREE SLAG

employed. As the acid mine water flow rate was decreased to about 145cc per minute, a much lower neutralization rate was obtained, indicating that diffusion within the liquid phase surrounding the slag particles becomes the primary resistance at lower flow rates. If the liquid phase diffusional resistance were the only controlling step in the neutralization reaction, it would be expected that a constant neutralization rate independent of throughput would be obtained. As can be seen from the data, neutralization rate decreased slightly with increasing throughput. Such a phenomenon indicates that diffusion within the slag particle contributes to the overall neutralization reaction rate at this low flow rate.

At the lowest acid mine water flow rate (145cc per minute) the space velocity (volume of acid mine water per volume of packed bed) was relatively low at 2.19. At his space velocity, the apparent residence time of the acid mine water while in contact with slag was approximately 27 seconds. Even at this relatively long contact time the pH of the effluent leaving the slag bed was not raised appreciably. This result is presented in Figure 41 which shows the effect of acid mine water throughput on pH of about 4.7 was obtained at the onset of flow but the effluent pH rapidly decreased as throughput increased. This is the result of some precipitation and/or the increase in the diffusion path to the interior of the particle as lime is consumed topochemically. Erratic behavior of the pH at throughputs in excess of 40 was due to poor control on the feed rate as the feed reservoir was depleted of acid mine water.

The packed bed contained approximately 100 times the equivalent of lime required to neutralize all acid mine water in the feed reservoir. Consequently, a series of experiments were completed whereby the acid mine water was continuously recirculated through the packed bed in a closed loop system to determine the ultimate or steady state pH that could be achieved. Based on the alkali utilization factor test it was expected that only about 30 percent of the slag alkali would be effective in the neutralization. Since the latter tests were obtained under rather strong neutralization conditions, continuous recirculation of the acid mine water would establish effectiveness of this slag in neutralizing relatively mild acid liquids. Results of these tests showed that steady state pH values of 4.6 and 4.1 were obtained for the -¼ + 10 and -10 + 20 mesh materials respectively. These data tend to support the conclusions obtained from the alkaline utilization factor i.e., slag alkali utilization decreases with increasing slag particle size.

AMW Neutralization

After the completion of the recycle tests, the -10 + 20 mesh slag particles were screened to determine their extent of degradation. Screen analysis showed that less than 1.6 percent passed through -20 mesh with 0.04 percent passing 100 mesh. Thus it can be expected that slag degradation will not occur during neutralization causing an increase in the overall reaction rate.

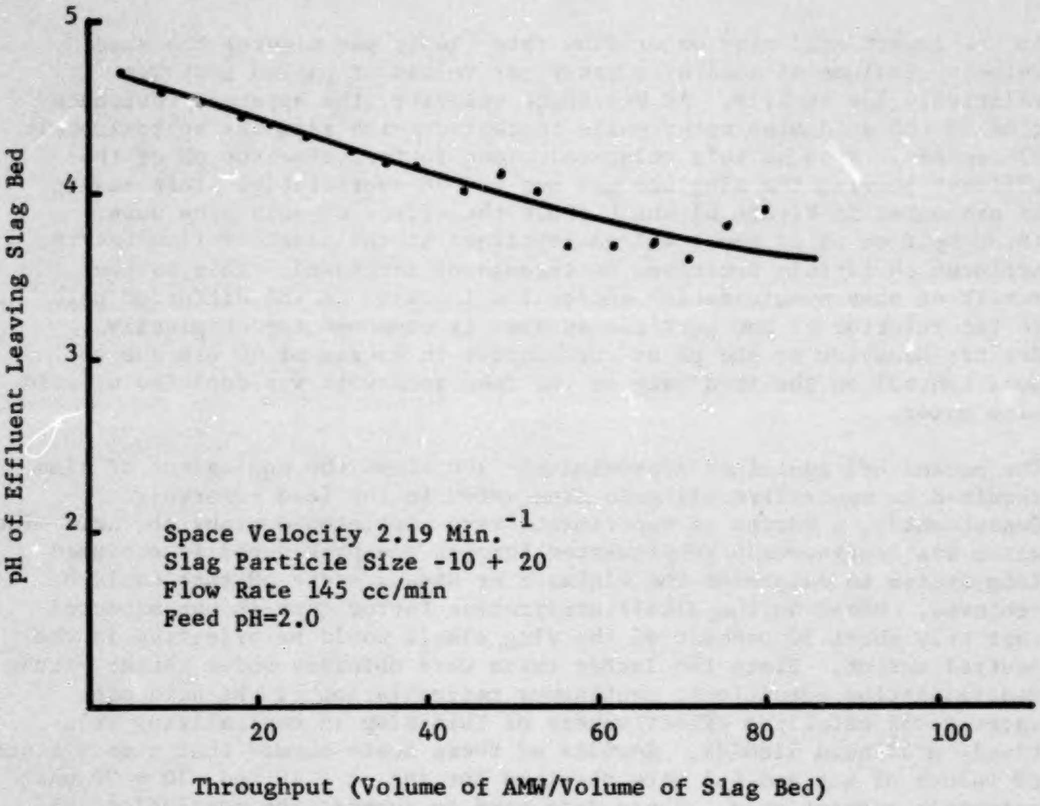

FIGURE 41 - EFFECT OF THROUGHPUT ON pH OF EFFLUENT LEAVING FLOW NEUTRALIZING REACTOR

Because the alkali utilization factor and continuous neutralization tests indicate that very fine grinding of the slag will be required to neutralize the acid mine water to a pH of seven in reasonably sized equipment, the continuous tests were terminated in favor of batch neutralization studies. Calculations based on the continuous rate study, which assume that the major resistance is liquid diffusion, indicate that the slag particles must be ground to finer than 200 mesh. At this size consist, a pH of seven can be achieved. However, capital equipment and operating costs would be substantial.

Batch Neutralization Studies

Because of the slow neutralization rates and poor alkali utilization factors achieved in the earlier work, batch neutralization tests were completed on a 1.2 basicity slag over a wide range of particle sizes. Figure 42 presents results of this work and shows effect of slag particle size and time on resultant pH of the neutralized acid mine water. Neutralization rate increases with decreasing slag particle size. However, neutral (pH = 7) water was obtained only with slag particle sizes finer than 270 mesh. Extremely long neutralization times were required for all slags having larger particle size. Although all of the data are not shown in Figure 42, residence times in the order of days were required to bring the pH to seven for the larger slag particles. Based on these results, it does not appear that the synthetic slags produced in this work are commercially attractive for neutralization of acid mine water.

Because all of the neutralization tests were completed with sulfur free slags, a second series of batch neutralization tests were completed on slag obtained from the desulfurization unit. For these tests, slags containing about eight percent sulfur initially were desulfurized by the air water reaction to sulfur levels of one percent or less. It was anticipated that the removal of sulfur from the slag might increase the internal porosity of the slag particles and high neutralization rates could be achieved. The results of this work are presented in Figure 43 which shows the effect of contact time, basicity, and particle size on acid mine water pH. Only typical data are presented in this figure. In particular, representative data were selected to show the effect of decreasing particle size with decreasing basicity. For example, for a 0.92 basicity slag ground to -100 mesh, the neutralization rate is comparable to the lower basicity 0.82 basicity slag ground to -200 mesh. This would be expected because the alkali utilization factor increases with increasing basicity and decreasing particle size.

Extensively long residence times are required to obtain neutral water. As a point of reference, a commercial grade of limestone ground to -200 mesh is shown for comparison. As is evident limestone is more effective for neutralization than desulfurized slag.

If the desulfurized slag contained residual sulfur considerable hydrogen sulfide was generated during the neutralization step. Inasmuch as it is unlikely that desulfurization will be 100 percent effective in recovery of sulfur, use of desulfurized slag for neutralization is not recommended. Production of hydrogen sulfide will necessitate use of an enclosed neutralization tank or a pond to prevent an air pollution problem. This

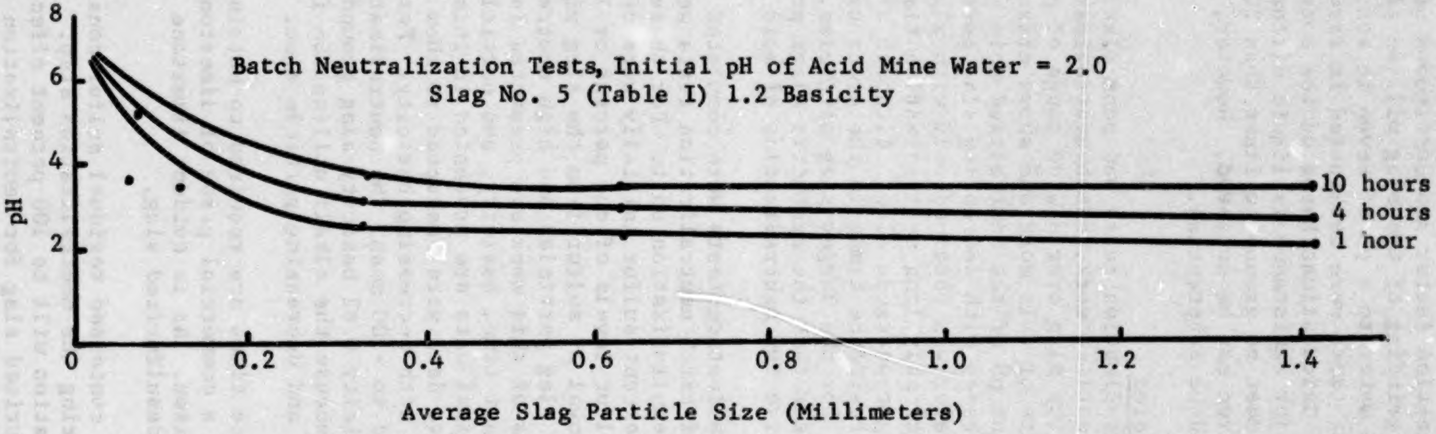

FIGURE 42 - EFFECT OF SLAG PARTICLE SIZE ON pH AS A FUNCTION OF NEUTRALIZATION TIME

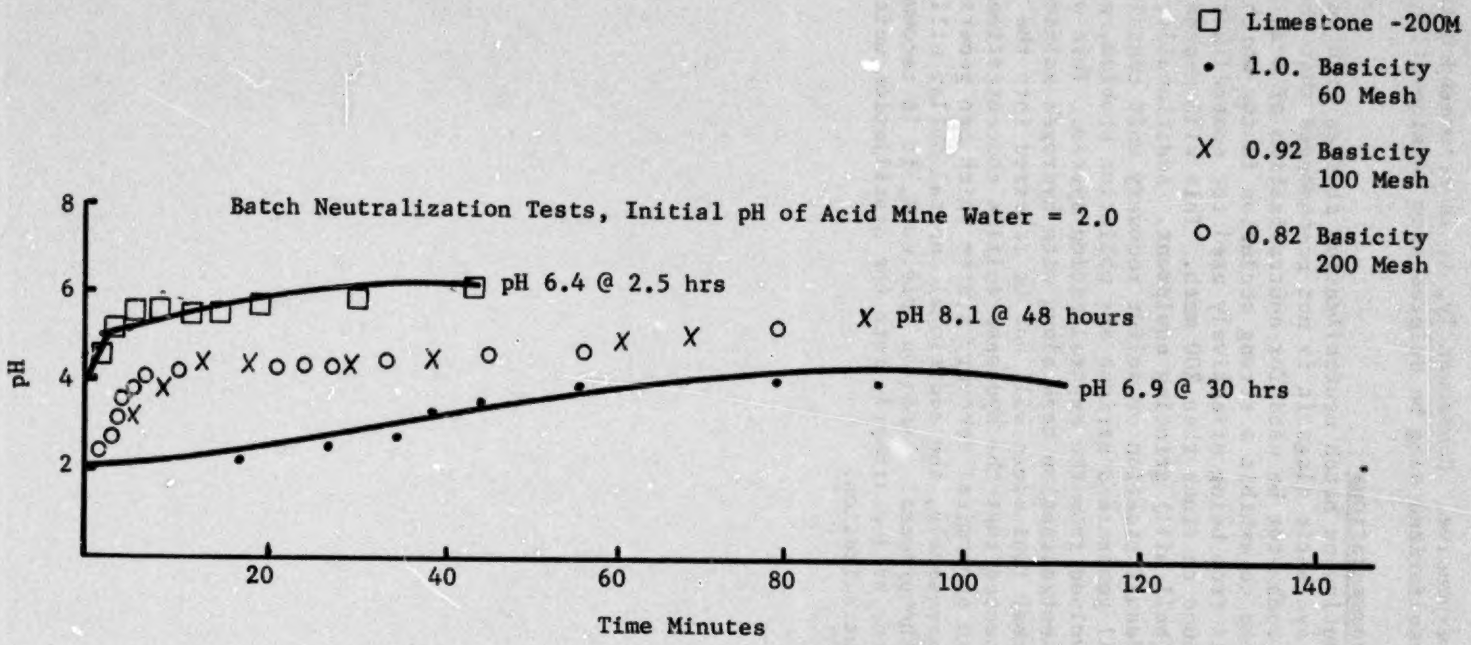

FIGURE 43 - VARIATION OF pH WITH TIME AS A FUNCTION OF SLAG BASICITY

becomes prohibitively expensive. Consequently, it is recommended that neutralization with desulfurized slag be deleted from consideration.

Engineering Design Recommendations

Based on results of continuous batch neutralization studies with sulfur-free and desulfurized synthetic slags it is not recommended that the slags produced in the combustor be used for neutralization of acid mine water. These slags tend to exhibit a strong occlusion factor which prevents all of the alkali from being effectively used for neutralization unless the slag is ground to finer than 200 mesh. This will necessitate the use of expensive (ball mill) grinding equipment. Additionally, if the slag leaving the desulfurization or sulfur recovery unit contains residual sulfur it will generate a serious air pollution problem, as hydrogen sulfide is evolved from the neutralization system. This will necessitate a closed neutralization tank along with hydrogen sulfide removal equipment so that foul odors will not be released into the atmosphere. It is expected that the hydrogen sulfide concentrations will be too low to afford an economical recovery system which can generate elemental sulfur. Consequently, the additional capital outlay will only increase the cost of the process. Based on this work, it is recommended that the acid mine water be fed directly into the distillation unit without benefit of neutralization.

KINETICS OF SULFUR RECOVERY FROM SLAG

Introduction

The economics of the process depend upon the kinetics and efficiency of sulfur recovery from slag. Sulfur can be recovered from the slag in two ways. One is to react the slag with carbon dioxide in the presence of moisture to produce calcium carbonate and hydrogen sulfide.

$$CaS + H_2O + CO_2 = CaCO_3 + H_2S \tag{1}$$

The hydrogen sulfide can be treated by the Claus process to produce elemental sulfur according to the simultaneous reactions.

$$\begin{aligned} 2H_2S + 3O_2 &= 2H_2O + 2SO_2 \\ 2H_2S + SO_2 &= 2H_2O + 3S \end{aligned} \tag{2}$$

These reactions are well known[22-26]. In general, the hydrogen sulfide production step is carried out at low temperatures with water in the liquid phase. The Claus reaction for conversion of hydrogen sulfide to elemental sulfur is completed at elevated temperatures (about 800°F depending upon the process). Reaction (1) is a preferred route for the recovery of sulfur when calcium sulfide bearing slags are available at ambient temperatures. In this manner, heat requirements can be minimized. However, when slag is available at high temperatures (2000°F or more) the following reaction

$$(CaS)_{slag} + H_2O = H_2S + (CaO)_{slag} \tag{3}$$

affords a more economically attractive approach to sulfur recovery. The mechanism of this reaction is not well known and as yet cannot be explained[6]. However, it is generally believed that an oxygen deficiency exists in the slag which permits the decomposition reaction (3) to occur. Inasmuch as high temperature hydrogen sulfide is available, the addition of air to the gas stream should generate SO_2 and permit the thermal conversion of H_2S to elemental sulfur according to equation (2).

Because carrying out hydrogen sulfide generation and reduction to sulfur simultaneously offers a substantial capital and operating cost reduction, the CO_2 treatment cost emphasis was placed on this approach. No attempts were made to evaluate the mechanism of reaction (1). Instead, efforts were concentrated on evaluating the yield of H_2S and elemental sulfur in one single step.

Theory

It is generally assumed[5] that the sulfur that chemically combines with slag during the desulfurization of steel exists in the form of calcium sulfide. However, the form and nature of the CaS found in solid slags is subject to speculation. For example, various authors[27-28], in studies on CaO-MgO-SiO_2 slags, have shown that calcium sulfide exists in crystalline form as well as a solid solution possessing complex formula structure. Consequently, equilibrium data based on theoretical and experimental work associated with pure calcium sulfide as given by

(4) $$CaS + H_2O = CaO + H_2S$$

(5) $$CaS + \frac{1}{2}O_2 = CaO + \frac{1}{2}S_2 \text{ (gas)}$$

(6) $$CaS + xH_2O + yO_2 = CaO + aH_2S + bSO_2 + cS$$

are not necessarily valid for desulfurization of sulfur containing slag. Nevertheless, the theoretical considerations do provide valuable insight into the desulfurization reaction and are presented in Figure 44.

As is evident from Figure 44, reaction (5) has a favorable thermodynamic effect for completion because of its high negative free energy. The high equilibrium constant explaining why the desulfurization reaction in steel refining requires that the oxygen level in the steel be maintained as low as possible to prevent the spontaneous decomposition of calcium sulfide. For this reason, the process operates with a high carbon level in the iron bath during carbon combustion. By maintaining a high carbon level in the iron bath, oxygen content in the pig iron is maintained at an extremely low level[5]. However, in the desulfurization reaction for recovery of sulfur from the spent slag, the reverse situation must be maintained to obtain high sulfur yields.

Equation (4) is another reaction tending to promote the desulfurization of spent slag. Desulfurization of calcium sulfide is favored by increasing temperatures. It is interesting to note that even though the equilibrium constant is low, generation of hydrogen sulfide by this technique compares favorably with the commercial reaction[29] given by Equation (1).

To determine the probable gas phase compositions for the reactant species, defined in Reaction (6), a free energy minimization program was developed in a computer assessment of the reaction products that may be obtained under equilibrium conditions as a function of temperature and molar water-to-oxygen ratios. Typical results for these equilibrium calculations at a temperature of 1400°K are presented in Figure 45. At low water-to-oxygen ratios conversion proceeds almost entirely to elemental sulfur. This is attributed mainly to the high negative energy free change associated with reaction (5). As the water-to-oxygen ratio increases to ten and higher, equilibrium sulfur conversion tends to decrease. Although not shown, the effect of temperature is to increase the conversion to sulfur at all water-to-oxygen ratios.

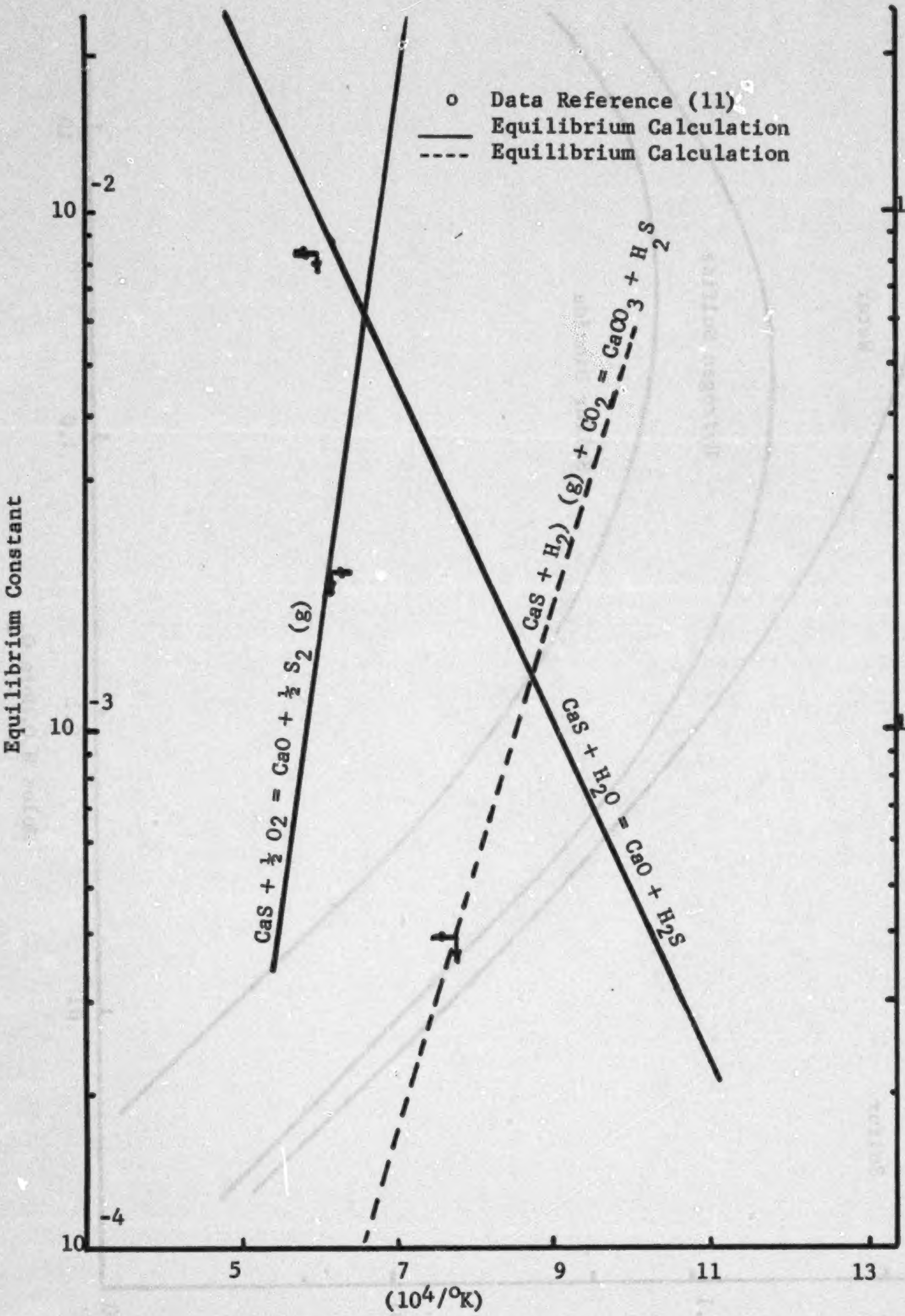

FIGURE 44 - VARIATION OF EQUILIBRIUM CONSTANT WITH TEMPERATURE

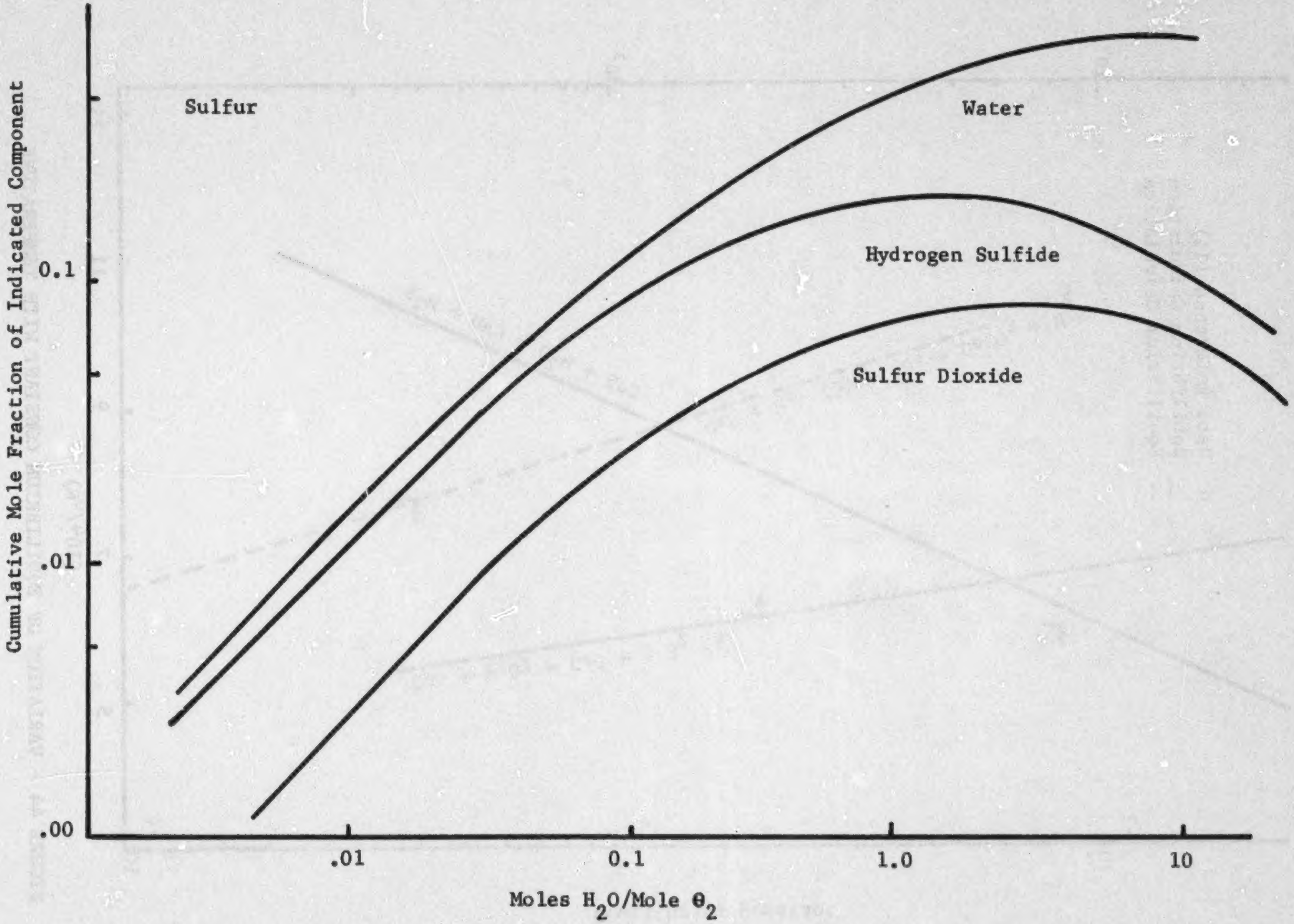

FIGURE 45 - EQUILIBRIUM DATA FOR THE SYSTEM, $CaS + xH_2O + yO_2 = CaO + aSO_2 + bH_2S + cS_2 + dS_8$ at 1400°K

Literature data[30] are available which indicate that the water granulation of liquid slag under oxidizing conditions tends to promote the formation of a high concentration of hydrogen sulfide as compared to sulfur dioxide. Contrary to equilibrium calculations, ratios of hydrogen sulfide to sulfur dioxide as high as 100 to one have been obtained. Additionally, during the quenching reaction, a large amount of hydrogen was also formed. Although it was stated that the nature of the reaction mechanism leading to hydrogen formation during granulation was not known nor could it be explained, a tentative hypothesis for the desulfurization of slag was put forth which indicated that kinetics, rather than equilibria, dictated the overall yield of products.

Inasmuch as literature on desulfurization of blast furnace slags (and those comparable to the type used in our process) was rather scant, an experimental program was undertaken to determine effect of temperature, particle size, and reactant flow rates on the yield of sulfur and/or hydrogen sulfide. A theoretical kinetic model based on the concepts outlined by Wen[31] for non-catalytic heterogenous (solid-fluid) reactions was adopted. The model assumes that a shrinking spherical unreacted core of radius r_c exists within each spherical slag particle of radius R. Using a pseudo steady-state solution of the equation describing the change in reactant concentration with time at various locations within the spherical particle, a solution was obtained relating reaction time, t, to reactant concentrations. This solution is shown as equation (7).

$$(7)\quad t = \frac{RC_{so}}{S_{so}}\left(\frac{1}{3}\left(\frac{1}{k_m} - \frac{R}{D}\right)\left(1 - \frac{r_c^3}{R^3}\right) + \frac{1}{k_s}\left(1 - \frac{r_c}{R}\right) + \frac{R}{2D}\left(1 - \frac{r_c^2}{R^2}\right)\right)$$

where:

a = interfacial area, sq ft/cu ft of solids
C = weight fraction of sulfur in solids at any time
C_{so} = concentration of reactant fluid in bulk phase, mole/ft^3
C_o = weight fraction of sulfur in solids at time zero
C_{so} = initial concentration of solid reactant, mole/cu ft
D = diffusivity, sq ft/min
k_m = mass transfer coefficient across fluid film, ft/min
k_s = reaction rate constant based on surface, ft/min
r_c = distance from center of sphere to reaction surface ft
R = radius of particle ft
t = time, minutes

The first product term within the brackets of Equation (7) defines the fluid film resistance, that is, the transport of reactant from the bulk gas phase across the boundary layer surrounding the particle. The second term defines the contribution of chemical resistance and the last term relates to the resistance afforded by diffusion through the ash or reacted layer surrounding the unreacted core. Depending upon which resistance controls the overall reaction rate, it is possible to simplify Equation (7) substantially. Assuming that chemical reaction controls (it will be shown later that this indeed is true) Equation (7) can be rewritten as

$$t = \frac{RC_{so}}{k_s C_{ao}} \left(1-(1-X)^{1/3} \right) \tag{8}$$

where X is the fraction of calcium sulfide converted to the sulfur-free form. If chemical reaction controls the overall desulfurization rate, a logarithmic plot of $1-(1-X)^{1/3}$ versus t should have a slope of unity. Similarly, it can be shown that, if the slope of the log-log plot is 1/2, then ash diffusion controls the overall reaction rate. It will be shown in the discussion of the experimental results, that the mathematical model presented by Wen adequately represents the experimental data and affords the opportunity for scale up to commercial equipment.

Experimental Procedure

Two types of experimental equipment were used in this work. The first employing stainless steel and glass equipment is shown in Figure 46. Air and water were introduced by rotameters into a preheater maintained at reaction temperature so that vaporization of the water occurred outside of the reactor proper. The heated gases were introduced into a stainless steel reactor (1.5 inches I.D. by eight inches long) flanged on both ends and heated by means of a muffle furnace. The muffle furnace was controlled at the desired reaction temperature. The outlet of the reactor was connected to an air condenser heated to a temperature of approximately 400°F by means of an electrical resistance tape. This condenser was used to collect sulfur. The outlet of the sulfur condenser was connected to a water cooled glass condenser for removal of water vapor which was collected in a graduated flask. A gas sampling port for chromatographic analysis was located between the steam condenser and a wet test flow meter. Gases exiting the wet test meter were collected in a water displacement vessel for cumulative gas analysis.

Difficulties were experienced in operation of this equipment because of the reaction of sulfur compounds with the vessel. Consequently, an alternative experimental apparatus was constructed to obtain meaningful kinetic data as shown in Figure 47. A variable speed positive displacement pump was used to maintain a constant flow of water into an inconel preheater (straight pipe) that was inserted within a high temperature furnace set at the desired reaction temperature. Sufficient surface area was allowed for heat transfer from the furnace to preheat and vaporize the water to the approximate reaction temperature. The steam was directed onto a ceramic combustor boat maintained within a ceramic combustion tube located within an electrical resistance heated furnace. One half to

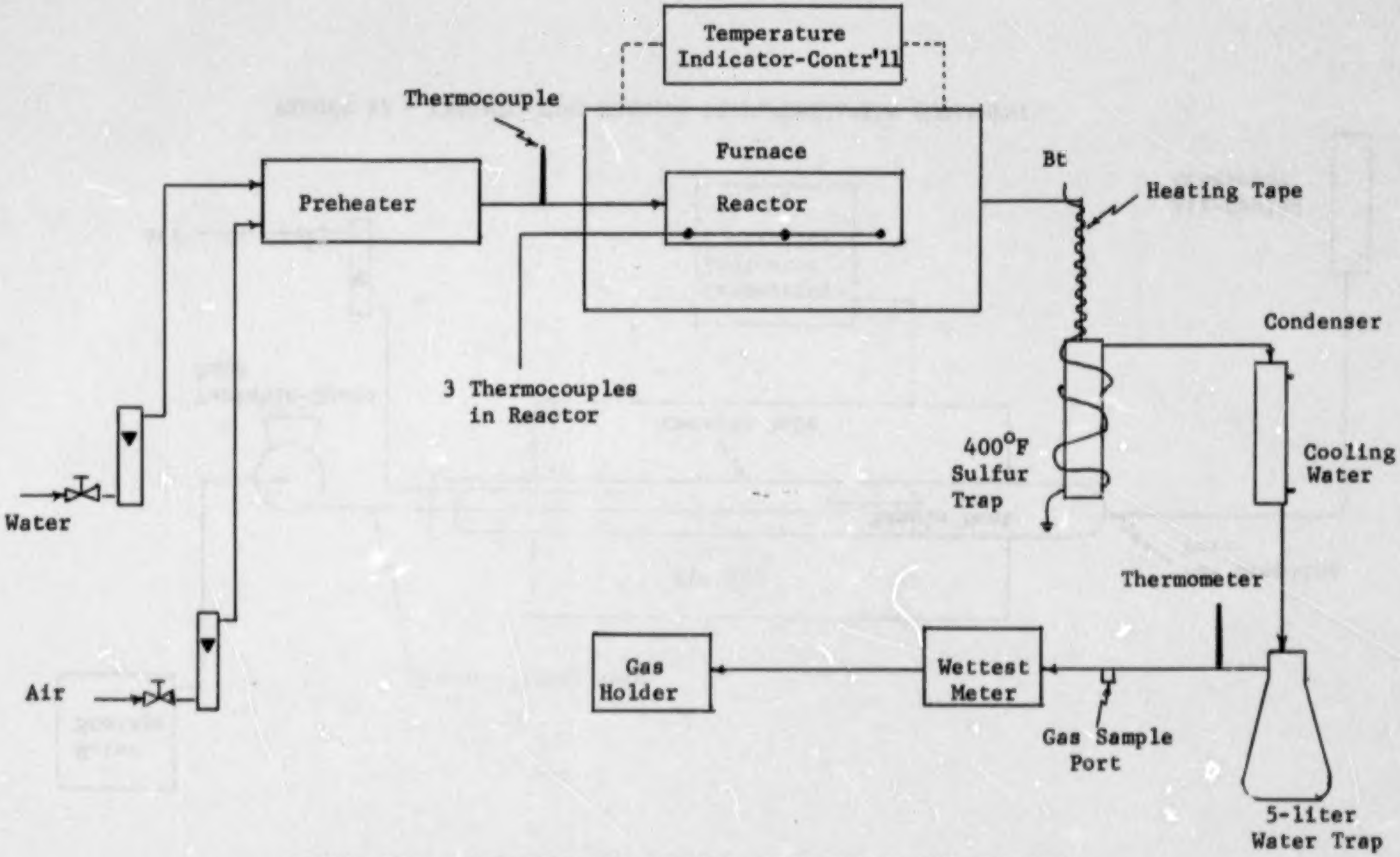

FIGURE 46 - STAINLESS-STEEL REACTOR DESULFURIZATION EQUIPMENT

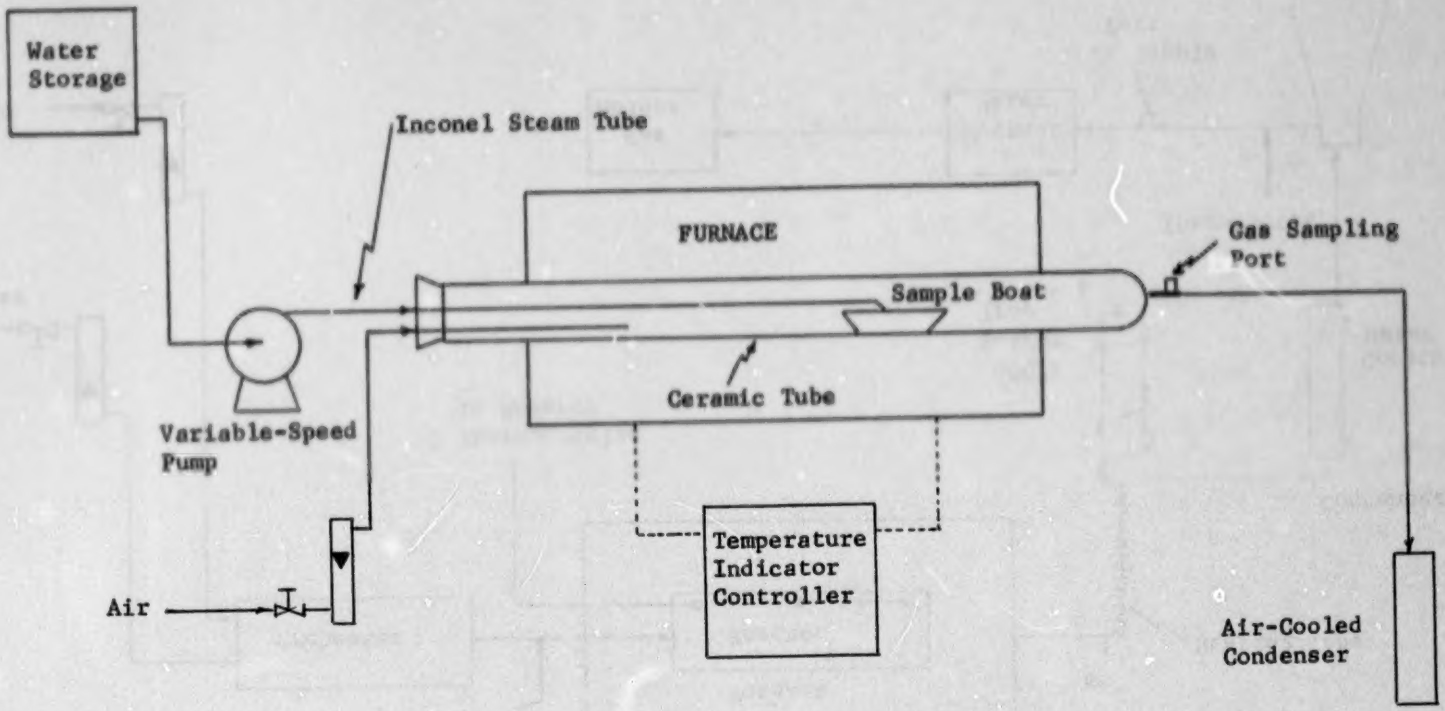

FIGURE 47 - CERAMIC-TUBE REACTOR DESULFURIZATION EQUIPMENT

one gram samples of slag were spread in a single layer of particles across the ceramic combustion boat and the steam was directed across the particles. Air or argon was introduced into the combustion tube and across the ceramic boat by means of a rotameter. Effluent gases from the combustion tube were air cooled and periodic spot samples were obtained for gas chromatographic analysis.

The experimental procedure consisted of introducing a known amount of slag material into the combustion boat and reacting it with air and water for a known period of time. The entire combustion boat sample was then analyzed for residual sulfur content. Reaction time was varied for a given sample to determine rate of desulfurization.

Discussion of Results

A considerable number of experiments employing pure calcium sulfide and slags of various basicity and particle size was completed over the temperature range of 1000 to 1700°F in the stainless steel reactor shown in Figure 32. However, because of experimental difficulties and side reactions only qualitative data were obtained for this system. Three problems proved to be insurmountable in terms of obtaining qualitative data. The first was inability to collect all of the sulfur formed in the steam-calcium sulfide or steam-slag reaction. In the pure calcium sulfide experiments, reagent grade powdered (-100 mesh) calcium sulfide was employed. At the steam flow rates employed, sufficient plugging of dust carryover and sulfur condensate was observed. Additionally, the sulfur condenser was unable to effectively trap all of the sulfur vapors generated during reaction and substantial quantities were carried over with steam to the steam condenser. Consequently, a cloudy steam condensate was collected containing substantial quantities of sulfur. For these reasons it was not possible to quantitatively define the amount of elemental sulfur obtained as a function of time. The third and final anomaly was substantial corrosion of the stainless steel reactor and deposits of scale in the desulfurized calcium sulfide slag samples. A magnetic separation of the partially desulfurized slag and scale materials was made. Sulfur analysis on the magnetic fraction indicated substantial quantities of sulfur present in the scale material. All of the scale deposits could not be magnetically separated from the desulfurized slag. Consequently, it was not possible to determine the extent of desulfurization by a sulfur analysis of the spent slag. However, estimates have shown that approximately 60 percent of the sulfur was removed from the slag.

Even though the data could not be used for a quantitative assessment of the reaction kinetics, several pertinent conclusions were drawn. Typical data to show the effect of temperature obtained in these experiments are presented in Figure 48. These data are presented only as a relative guide and show that the rate of evolution of hydrogen sulfide increases with increasing temperature. In addition to H_2S, elemental sulfur was produced in substantial quantities. In general, the results of these qualitative experiments indicate that desulfurization rate increases with decreasing particle size and increasing temperature.

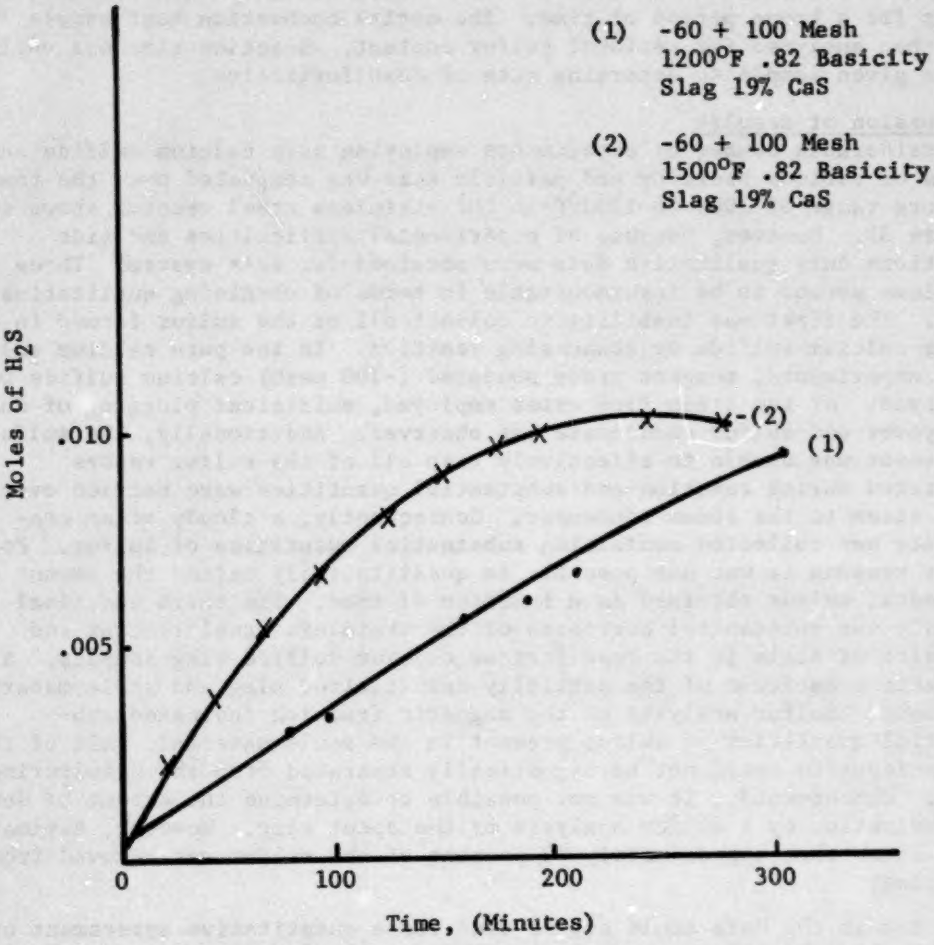

FIGURE 48 - TEMPERATURE EFFECT ON STEAM-SLAG REACTION

Even though the data are relatively inaccurate with regard to rate of desulfurization, the fact that only approximately 60 percent of the sulfur was removed in a reaction time of about five hours invalidates the feasibility of desulfurization at these low temperatures (less than 1700°F). For commercial utility, to obtain a reasonable size reactor, residence times of the solid particles should be maintained at less than one hour.

An important consideration derived from these experiments was the fact that the slag desulfurization reaction was topochemical in nature. Coarse slag particles of approximately ¼ inch in diameter were desulfurized using steam at a temperature of about 1700°F. An examination (both visually and microscopically) of the desulfurized slag showed a white outer layer surrounding a gray unreacted core. This tended to substantiate the hypothesis that experimental results could be treated using a model based on a particle with a shrinking unreacted core. An additional factor observed during these desulfurization experiments was that the particle size did not change significantly during desulfurization. A screen analysis on the desulfurized slag initially sized at -6 +10 U.S. mesh showed that about 1.5 percent passed through the ten mesh screen after desulfurization (approximately 60 percent sulfur removal).

Gas analysis of samples withdrawn during the course of these experiments indicated the existence of nitrogen, oxygen, carbon dioxide, carbon monoxide, hydrogen and hydrogen sulfide. In general, hydrogen sulfide concentration in cumulative gas samples approached 12 percent by volume on a water-free basis. Formation of hydrogen sulfide and hydrogen along with the absence of sulfur dioxide tends to support the hypothesis put forward in the literature with regard to slag desulfurization by water or steam[25].

Experimental difficulties inherent in the steel reactor resulted in expenditure of considerable quantities of slag. Because of limited availability of slags, the all-ceramic desulfurization apparatus shown in Figure 47 was designed to use only 0.5 to one gram slag samples. As small quantities of slag were involved, it was not possible to quantitatively collect sulfur produced. However, sulfur deposition was evidenced in the cooler regions of the reaction tube. Periodic spot samples obtained for gas analysis (particularly during the early portions of the run) indicated no sulfur loss as gaseous SO_2 or H_2S. Consequently, it is assumed that all sulfur loss from the desulfurized slag sample occurred by formation of elemental sulfur. The latter assumption requires further experimentation on larger quantities of material using more refined experimental equipment. Kinetics of sulfur removal were followed by determining residual sulfur content in the slag after a known period of reaction time. Results of this work are presented in Figures 49, 50 and 51.

Figure 49 shows the desulfurization that occurs as a function of time when correlated according to the topochemical reaction model proposed by Wen (Equation 8). The data correlate for a model that assumes chemical

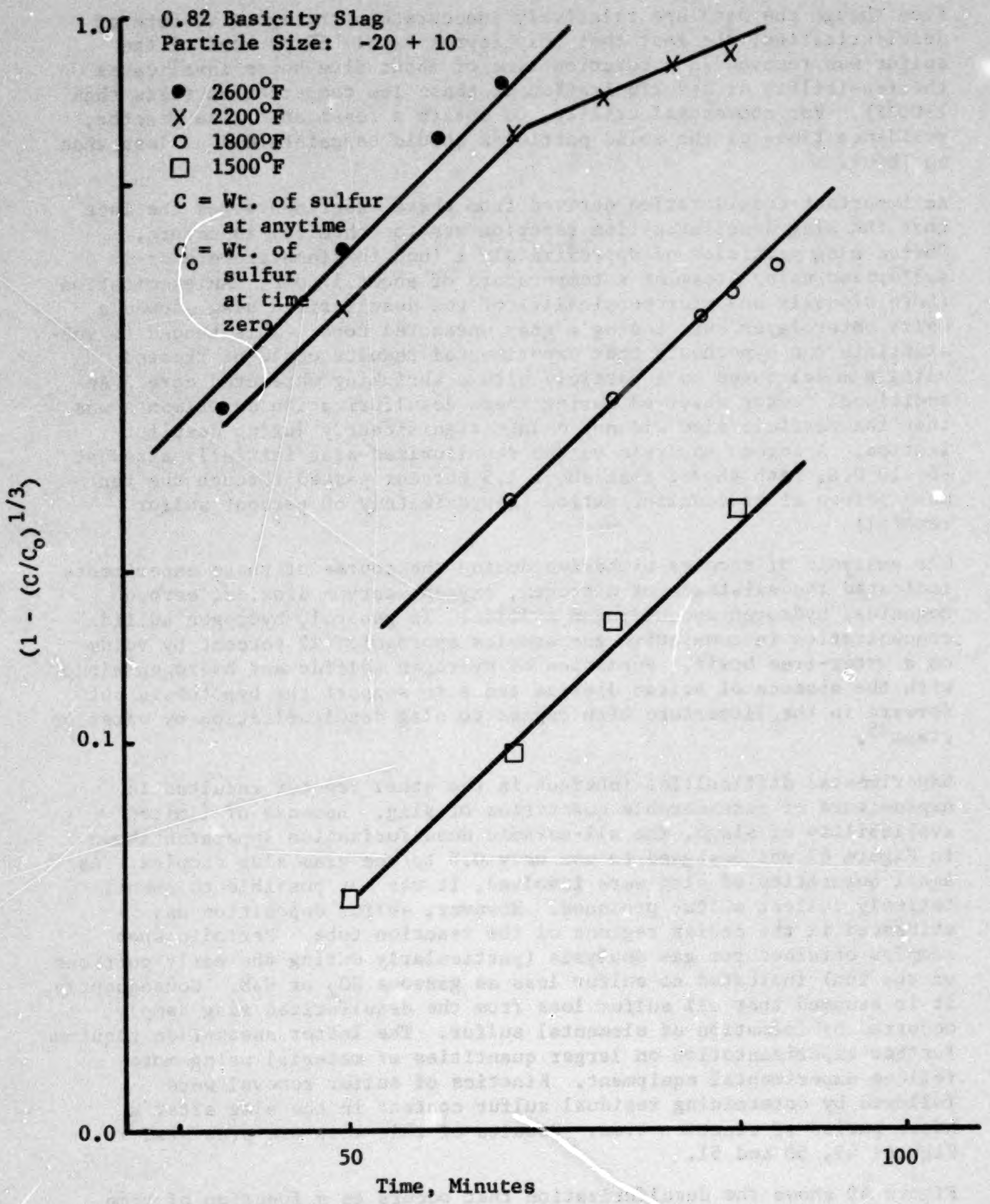

FIGURE 49 - EFFECT OF TIME ON DESULFURIZATION, SLAG BASICITY OF 0.82

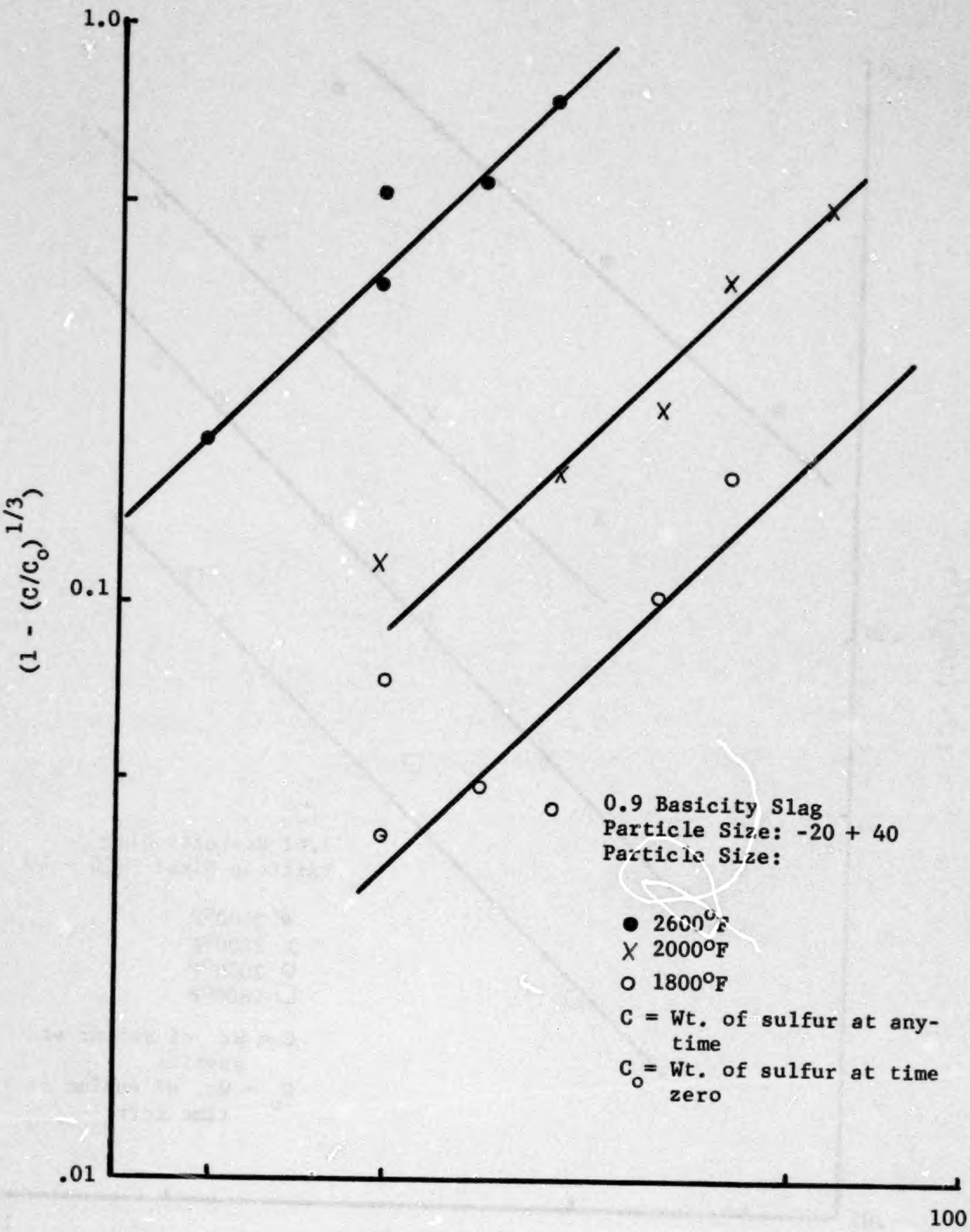

FIGURE 50 - EFFECT OF TIME ON DESULFURIZATION SLAG BASICITY OF 0.90

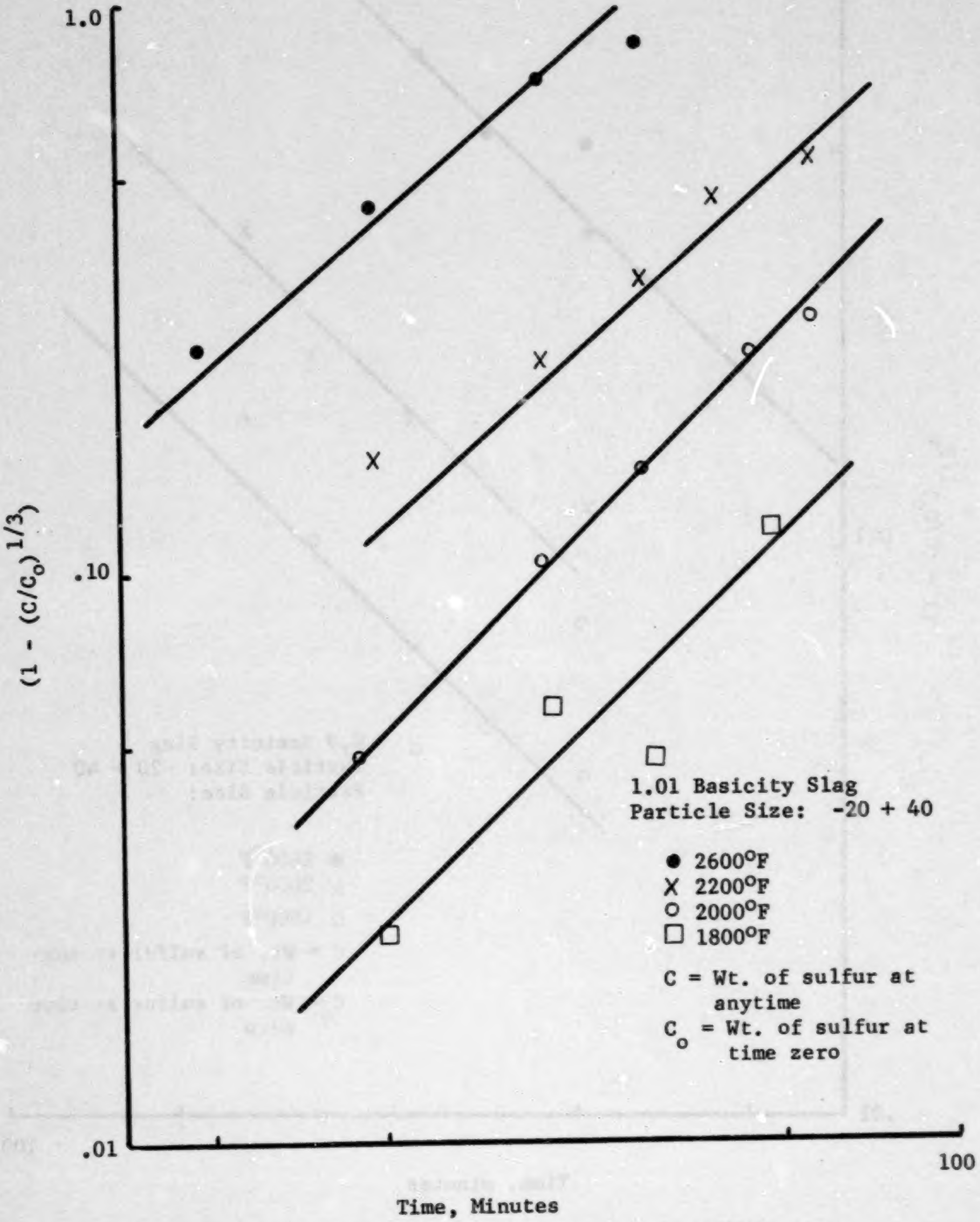

FIGURE 51 - EFFECT OF TIME ON DESULFURIZATION
SLAG BASICITY OF 1.01

reaction controls, inasmuch as a slope of one prevails. The reaction temperature shown is the furnace temperature and not the temperature of the slag. Since steam and air were introduced into this system as soon as the slag was placed in the hot zone of the furnace, desulfurization occurs over a range of temperatures varying from somewhat above room temperature up to the final reaction temperature for a given run. Since the overall reaction rate thus determined is less than the true reaction rate for the stated temperature, subsequent reactor design based on these data should be conservative in nature.

Desulfurization data for the 0.82 basicity slag followed a pattern that was consistent with that obtained earlier in the stainless steel reactor experiments. Figure 49 shows that the rate of desulfurization increases with increasing reaction temperature. At temperatures below 1800°F chemical reaction controls desulfurization rate and the data are correlated by a straight line of slope one. A change in slope occurred for the 2200°F test at a desulfurization level to approximately 94 percent. The departure from chemical reaction as exemplified by the change of slope from one to 0.5 indicates that ash diffusion is controlling in this region. This implies that the topochemical nature of the reaction observed earlier with coarse particles in the steel reactor experiments persists for the 0.82 basicity slags. As will be seen later, this phenomenon did not exhibit itself in the higher basicity slags. It is not known at this time why the 0.82 basicity slag shows this effect whereas the other slags do not. As the furnace temperature was increased to 2600°F, the desulfurization data exhibit chemical reaction control over the entire sulfur removal range studied (residual slag sulfur content at the end of 20 minutes was 0.01 percent which corresponds to 95 percent sulfur removal). The reason for the apparent anomaly of reversion to chemical reaction control lies in the fact that the slag particles became liquid after 20 minutes in the furnace at 2600°F. In this manner the unreacted core containing the residual sulfur was exposed to the reaction gases. Consequently, diffusion through the solid ash (reacted layer) region of these solid particles no longer existed.

Desulfurization data for 0.9 and 1.01 basicity slags are presented in Figures 50 and 51 respectively. As is evident, they all follow a chemical reaction controlled regime with the data lying along a straight line of slope one. A comparison of the desulfurization data tends to indicate that the ease of desulfurization increases with decreasing basicity. However, subsequent calculations show that the apparent desulfurization rate when corrected for the differences in external specific surface for each of the slags, reduces the desulfurization data to a common denominator.

Using Equation (8), and the curves of Figures 49, 50 and 51, specific reaction rates were calculated from the intercepts of the straight lines shown in these figures. Correction of the specific reaction rate for differences in external specific surface permits a correlation of reaction rate as a function of temperature as shown in Figure 52. It

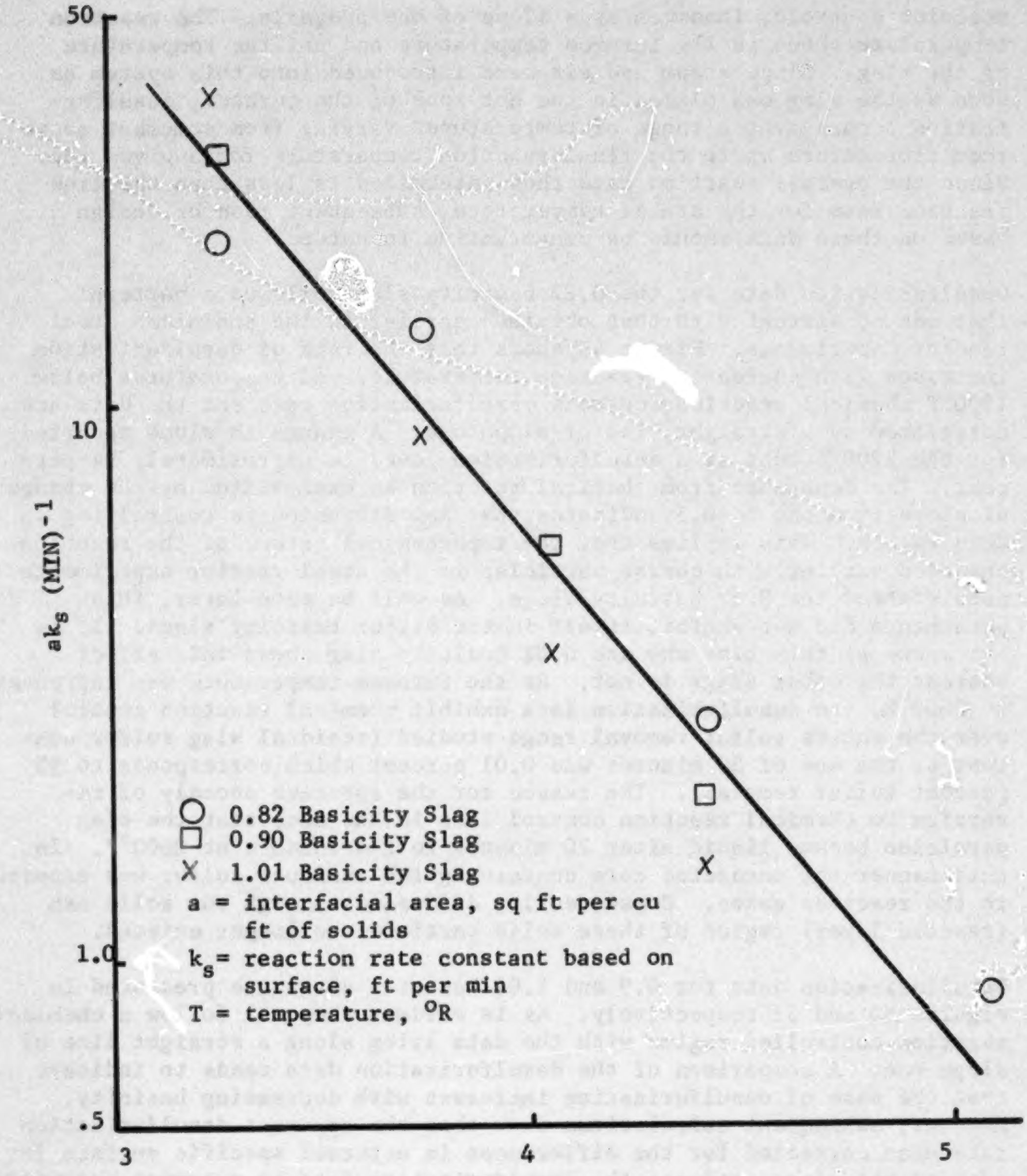

FIGURE 52 - EFFECT OF TEMPERATURE ON SPECIFIC REACTION RATE

can be seen that the data are correlated reasonably well by the Arrhenius plot. For these data, the correlating equation is given by

$$(9) \qquad ak_s = 3.036 \times 10^4 \, \text{Exp}(-21{,}442/T)$$

where:

a = interfacial area, sq ft per cu ft of solids

k_s = reaction rate constant based on surface, ft per min

T = temperature, ^oR

Substitution of Equation (9) into Equation (8) and rearranging results in

$$C = Co \left(1 - \frac{3.86 \times 10^{-8} \, t \, \exp\,(-21{,}442/T)}{aT \, C_{so}} \right)$$

where:

C = weight fraction of sulfur in solids at any time
C_o = weight fraction of sulfur in solids at time zero
C_{so} = initial concentration of solid reactant, made per cu ft
t = time, minutes

This is the correlating equation of all of the data presented in Figures 49, 50 and 51. By use of this equation, it is possible to determine the residual sulfur content in a slag (over the basicity range studied) as a function of time, temperature, specific surface and initial sulfur content.

A comparison of the calculated percent sulfur in the slag versus the experimental sulfur actually obtained is presented in Figure 53. The data correlated reasonably well and it should be pointed out that Equation (10) tends to be conservative for the lower basicity slag. By and large, the bulk of the data lying above the line on Figure 53 associated with 0.82 basicity slag. This is to say that Equation (10) yields a higher residual sulfur content than was actually achieved in the experimental program. Inasmuch as the lower basicity slags tend to favor the overall economics of the process, an engineering reactor design based on Equation (9) will prove to be conservative.

Engineering Reactor Design Recommendations

The experimental effort was completed using synthetic slags in an attempt to anticipate results that may be achieved from slags produced under commercial conditions. The synthetic slags contained no iron or alkali compounds that may be expected to combine with a slag under actual operating conditions. Additionally, slags produced in this work were of low surface

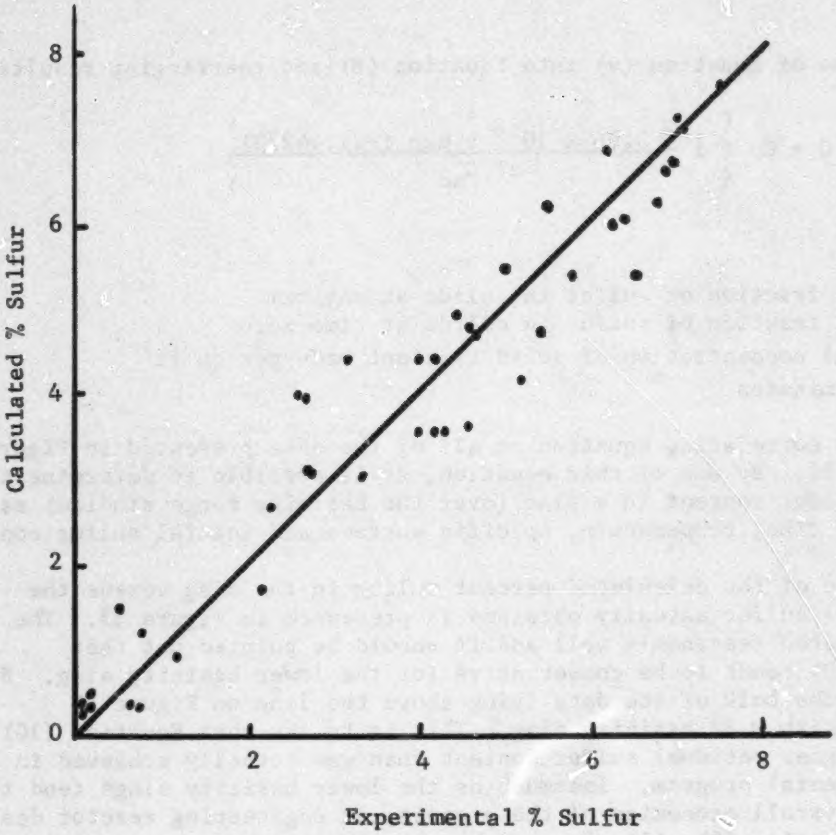

FIGURE 53 - CORRELATION BETWEEN ACTUAL & PREDICATED DESULFURIZATION RESULTS

area and high density unlike those that may be anticipated in commercial production. Consequently, it is assumed that the desulfurization rate data derived from this work will be conservative with regard to the actual rate experienced in commercial equipment. Although conservative desulfurization rate data were obtained, it is not possible to quantitatively state the degree of conversion of sulfide materials to elemental sulfur. Data would tend to indicate that conversion of elemental sulfur is high; however, absolute conversion levels were not established. Although material balances could not be obtained, the qualitative data available indicate that conversion to elemental sulfur can be assumed to be in excess of 90 percent. Until more detailed experiments can be completed on desulfurization of the slag, it is recommended that 90 percent conversion be assumed for further engineering and economic feasibility studies.

Using this assumption, and the design Equation (9) it is recommended that the engineering feasibility study assume the following:

(1) A slag of approximately 0.8 basicity should be employed in the combustor.
(2) Either a liquid or solid slag can be used for desulfurization. When using a liquid slag, reaction temperature should be maintained as high as possible above the melting point. Reaction times under this condition will be approximately 30 minutes.
(3) When using a solid slag, a reaction temperature in excess of 2000°F, and a slag residence time of one hour should be employed.
(4) Solid slags should be crushed to minus 20 U.S. mesh prior to desulfurization.
(5) Desulfurization reaction is controlled by chemical reaction. Consequently, fluid mass flow rates through the reactor can be set at a minimum level so that gas phase mass transfer balances the reaction rate for a given set of conditions.
(6) Further degradation of the slag particles due to desulfurization will not occur.

REFRACTORY LINING LIFE

Introduction

The combustor is the most critical piece of equipment in the acid mine water process because it must contain molten iron and slag at temperatures up to 2700°F. The frequency of maintenance shutdowns to reline the combustor will not only determine the technical and operating feasibility of the process but will also establish the economic potential of the operation.

The main factor which determines the time interval between maintenance shutdowns is the combustor refractory lining's resistance to slag attack. Molten high-carbon iron does not reduce refractory life to a serious degree. However, slags through mechanical erosion and chemical reaction bring about a significant decrease in refractory life. Mechanical erosion of the refractory occurs at the slag-refractory interface, and is often intensified by a softening of the refractory brought on by reactions between the slag and refractory. Chemical attack results from reaction between the refractory and slag that has penetrated deeply into the refractory. Such reactions cause refractory failure either by softening due to formation of low melting compounds or by crumbling of the refractory due to recrystalization.

The life expectancy of refractory linings in contact with low-sulfur (less than three percent) slags found in commercial processes is well known. However, a search of the literature and discussions with vendors failed to uncover any information on life of refractories subjected to slags of high-sulfur content (to minimize the amount of slag processed and to facilitate sulfur recovery, combustor slags will contain approximately ten percent sulfur). Accordingly, a laboratory study was conducted to determine effect of high-sulfur slags on various refractories.

Experimental Procedure

The experimental method used in this study is best described as a compromise between two commonly used refractory tests: the slag button test and the slag drip test. In the commonly used version of the slag button test, a hole drilled in the sample brick is filled with slag. After the two materials have been in contact at high temperature for a predetermined length of time, the brick is cooled and sectioned to measure the slag penetration into the brick. Because this test requires a minimum of furnace space, a large number of samples can be held at temperature for prolonged periods of time. However, the slag in the sample hole is stationary. Consequently, this test does not provide information on mechanical erosion. The button test imposes a severe refractory temperate evaluation. In commercial operations, the refractories are generally exposed to high temperatures on only one face of the brick. The other face is usually at a much lower temperature. In this manner, a temperature gradient is established which is sufficient to solidify any slag or molten material that has penetrated the brick. The solidified material thus acts as a barrier between the brick and molten slag and tends to prevent further chemical attack. In the button test, temperature gradients within the brick are very small or nonexistent, which precludes the possibility of preventing chemical corrosion by solidification of the molten corrosive materials. To some degree, this temperature gradient effect is off-set by a compensating slag-dilution effect. The slag dilution is the result of slag-refractory reactions that may alter the properties of the small amounts of slag used in the test to such an extent that reactions between slag and refractory are inhibited.

With exception of the temperature gradient effect, these limitations do not exist in the slag drip test. In this test, molten slag is caused to drip slowly onto a refractory sample to bring about some mechanical erosion along with a strong chemical attack. However, this test requires considerable space in a high temperature furnace and equipment for feeding the slag into the furnace. As a compromise between the two types of tests, the slag button test was modified to include periodic additions of fresh slag to the test hole of the refractory sample. This modification tends to minimize the neutralization of slag by reaction with the refractory. The test still does not induce mechanical erosion but it does provide a valid comparison between various refractories.

For this study, five conventional types of bricks and three new more expensive high-density bricks were selected, as shown in Table XVII. The super duty fireclay was chosen as reference material, because it is a widely used low-cost refractory. The other conventional refractories consisted of two alumina and two magnesia bricks. The alumina can be expected to resist attack from acid slags. A slag is classified as acid if its acid oxide (silica and alumina) content by weight exceeds the basic oxide (lime and magnesia) content. Since it was not known whether calcium sulfide acts as a neutral compound, weak acid or weak base, alumina as well as basic-slag-resistant magnesia were selected for testing. Both the alumina and magnesia bricks were also tested in tar-impregnated versions. Impregnating the brick with tar results in a deposit of graphite in the pores of the refractory after the brick is heated to operating temperature. The graphite fills and coats the refractory pores, thereby minimizing slag penetration and attack of refractory.

In addition to conventional refractories, three new types of refractories were studied. One of these is an isostatically pressed alumina of extremely low porosity (0.1 percent). In the future, a wider variety of refractory materials is expected to be available as isostatically pressed very low porosity bricks. The remaining two samples were both melted and cast to shape alumina produced by two different manufacturers. The fused cast alumina designated as Type I was a grade that contained air bubbles (blow holes) that were not removed during solidification. The second alumina, Type II was a better quality brick free of blow holes. No fused basic refractories were tested because their tendency to crack under thermal shock would have severely complicated the test procedure. No sudden temperature changes are anticipated during combustor operation, including start-up and shut-down. Accordingly, fused basic refractories should not be excluded from consideration.

TABLE XVII
Refractories Used in Laboratory Tests

Conventional
Superduty Fireclay
High Alumina
Tar Impregnated Alumina
Magnesite-Chrome
Tar Impregnated Magnesia
New
Isostatically Pressed (High Density) Alumina
Fused & Cast Alumina Type I (with "Blow Holes")
Fused & Cast Alumina Type II (without "Blow Holes")

Although it is anticipated that a commercial combustor will contain castable refractories as well as bricks, all samples were cut from brick to insure that each refractory sample was prepared under controlled conditions of mixing, forming and firing. The brick samples used were approximately three inch cubes containing a one-inch diameter hole 1-½-inch deep to hold the slag.

Slag used in this study contained 18.6 percent calcium sulfide and had a basicity ratio of 0.8 where basicity is defined as the weight percent ratio $(CaO + MgO)/SiO_2 + Al_2O_3)$. Chemical composition for the slag is shown in Table XVIII. Preparation of the slag consisted of heating the pure components to 2600°F, cooling, crushing and reheating the mixture three times to insure a uniform composition. The resulting slag was crushed to pass through 100 mesh U.S. sieve, and 12 gram portions were briquetted to yield a 7/8-inch diameter by ½-inch high briquette. Slag briquettes were sized for easy placement in the sample brick test holes while the samples were in the high-temperature furnace.

Twenty-six refractory samples were prepared for testing by preheating to the 2640°F test temperature at a temperature rise of less than 50°F per hour to avoid refractory fracture due to thermal shock. The 2640°F test temperature was chosen as the highest temperature at which the test furnace could be expected to operate continuously for the two-week minimum test duration. Slag briquettes were inserted in the test holes of the brick samples. The samples were periodically inspected and slag was added to those that could hold more (as determined by the slag level being lower than ½-inch from the top of the test hole). Table XIX shows total grams of slag added to each refractory sample. This table also shows the duration of contact of each sample with slag at 2640°F. After each refractory sample completed its scheduled time of contact with slag in the furnace, it was removed and air cooled.

TABLE XVIII
Slag Composition Used in Refractory Study

Component	Percent by Weight
CaS	18.6
CaO	19.3
MgO	17.7
Al_2O_3	17.7
SiO_2	26.7

TABLE XIX
Summary of Test Results

Refractory Type	Hours of Exposure to Slag	Grams of Slag Added	Change in Hole Radius, In.	Change In Hole Depth, Inches
Superduty Fireclay	7.5	12	0	0
Superduty Fireclay	25	60	0.3	0.5
Superduty Fireclay	176	60	0.45	0.7
High Alumina	46	24	0	0
High Alumina	49	60	0.15	0.1
High Alumina	176	72	0.2	0.3
High Alumina	384	60	0.3	0.3
Tar-Impregnated Alumina	176	60	0.2	0.1
Tar-Impregnated Alumina	384	72	0.2	0.1
Magnesite Chrome	46	24	0	0
Magnesite Chrome	176	72	0	0
Magnesite Chrome	384	72	0	0
Tar-Impregnated Magnesia	46	24	0	0
Tar-Impregnated Magnesia	49	72	0	0
Tar-Impregnated Magnesia	176	84	0	0
Tar-Impregnated Magnesia	384	72	0	0
Isostatically Pressed Alumina	7.5	12	0	0
Isostatically Pressed Alumina	384	72	0	0.1
Fused & Cast Alumina I	7.5	12	0	0
Fused & Cast Alumina I	176	72	0.05	0.1
Fused & Cast Alumina I	384	72	0.05	0.2
Fused & Cast Alumina II	176	60	0	0
Fused & Cast Alumina II	384	84	0.05	0.1

To determine the effect of slag attack on the refractory material, the cooled brick sample was cut in a vertical plane as nearly through the center of the hole as possible. The cut sample was first photographed for a permanent record, and then was placed on an office copier when an image was recorded on paper. The image was then used to determine depth of the test hole. The cut sample was then cut on the horizontal plane and the cut fraction was placed on the office copier and an image recorded. This image was then used to measure length of the chord generated by the cut and distance from the chord to the eroded brick hole surface. From these measurements, the diameter of the test hole after exposure to the slag was determined. This procedure was used because of the difficulty in cutting the brick sample exactly on a diameter of the test hole. Amount of erosion was determined by subtracting the original radius from the radius after exposure of the test hole to slag.

Results

Results of this study are shown in Table XIX and Figure 54 where it is seen that there is no measurable erosion of the magnesia samples Figure 54 A, and very little erosion of the new high-density refractories Figure 54 B. There is some erosion of the alumina samples (Figure 54 C) and considerable erosion of the superduty fireclay Figure 54 D a standard low-cost refractory used as reference material. The latter suffered 0.45 inches of erosion after 176 hours of exposure. The high alumina brick showed approximately one-half the erosion of the superduty fireclay for the same 176 hour exposure to slag. The attack on tar-impregnated high alumina was even less than that of the plain high alumina.

The superior erosion resistance of tar-impregnated high alumina brick compared to high alumina brick is attributed to the carbon coating formed within the tar-impregnated brick after firing. Samples of fused and cast alumina (Types I and II) showed very little erosion after 384 hours of exposure to slag. These materials have relatively low porosities (one percent to four percent) but the isostatically pressed alumina has even a lower pososity (0.1 percent) and tends to show a slightly greater resistance to slag erosion. After 384 hours of contact to slag, this material exhibited no significant slag penetration. Thus the alumina data indicate that the fused and cast materials will be acceptable refractories.

The magnesia samples (including the magnesite-chrome) indicated no change in test hole dimensions after being in contact with slag for up to 384 hours. However, observation of the brick samples after testing indicated that a large percentage of the slag effected an erosion-free penetration of the brick. This implies a high degree of wettability of the brick by the slag so that the slag freely entered the pores of the brick. The slag-refractory reaction appeared to be minor with no evidence of refractory softening or crumbling. For these reasons, it can be expected that, in a commercial operation where the bricks have a temperature gradient imposed on them, the slag will freeze after penetrating the pores of the brick. In this manner, refractory life will be enhanced.

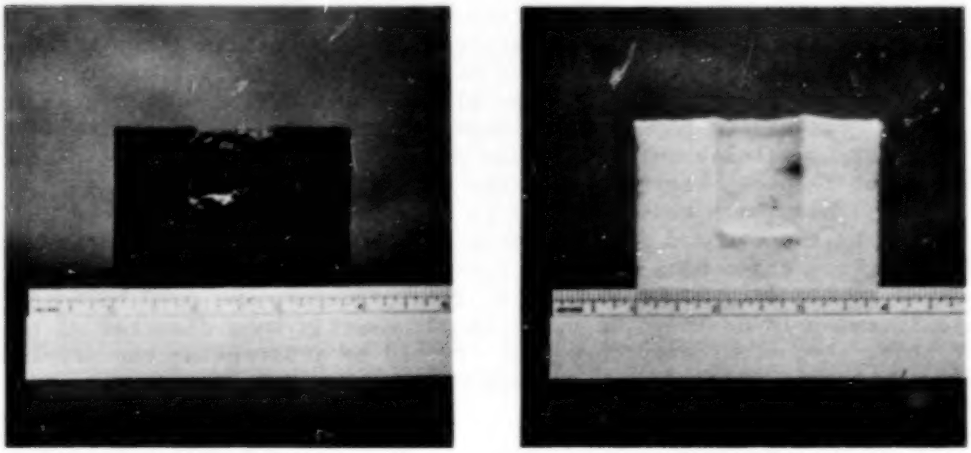

Figure 54 A
Magnesite-Chrome
Brick
384 Hours

Figure 54 B
Fused Alumina-Type II
384 Hours

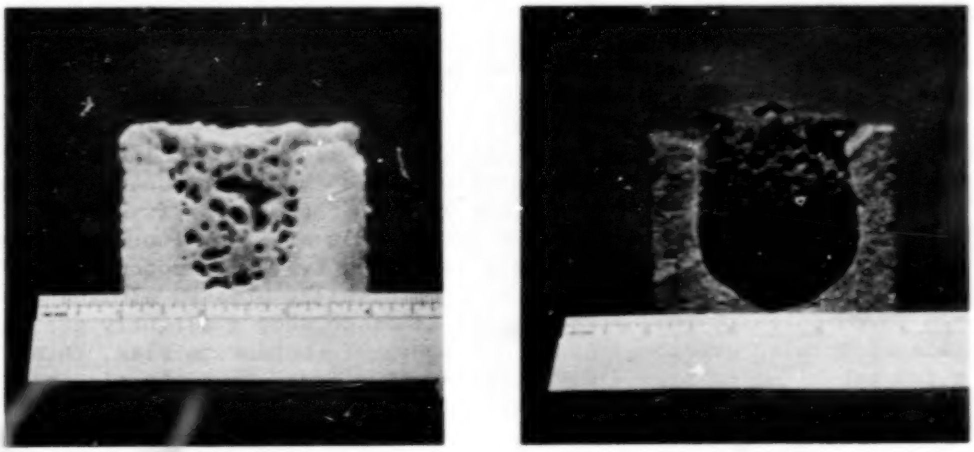

Figure 54 C
High Alumina
384 Hours

Figure 54 D
Fireclay
176 Hours

FIGURE 54 - THE EFFECT OF SLAG CONTACT ON REFRACTORY EROSION

Time Parameters: Hours of Slag-Refractory Contact

Above results show that calcium sulfide in the slag acted as a mild base; and, in conjunction with the lime and magnesia content of the slag (see Table XVIII), caused it to act as a base. This basic slag attacked the alumina bricks, but not the magnesia bricks. As is the case with most slags, this was better contained by the less porous refractories.

Design Recommendations

The refractory study shows that the high sulfur content of the slag being considered for the combustor does not significantly effect reactivity of these slags with refractories.

For economic evaluation of the process use of the magnesite-chrome brick that performed so well in these tests should be assumed.

Prior to final design of the commercial installation, price and availability of fused or other low-porosity basic bricks should be investigated.

APPENDIX B
THE PROCESS WORKING AREA DIAGRAM

To generate a process working area diagram (PWAD) requires that the energy and material balance computer program be run using ranges of slag recycle fraction and flux rate at the selected heat rate. For illustration purposes, a two million gallon per day acid mine water plant utilizing partially neutralized dilute AMW will be used. The PWAD will be generated for a process operating at a heat rate of two million BTU/1,000 gallon AMW using a ten percent sulfur coal refuse having a heating value of 6,000 BTUs/lb. The computer program was run using flux rates of 100, 200, 300 and 400 tons per day with spent slag recycle fractions of 0, 0.4, and 0.8. Results from these runs are shown in Table XX where the flux rate, spent slag recycle fraction, resulting slag basicity, air preheat temperature, and percent sulfur in slag are presented.

TABLE XX
Computer Results Used to Generate Process Working Area Diagram*

Flux Tons/Day	Spent Slag Recycle Fract.	Slag Basicity	Air Temperature, °F	Percent Sulfur In Slag
100	0	0.00	1507	18.44
100	.4	0.19	1610	12.17
100	.8	0.42	2051	4.10
200	0	0.47	1562	14.41
200	.4	0.67	1701	9.19
200	.8	0.90	2314	3.27
300	0	0.94	1616	11.83
300	.4	1.15	1786	7.43
300	.8	1.37	2556	2.60
400	0	1.42	1669	10.03
	.4	1.63	1869	6.25

* Partially neutralized dilute acid mine water heat rate-2 MM BTU/1,000 gallon AMW, ten percent S coal refuse, combustor temperature 2700°F, 2,000,000 gallon AMW plant.

The first step in generating a PWAD is to prepare a plot of basicity versus spent slag recycle fraction at various flux rates into the kiln. Figure 55 is such a plot and was prepared using the data of Table XX. In Figure 56 is presented a plot of air preheat temperature versus slag recycle fraction at various flux rates. From this figure it is seen that at a given flux rate the required air preheat temperature increases as the slag recycle fraction increases. Also shown is the fact that at a given slag recycle fraction the air preheat temperature increases as the flux rate increases. Constructing a line at the 2000°F air preheat

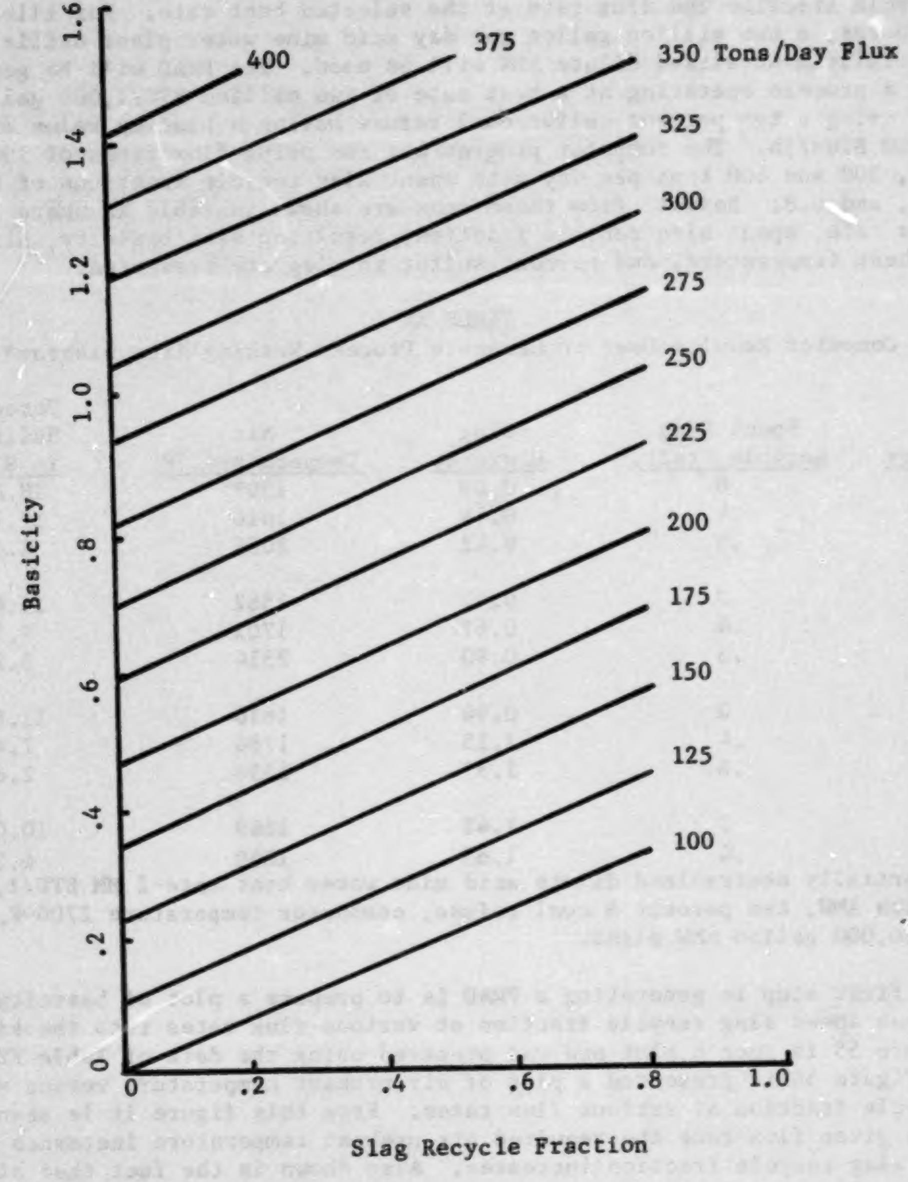

FIGURE 55 - SLAG BASICITY VS. SPENT SLAG RECYCLE FRACTION OF VARIOUS FLUX RATES

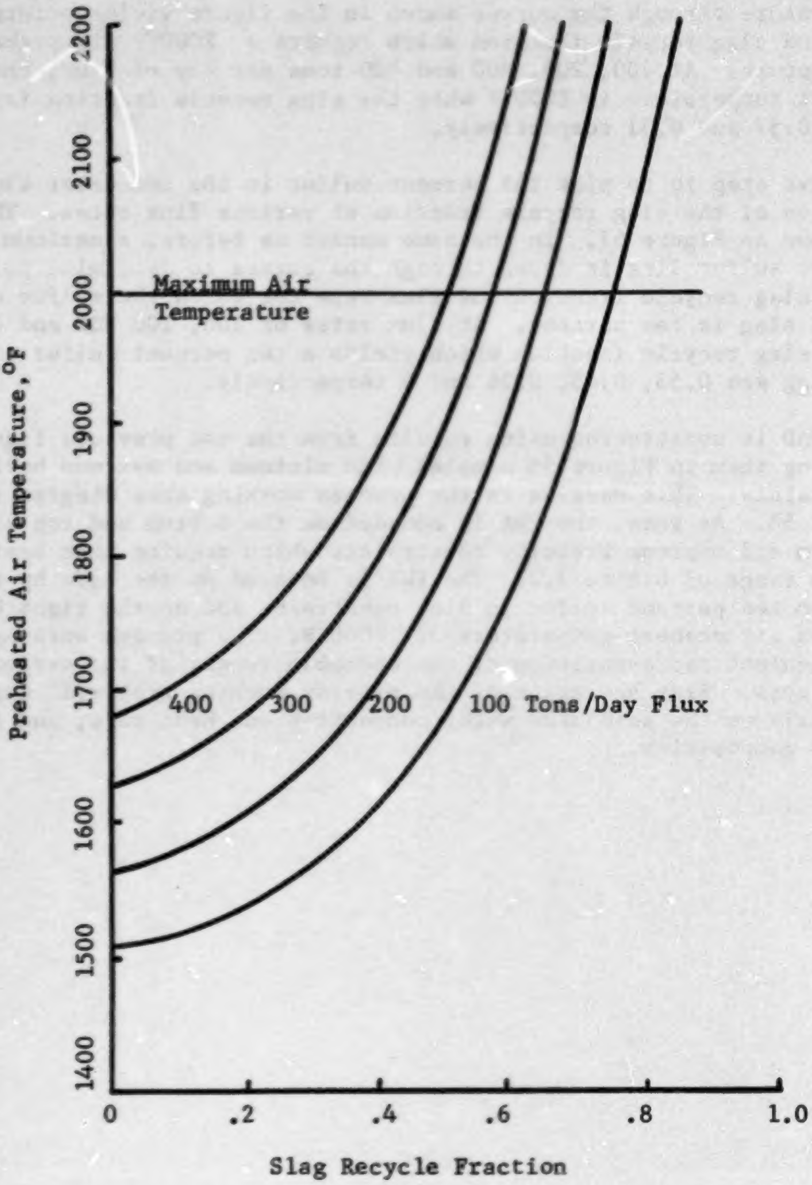

FIGURE 56 - REQUIRED PREHEATED AIR TEMPERATURE VS. SLAG RECYCLE FRACTION OF VARIOUS FLUX RATES

temperature through the curves shown in the figure yields points of flux rate and slag recycle fraction which require a 2000°F air preheat temperature. At 100, 200, 300 and 400 tons per day of flux, the air preheat temperature is 2000°F when the slag recycle fraction is 0.77, 0.64, 0.57 and 0.51 respectively.

The next step is to plot the percent sulfur in the combustor slag as a function of the slag recycle fraction at various flux rates. This plot is shown as Figure 57. In the same manner as before, a maximum ten percent sulfur line is drawn through the curves to determine points of spent slag recycle fraction and flux rate for which the sulfur content of the slag is ten percent. At flux rates of 100, 200 300 and 400 the spent slag recycle fraction which yields a ten percent sulfur content in the slag are 0.53, 0.43, 0.26 and 0 respectively.

The PWAD is constructed using results from the two previous figures and applying them to Figure 58 coupled with minimum and maximum basicity constraints. This results in the process working area diagram shown in Figure 58. As seen, the PWA is bounded on the bottom and top by the minimum and maximum basicity constraints which require that basicity be in the range of 0.8 to 1.2. The PWA is bounded on the left by the maximum ten percent sulfur in slag constraint and on the right by the maximum air preheat temperature of 2000°F. The process working area is a convenient representation of the operable ranges of the various process parameters. Size and shape of the process working area will depend primarily on the acid mine water concentration, heat rate, and the coal refuse composition.

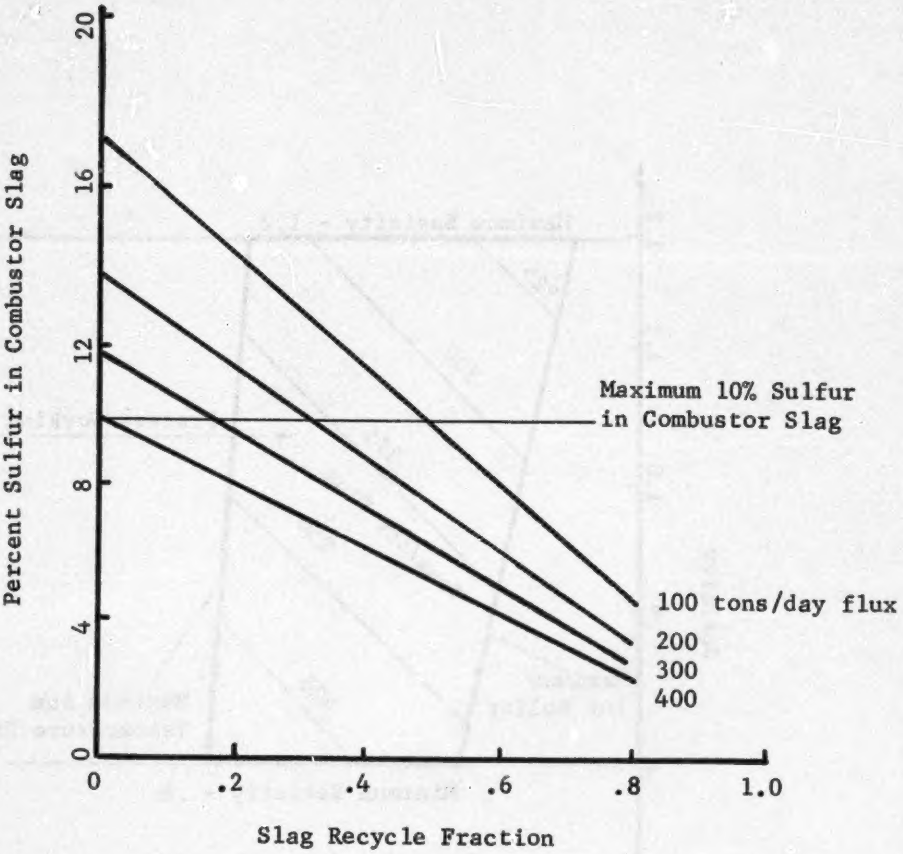

FIGURE 57 - PERCENT SULFUR IN COMBUSTOR SLAG VS. SLAG RECYCLE FRACTION AT VARIOUS FLUX RATES

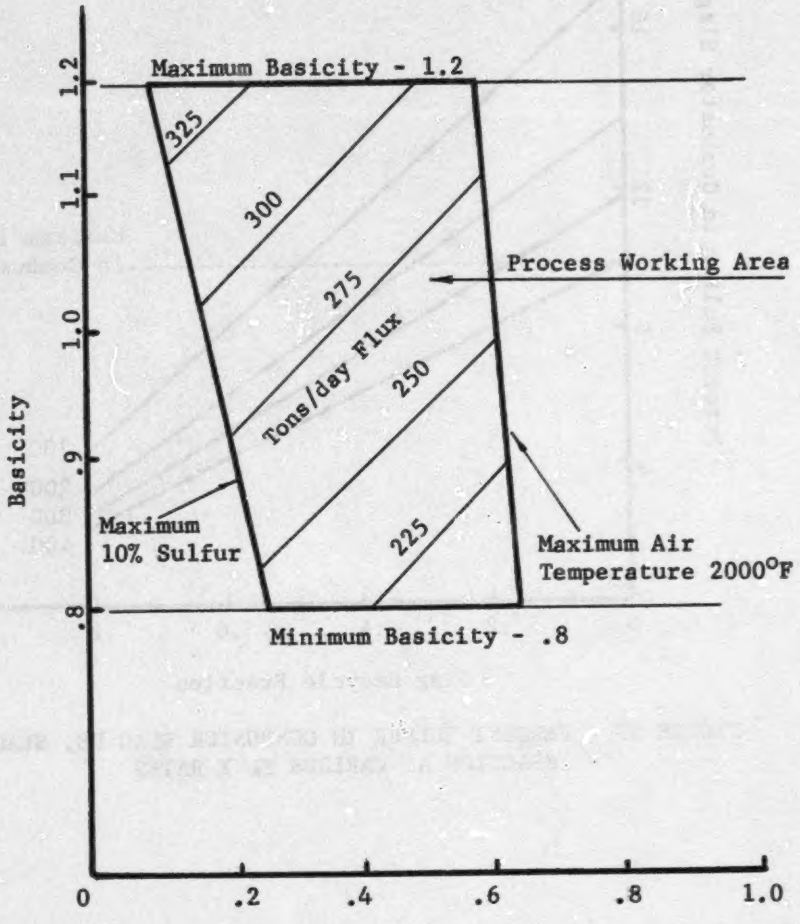

FIGURE 58 - PROCESS WORKING AREA DIAGRAM FOR A 2 MM GAL/DAY PLANT USING PARTIALLY NEUTRALIZED DILUTE AMW AND A HEAT RATE OF 2 MM BTU'S/1,000 GALS AMW

APPENDIX C
EQUIPMENT COSTS

To determine the capital investment requirement for the process, the process equipment was grouped into nine equipment complexes. These equipment complexes were designated as (1) coal handling system, (2) neutralization, (3) steam turbine--air compressors, (4) direct-fired air heater, (5) waste heat boiler, (6) combustor, (7) distillation, (8) desulfurization, and (9) rotary kiln dryer. Individual costs of these complexes were determined for a two MM GPD AMW plant utilizing partially neutralized dilute AMW, a ten percent sulfur coal refuse with a heating value of 6,000 BTU/lb., a heat rate of two MM BTUs/1,000 gallon AMW, a flux rate of 230 tons/day and a spent slag recycle fraction of 0.4. The energy and material balance computer program was run, using the above values to determine the capacity and/or temperature of the process streams which control the size and consequently the cost of the equipment complexes. These costs and capacities are then used to scale up or down the equipment complex costs for any plant size and operating conditions.

The process streams which control the size and cost of the various equipment complex are as follows:

Equipment Complex	Process Stream(s) Determining Capacity
Coal Handling System	Coal Rate, Tons/Day
Neutralization	Acid Mine Water, Gallons/Day
Steam Turbine--Air Compressors	Coal Rate, Tons/Day
Direct Fired Furnace	Air Preheat Temperature, °F, and Air Rate, Tons/Day
Waste Heat Boiler	Acid Mine Water, Gallons/Day
Combustor	Combustor Offgas, Tons/Day
Distillation	Acid Mine Water, Gallons/Day
Desulfurization	Combustor Slag, Tons/Day
Rotary Kiln Dryer	Dry Solids Leaving Kiln, Tons/Day

Based on 333.3 tons/day of coal refuse, the coal handling system will cost $91,290 (mid - 1970, purchase price at factory). The coal handling system consists of a belt conveyor to transport coal from a storage pile to a hammer mill, a rotary dryer to dry the crushed coal, pneumatic conveying equipment to transport the crushed coal to process storage, a storage tank, a hopper, and pneumatic conveying equipment to transport the coal to the combustor lances. Individual costs for this equipment plus relevant sizes and/or capacities are presented in Table XXI.

Based on partially neutralizing two MM GPD of AMW, the neutralization complex will cost $50,795. The neutralization complex consists of a stainless steel pump to pump AMW into a neutralization tank, a pneumatic conveying system to transport limestone into the neutralization

TABLE XXI
Coal Handling Complex Cost

Item of Equipment	Size/Capacity	Cost
Coal Refuse Belt Conveyor with Motor & Drive Equip.	14" Belt x 22 Ft. @ 150 Ft/Min.	$ 2,910
Hammer Mill	14 tons/hr	5,620
Rotary Kiln Coal Dryer	7.5 ft. dia. x 55 ft.	69,000
Complete Pneumatic Conveying System for Crushed Coal to Process Storage	13.5 tons/hr	7,870
Process Storage Tank Carbon Steel	1,000 Gallons	3,050
Pneumatic Conveying System for Crushed Coal Into Combustor Lances	13.5 tons/hr	2,050
Hopper, Carbon Steel	8 hr. hold-up	790
Total Cost, Coal Handling System		$91,290

tank, two agitators to stir the AMW in the neutralization tank, and a bronze pump to pump partially neutralized AMW to the distillation unit. The individual equipment costs for the neutralization complex are presented in Table XXII.

TABLE XXII
Neutralization Complex Cost

Stainless Steel and Bronze Pump	2 MM GPD AMW	$11,650
Neutralization Tank Stainless Steel	42,000 Gallons	30,500
Limestone Pneumatic Conveying System	2 tons/hr	5,925
Agitators (2)	--	2,720
Total Cost, Neutralization Complex		$50,795

High pressure steam exiting the waste heat boiler will be used in two steam turbine-air compressors to generate compressed air at eight to ten psig to transport coal refuse into the combustor and air at four to five psig for combustion in the combustor. The low pressure steam exiting the compressors will be used as the steam source for distillation. Based on transport and combustion air requirements the steam turbine--air compressor complex will cost $28,500. The air compressor required to supply one ton/hr of air at eight to ten psig for pneumatic injection of coal will cost $5,500. The air compressor required to supply 25 tons/hr of combustion air at four to five psig will cost $23,000.

The cost of a direct fired heater which is used to preheat the combustion air entering the combustor depends on air preheat temperature and combustion air rate into the combustor. The air preheat temperature determines the material of construction used for the direct fired furnace and the heat transfer surface required. Based on heating 636 tons/day of air, the cost of the direct fired furnace at various air preheat temperatures is shown in Table XXIII.

TABLE XXIII
Direct Fired Heater Complex Cost

Air Preheat Temp., °F	Material of Construction	Cost
700	Carbon steel	$ 33,000
1000	Carbon steel	38,000
1300	Carbon steel	42,700
1300	Chrome/moly.	61,700
1700	Chrome/moly.	98,000
2000	Chrome/moly.	121,000

The waste heat boiler uses combustor offgas to generate steam for distillation. Based on generating 830 tons/day of steam at 100F superheat and 250 psig, the waste heat boiler costs $90,000.

The combustor is a refractory lined steel vessel containing air and coal lances, a slag-iron separation box, and a chrome/moly. star valve for admitting dryer solids. Based on 805 tons/day of combustor offgas, the combustor will cost $46,600. The individual costs associated with the combustor complex are presented in Table XXIV. The distillation complex consists of a complete flash distillation plant without equipment to generate steam and provide AMW to the distillation plant. In the process the waste heat boiler is used to supply the steam requirements for distillation. Cost of a distillation plant depends on the capacity of the plant, the economy factor used in the design and whether partially neutralized AMW is used. The economy factor, which is a function of the steam available for distillation, determines the heat transfer surface required to distill the acid mine water. Consequently, the economy factor affects the cost of the plant. Concentration of the acid mine water (if neutralization is not used) affects plant cost because it determines the materials of construction. When partial neutralization is used the AMW

TABLE XXIV
Combustor Complex Cost

Item of Equipment	Size/Capacity	Cost
Carbon steel combustor shell and slag-iron separator	14 ft dia. x 15 ft	$ 9,000
Refractory lining	Magnesite-Chrome Brick	21,600
Coal lances (2)	2" I.D. x 12 ft Copper	15,000
Air lances (6)	6" I.D. x 12 ft Copper	1,000
Total cost, Combustor complex		$46,600

composition does not affect the cost of the distillation plant. In Table XXV are presented the installed costs of distillation plants operating with and without partial neutralization at economy factors of five to ten for dilute and moderately concentrated AMW. These costs were provided by the manufacturer for a two MM GPD plant.

TABLE XXV
Distillation Complex Cost

Distillation Conditions	Size/Capacity	Cost
Distillation, neutralized Dilute acid mine water	2 MM GPD AMW, Economy factor of 10	$2,500,000
Distillation, neutralized Dilute acid mine water	2 MM GPD AMW, Economy factor of 5	2,000,000
Distillation, unneutralized Dilute acid mine water	2 MM GPD AMW, Economy factor of 10	2,500,000
Distillation, unneutralized Moderately concentrated of acid mine water	2 MM GPD AMW, Economy factor of 10	2,800,000

The desulfurization complex is used to remove sulfur from the combustor slag. Based on the desulfurization of 406 tons/day of slag the desulfurization complex is $73,000. The desulfurization complex consists of an enclosed belt conveyor to transport hot slag to a crusher, a cold slag belt conveyor to transport desulfurized slag to the hot slag conveyor to provide a protective covering for the belt, a desulfurized slag quencher and hood, a refractory lined steel reaction vessel where a sulfur rich gas is produced, a sulfur condenser to condense sulfur from the gas, and sulfur storage facilities. The costs for this equipment plus the relevant sizes and/or capacities are presented in Table XXVI.

TABLE XXVI
Desulfurization Complex Cost

Item of Equipment	Size/Capacity	Cost
Enclosed hot slag belt conveyor	18" Belt, 75 ft	$21,200
Cold slag conveyor	12" Belt, 30 ft	3,460
Crusher	20 tons/hr	7,850
Reaction Vessel	8 ft dia x 20 ft Refractory Lined	26,500
Sulfur Condenser	35 tons/day sulfur	5,620
Sulfur storage tank	150 ft^3	3,370
Desulfurized slag quencher & hood	388 tons/day spent slag	5,000
Total cost, Desulfurization Complex		$73,000

Equipment associated with the rotary kiln dryer are: kiln structure, combustion equipment to burn the combustor offgas and kiln refractory lining. Based on 283.9 tons/day of solids leaving the kiln the cost is $315,000 as shown in Table XXVII.

TABLE XXVII
Rotary Kiln Dryer Cost

Item of Equipment	Size/Capacity	Cost
Kiln structure	9 ft dia x 270 ft	$265,000
Combustion equipment	275 tons/day combustor offgas	30,000
Refractory lining	High alumina brick	20,000
Total Cost, Rotary Kiln Dryer complex		$315,000

Equipment costs for the various equipment complexes were determined using standard capital cost estimating procedures or obtained from manufacturer quotes.

APPENDIX D
THE THEORY OF CARBON SOLUBILITY RATES

Introduction

The steady state operation of the combustor requires that a balance exist between the rate of carbon removal by oxidation and the rate of carbon solution in the molten iron bath. Literature data are available which indicate that carbon removal rates in excess of one percent per minute can be achieved. In general, the rate of carbon removal is limited by the rate at which oxygen or air is introduced into the molten bath. Carbon solution rates, on the other hand, present a more difficult problem. Olsson, et. al.[27,32], in laboratory work pertaining to the rate of solution of solid carbon in molten iron, have shown that solubility is mass transfer controlled. Carburization of open hearth melts using anthracite, coke, graphite, gas carbon and charcoal has been reported by Leary et. al.[33]. In their work on commercial open hearth melts containing low carbon, they have reported carburization rates as high as two percent carbon per minute. Another significant aspect of this work was the conclusion that sulfur contained in the carbon was distributed between the slag and metal with essentially no evolution in the gas phase.

Because the literature data on recarburization were relatively scant and generally done in shallow metal baths, a theoretical study was completed to determine the effect of carbon particle size on residence time in the hot bath and the depth of hot metal required to essentially affect a complete dissolution of the carbon before it reaches the surface of the molten iron. This section presents results of this work.

Theory

Since the solution of solid carbon into an iron melt is mass transfer controlled[32], the rate of solution can be defined as

$$-(dn/dt) = KA\ (C_i - C_b) \tag{1}$$

where n is the weight of carbon in the particle, K is the mass transfer coefficient (cm/sec), A is the surface area of the particle (cm^2), C_i and C_b are the carbon concentration at the reaction interface and in the liquid phase respectively (g/cm^3). The mass transfer coefficient is dependent on the relative velocity between the carbon and the liquid interface, on the diffusion coefficient and on the shape of the solid particle. A generalized mass transfer correlation is given by

$$(Kr/D) = 1.0 + 0.3\ (N_r)^{\frac{1}{2}}\ (N_s)^{1/3} \tag{2}$$

where r is the radius of the particle (cm), D is the diffusivity of carbon in iron (cm^2/sec), and $N_r N_s$ are the Reynolds and Schmidt numbers respectively (dimensionless).

Combining these two equations with a carbon material balance and a particle force balance completely defines the physical system of rising carbon particles dissolving in a molten iron bath. The material balance for each particle (assumed spherical) is

$$(dn/dt) = p_s \, d\,(4\, r^3/3)/dt \qquad (3)$$

where t is the time (sec), P_s is the solid density (g/cm^3) and d represents the differential operator.

The force balance about the particle rising in the molten iron bath at its terminal velocity indicates that the buoyancy force is equal to the sum of the drag and gravitational forces. Mathematically

$$4\ (r^3 p_f g/3) = 4\ (f r^2 V_t^2\ p_f) + 4\ (r^3 p_s g) \qquad (4)$$

where p_f is the density of the fluid (g/cm^3), f is the drag coefficient (dimensionless), g is the gravitational constant (cm/sec^2) and V_t is the terminal velocity of the particle (cm/sec). The drag coefficient is a function of the Reynold's number[19] and is given by

$$f = 18.5/(N_r)^{0.6} \qquad (5)$$

Combining equations (1-5) and solving for the change of particle radius with residence time in the molten iron bath yields

$$-(dr/dt) = a_1(1/r + a_2 r^{0.071})\ (C_i - C_b) \qquad (6)$$

where

$$a_1 = D/p_s$$

$$a_2 = 0.31\ N_s^{1/3}\ P_f^{0.4}\ (P_s - P_f)^{1/4}\ g^{1/4}\ /v^{0.65}$$

and v = viscosity (g/cm sec) and the other terms are as defined previously.

By maintaining the carbon composition and temperature in the bath constant at steady state, Equation (6) can be integrated to find the residence time of the carbon particle in the bath at any fraction of its initial weight.

To compute the metal bath depth required to dissolve a particle, the force balance (Eq. 4) can be solved for the terminal rising velocity and combined with Equation (6) to yield

$$-(dh/dr) = 1/(a_3 r^{-2.142} + a_4 r^{-1.071}) \qquad (7)$$

where h is the bath depth required to dissolve a carbon particle to any desired fraction of its initial weight and

$$a_3 = a_1/a_5$$

$$a_4 = a_2 a_3$$

$$a_5 = \left\{0.289\ (p_s - p_f) g/p_f^{\ 0.4}\ v^{0.6}\right\}^{1/2}$$

Specification of the carbon feed rate into the combustor and a desired carbon solution rate determines the amount of hot metal required in the combustor. This results because the amount of hot metal is directly proportional to the carbon feed rate and inversely proportional to the carbon solution rate at steady state. Consequently, knowing the weight of hot metal required and the depth of hot metal necessary to dissolve the carbon particle the diameter of the combustor is readily established.

Discussion of Theoretical Calculations

To determine the effect of particle radius on the particle residence time required to dissolve 99.9 percent of the carbon particle Equation (6) was integrated numerically on a digital computer. The results of this work are presented in Figure 59. The parameters on the figure refer to a surface factor which relates the actual surface area of the particle to the surface area of a smooth sphere having the same diameter as the particle in question. As is evident, the residence time requirement for a given surface factor decreases with decreasing particle radius. Numerical integration of Equation (7) shows a similar effect (Figure 60) for the molten metal bath depth requirement as a function of carbon particle radius.

The actual specific surface of the coal refuse after injection into the molten iron bath is not known. However, it is believed that a considerable expansion (somewhat like a popcorn effect) will occur due to the evolution of volatile matter and thermal shock. It is believed that the surface factor under these conditions will lie in the range of 10 to 100.

For the economic and engineering evaluation, the combustor was sized conservatively using a surface factor of one. A closely sized coal fraction was injected into the combustor having an average particle diameter of 1.6 mm (-10 + 20 U.S. mesh). As would be expected, in actual operation of the combustor the coal will be ground to a wide size distribution such as -10 mesh rather than cut to a close particle size. However, for a conservative estimate on the combustor dimensions, closely sized coal was used.

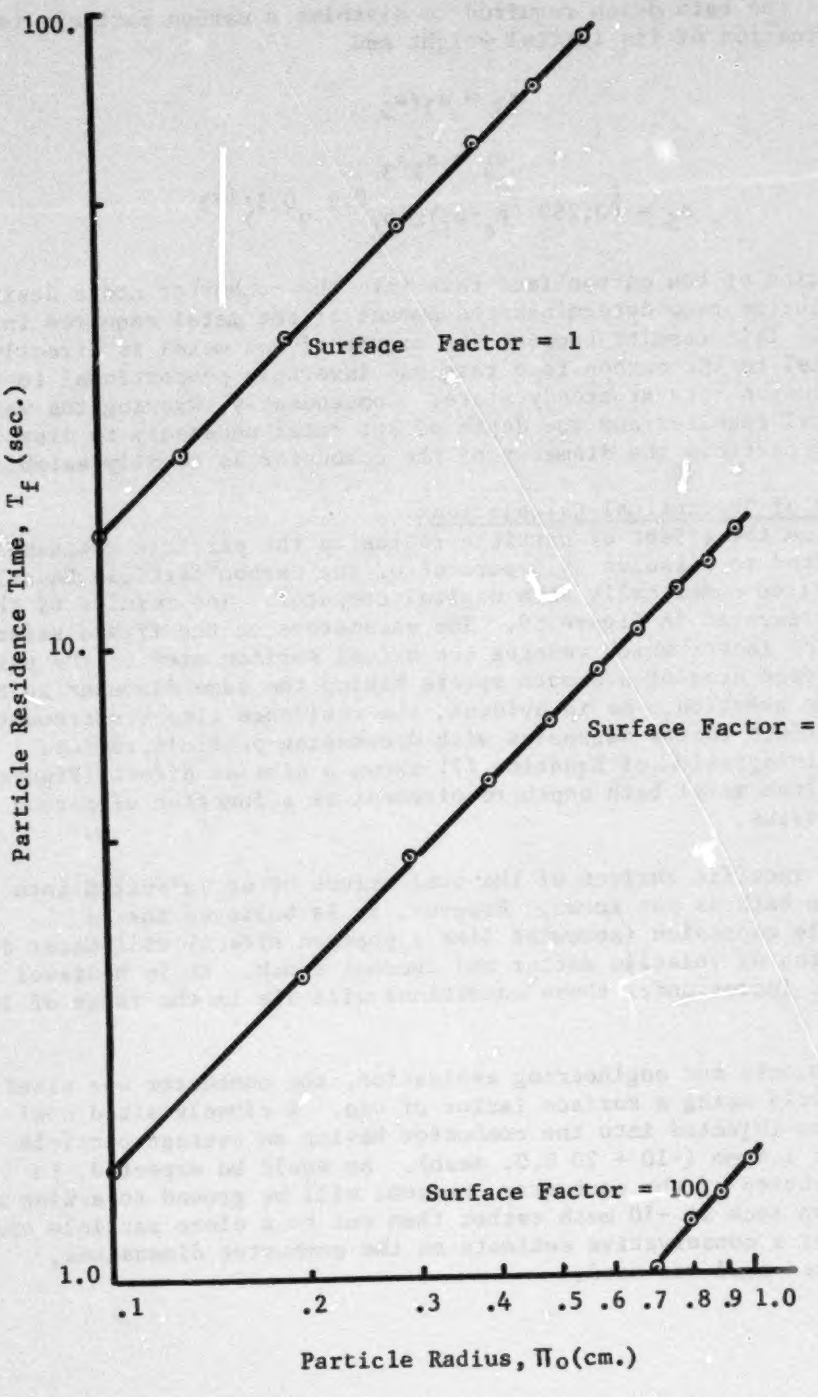

FIGURE 59 - EFFECT OF PARTICLE RADIUS ON RESIDENCE TIME NEEDED IN IRON MELT TO DISSOLVE CARBON

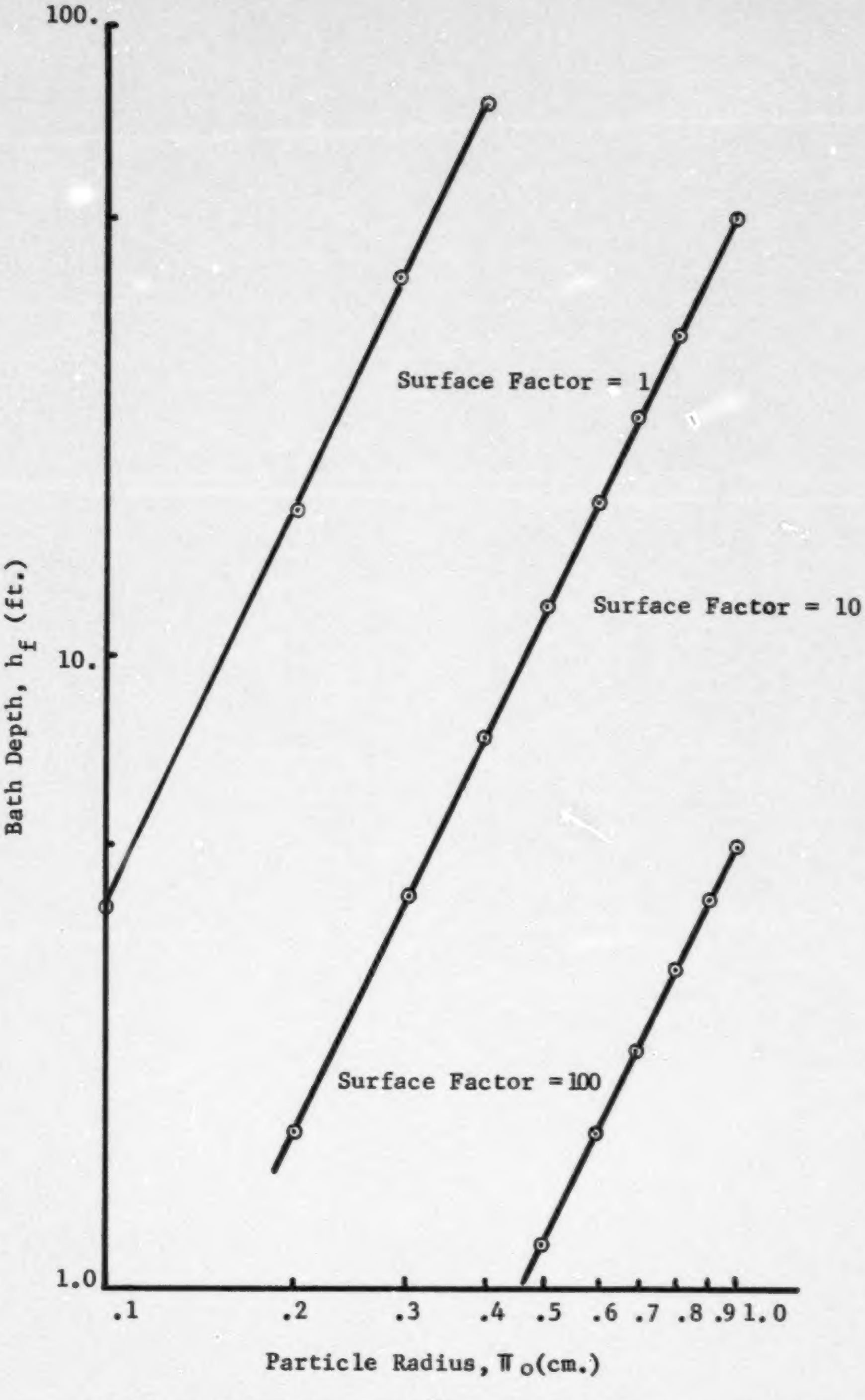

FIGURE 60 - EFFECT OF PARTICLE RADIUS ON HOT METAL DEPTH REQUIRED TO DISSOLVE CARBON

BIBLIOGRAPHIC:
Applied Technology Division, Black, Sivalls & Bryson, Inc., Evaluation of Acid Mine Water Drainage Treatment Process, Final Report, FWQA Contract No. 14-12-529

ABSTRACT

An economic and engineering evaluation of a submerged coal refuse combustion process to convert acid mine water (AMW) to potable water has been made. In this process coal refuse is burned in molten iron to supply energy for distillation or reverse osmosis, and the coal refuse sulfur is trapped in a slag for eventual recovery of sulfur. Laboratory experimentation was conducted

ACCESSION NO.

KEY WORDS
Acid Mine Water,
Distillation,
Slag Desulfurization,
Slag Characterization,
Submerged Coal Combustion,
Two-Stage Coal Combustion,
Coal Refuse

BIBLIOGRAPHIC:
Applied Technology Division, Black, Sivalls & Bryson, Inc., Evaluation of Acid Mine Water Drainage Treatment Process, Final Report, FWQA Contract No. 14-12-529

ABSTRACT

An economic and engineering evaluation of a submerged coal refuse combustion process to convert acid mine water (AMW) to potable water has been made. In this process coal refuse is burned in molten iron to supply energy for distillation or reverse osmosis, and the coal refuse sulfur is trapped in a slag for eventual recovery of sulfur. Laboratory experimentation was conducted

ACCESSION NO.

KEY WORDS
Acid Mine Water,
Distillation,
Slag Desulfurization,
Slag Characterization,
Submerged Coal Combustion,
Two-Stage Coal Combustion,
Coal Refuse

BIBLIOGRAPHIC:
Applied Technology Division, Black, Sivalls & Bryson, Inc., Evaluation of Acid Mine Water Drainage Treatment Process, Final Report, FWQA Contract No. 14-12-529

ABSTRACT

An economic and engineering evaluation of a submerged coal refuse combustion process to convert acid mine water (AMW) to potable water has been made. In this process coal refuse is burned in molten iron to supply energy for distillation or reverse osmosis, and the coal refuse sulfur is trapped in a slag for eventual recovery of sulfur. Laboratory experimentation was conducted

ACCESSION NO.

KEY WORDS
Acid Mine Water
Distillation,
Slag Desulfurization,
Slag Characterization,
Submerged Coal Combustion,
Two-Stage Coal Combustion,
Coal Refuse

on those areas which could profoundly affect the process. These areas were: A laboratory demonstration of slag desulfurization to produce sulfur, the evaluation of slag sulfur retention characteristics, slag capability for neutralizing AMW and the determination of slag compositions having acceptable fluidities. Laboratory results indicated that sulfur is obtained, high slag sulfur partition ratios were achieved, fluid slags are produced and desulfurized slags are not suitable for neutralization.

Engineering studies show that the process has potential for supplying inexpensive energy for distillation and permits the recovery of sulfur so that distilled water is economically produced. Depending upon the AMW composition and sulfur selling price ($20 to $30/ton) the break-even price of water for a 5 MM GPD plant varies between $.42 and $.16/1000 gals when a 14 percent capital interest charge is used.

on those areas which could profoundly affect the process. These areas were: A laboratory demonstration of slag desulfurization to produce sulfur, the evaluation of slag sulfur retention characteristics, slag capability for neutralizing AMW and the determination of slag compositions having acceptable fluidities. Laboratory results indicated that sulfur is obtained, high slag sulfur partition ratios were achieved, fluid slags are produced and desulfurized slags are not suitable for neutralization.

Engineering studies show that the process has potential for supplying inexpensive energy for distillation and permits the recovery of sulfur so that distilled water is economically produced. Depending upon the AMW composition and sulfur selling price ($20 to $30/ton) the break-even price of water for a 5 MM GPD plant varies between $.42 and $.16/1000 gals when a 14 percent capital interest charge is used.

on those areas which could profoundly affect the process. These areas were: A laboratory demonstration of slag desulfurization to produce sulfur, the evaluation of slag sulfur retention characteristics, slag capability for neutralizing AMW and the determination of slag compositions having acceptable fluidities. Laboratory results indicated that sulfur is obtained, high slag sulfur partition ratios were achieved, fluid slags are produced and desulfurized slags are not suitable for neutralization.

Engineering studies show that the process has potential for supplying inexpensive energy for distillation and permits the recovery of sulfur so that distilled water is economically produced. Depending upon the AMW composition and sulfur selling price ($20 to $30/ton) the break-even price of water for a 5 MM GPD plant varies between $.42 and $.16/1000 gals when a 14 percent capital interest charge is used.

1 *Accession Number*

2 *Subject Field & Group*
05D

SELECTED WATER RESOURCES ABSTRACTS
INPUT TRANSACTION FORM

5 *Organization*
Environmental Protection Agency
Washington, D. C.

6 *Title*
Evaluation of a New Acid Mine Drainage Treatment Process

10 *Author(s)*
Paul J. LaRosa
James A. Karnavas
Eugene A. Pelczarski

16 *Project Designation*
14010 DYI

21 *Note*

22 *Citation*
Environmental Control Research Service
14010 DYI 2/71
Environmental Protection Agency
Washington, D. C.

23 *Descriptors (Starred First)*
Acid mine water*, distillation*, slag desulfurization*, slag characterization*, coal refuse*

25 *Identifiers (Starred First)*
Submerged coal combustion*, two stage coal combustion*, acid mine water treatment*

27 *Abstract*
An economic and engineering evaluation of a submerged coal refuse combustion process to convert acid mine water (AMW) to potable water has been made. In this process coal refuse is burned in molten iron to supply energy for distillation or reverse osmosis, and the coal refuse sulfur is trapped in a slag for eventual recovery of sulfur. Laboratory experimentation was conducted on those areas which could profoundly affect the process. These areas were: A laboratory demonstration of slag desulfurization to produce sulfur, the evaluation of slag sulfur retention characteristics, slag capability for neutralizing AMW and determination of slag compositions having acceptable fluidities. Laboratory results indicated that sulfur is obtained, high slag sulfur partition ratios are achieved, fluid slags are produced, and that desulfurized slags are not suitable for neutralization.

Engineering studies show that the process has potential for supplying inexpensive energy for distillation and permits the recovery of sulfur so that distilled water is economically produced. Depending upon the AMW composition and sulfur selling price ($20 to $30/ton) the break-even price of water for a 5 MM GPD plant varies between $.42 and $.16/1,000 gals when a 14 percent capital interest charge is used.

This report was submitted in fulfillment of Program No. 14010 DYI, contract No. 14-12-529 under the sponsorship of the Environmental Protection Agency.

Abstractor

Institution

WR:102 (REV JULY 1969)
WRSIC

SEND TO: WATER RESOURCES SCIENTIFIC INFORMATION CENTER
U S DEPARTMENT OF THE INTERIOR
WASHINGTON, D C 20240

* GPO: 1969-359-339